UNIVERSITÀ DEGLI STUDI DI CATANIA

DOTTORATO DI RICERCA IN BIOMEDICINA TRASLAZIONALE

***CURRICULUM* IN BIOMEDICINA MOLECOLARE GENOMICA E DEI SISTEMI COMPLESSI: BASI CELLULARI E MOLECOLARI DEL FENOTIPO - XXXII CICLO**

DIPARTIMENTO DI MEDICINA CLINICA E SPERIMENTALE

DIPARTIMENTO DI SCIENZE BIOMEDICHE E BIOTECNOLOGICHE

SEZIONE DI BIOLOGIA E GENETICA "GIOVANNI SICHEL"

Angela Caponnetto

circSMARCA5-SRSF1 interaction is functionally involved in GBM pathogenesis

TESI DI DOTTORATO

Coordinatore del Dottorato: Prof. Lorenzo Malatino

Tutor: Prof. Michele Purrello

Anno Accademico 2018/2019

TABLE OF CONTENTS

ABSTRACT 1

1. INTRODUCTION 3

1.1 Glioblastoma multiforme 3

1.1.2 Cell biology of GBM 4

1.1.3 Molecular markers of GBM 6

1.2 Non-coding RNAs 8

1.2.1 Circular RNAs 9

1.2.2 Expression and conservation of circRNAs among species 12

1.2.3 Biogenesis of circular RNAs 13

1.2.4 Nuclear export and degradation of circRNAs 20

1.2.5 Circular RNA functions 21

1.2.6 CircRNAs and disease 26

1.2.7 CircRNAs and cancer 28

1.2.8 CircRNAs as putative biomarkers in cancers and therapeutic targets 31

1.2.9 CircRNAs in human brain 32

1.2.10 CircRNAs in gliomas 33

1.3 Alternative splicing 37

1.3.1 Cancer-associated alterations of splicing patterns 39

1.4 RNA binding proteins.....41

1.4.1 Serine/arginine (SR)-rich protein family.....44

1.4.2 SR protein functions 45

1.4.3 SR proteins in disease 45

1.4.4 Serine/arginine-rich splicing factor 1 (SRSF1 or ASF/SF2).....47

1.4.5 Serine/arginine-rich splicing factor 3 (SRSF3 or SRp20).....49

1.5 Angiogenesis.....50

1.5.1 Vascular endothelial growth factor (VEGF or VEGFA).....52

1.5.2 VEGFA in GBM.....54

1.5.3 Anti-angiogenesis therapeutic targets 56

2. AIM OF THE PROJECT 58

3. MATERIALS AND METHODS.....59

3.1 Collection of GBM specimens 59

3.2 GBM cell lines 60

3.3 Immunohistochemistry: percentage of GFAP+ cells in GBM biopsies 60

3.4 Circular RNA selection 61

3.5 Primer design for the detection of circRNAs and their linear counterparts 63

3.6 RNA isolation and purification 64

3.7 Vector construction 65

3.8 Transfection of GBM cell line 66

3.9 Northern Blotting 66

3.10 qRT PCR 66

3.11 Cell migration and viability assay 67

3.12 Prediction analysis of circSMARCA5 interactions 67

3.13 Primer sequence design to detect VEGFA transcripts 68

3.14 RNA Immunoprecipitation (RIP) 68

3.15 Protein Extraction 69

3.16 Immunoblotting 69

3.17 Immunostaining for CD31 70

3.18 Assessment of blood vascular microvessel density (MVD) 70

3.19 Identification of inverted sequences within introns franking circSMARCA5's exons 15 and 16 by *in silico* analysis 71

3.20 Conservation analysis among species of circSMARCA5's inverted sequences 71

3.21 eCLIP analysis 72

3.22 TCGA data.....72

3.23 Statistical Analyses.....72

4. RESULTS.....74

4.1 Expression profile of selected circRNAs.....74

4.2 Expression of circSMARCA5 correlates with glioma grade malignancy 76

4.3 Cloning of circSMARCA5 in GBM cell line.....77

4.4 CircSMARCA5 regulates GBM cell migration 80

4.5 Prediction analysis of interaction between circSMARCA5 and miRNAs or RBPs.....81

4.6 CircSMARCA5 regulates the splicing of SRSF3 pre-mRNA 85

4.7 Receiver Operating Characteristic (ROC) curve analysis 89

4.8 CircSMARCA5 physically interacts with SRSF1.....90

4.9 SRSF1, VEGFA and circSMARCA5 expression in GBM biopsies 92

4.10 Expression of SRSF1 and VEGFA transcripts in REMBRANDT and TCGA databases 94

4.11 Ratio of pro- to anti-angiogenic VEGFA mRNA isoforms in GBM biopsies and in U87-MG cells overexpressing circSMARCA5 98

4.12 Correlation between circSMARCA5/SRSF1/VEGFA expression and blood vascular microvessel density 101

4.13 CircSMARCA5 expression and GBM Patients' Overall Survival (OS) and Progression-Free Survival (PFS) 102

5. DISCUSSION.....105

6. BIBLIOGRAPHY.....110

ABSTRACT

Glioblastoma multiforme (GBM) is the most aggressive human brain tumor with a median survival of 15 months. The standard treatments of GBM and the total medical resection are unable to contrast this mortal cancer. For these reasons new diagnostic approaches and treatment strategies are needed: the identification of molecular features of this cancer may allow to create a personalized therapy. Circular RNAs (circRNAs) are a new class of non-coding RNAs (ncRNAs) highly enriched in brain, stable within the cells and detectable in body fluids. Even though a lot of studies have proposed their potential roles, the biological importance of circRNAs is still object of debate.

This thesis investigated the putative involvement of circRNAs in GBM pathogenesis. Our group has shown that circSMARCA5 is significantly downregulated in GBM biopsies and its expression is associated to the glioma grade malignancy. Functional analysis showed that circSMARCA5 negatively regulated migration of U87MG cells overexpressing circSMARCA5. Serine/arginine-rich splicing factor 1 (SRSF1) is one of the predicted interactors of circSMARCA5. Is has been proposed that circSMARCA5 may regulate the alternative splicing of serine and arginine rich splicing factor 3 (SRSF3), a known SRSF1 splicing target. Interestingly, SRSF3 is known to act together with other splicing factors, polypyrimidine tract binding protein 1 (PTBP1) and polypyrimidine tract binding protein 2 (PTBP2), that positively regulate glioma cells migration.

Successively, we have demonstrated the physical interaction between SRFS1 and circSMARCA5. One of the most interesting splicing targets of SRSF1 in GBM is the vascular endothelial growth factor A (VEGFA). Expression analysis of the total VEGFA (VEGFAtot) and its splicing variants (Iso8a to Iso8b) transcripts

showed that circSMARCA5 regulated the alternative splicing of VEGFA mRNA by binding to SRSF1. In addition, blood vascular microvessel density evaluated in GBM negatively correlated with the expression of circSMARCA5, while positively correlated with that of SRSF1 and Iso8a/Iso8b ratio.

Kaplan-Meier survival analysis showed that GBM patients with low circSMARCA5 expression had lower overall and progression free survival rates.

Collectively these data convincingly suggest that circSMARCA5 could be considered a promising druggable tumor suppressor in GBM. Moreover, the interaction with the splicing factor SRSF1 makes circSMARCA5 an upstream regulator of pro- to anti-angiogenic VEGFA isoforms ratio within GBM cells and a highly promising GBM prospective anti-angiogenic molecule.

1. INTRODUCTION

1.1 Glioblastoma multiforme

Glial tumors are classified in two major categories based on the grade of invasiveness into the surrounding parenchyma tissue: diffuse gliomas, characterized by a diffuse infiltration of the surrounding brain tissue, and gliomas that show a circumscribed growth behavior [1].

The World Health Organization (WHO) classifies gliomas based on their histological features. This classification of central nervous system tumors classifies diffuse gliomas in four histological grades: grade I, II, III and IV, also named glioblastoma multiforme (GBM) [1].

Diffuse gliomas, due to their ability to infiltrate surrounding normal brain tissue, tend to recur and they can be removed only by a total resection. Moreover, another aspect of diffuse gliomas is that low-grade tumors of WHO grade II not only recur but also may progress to high grade gliomas of WHO grade III and eventually secondary GBM of WHO grade IV [2].

Diffuse gliomas arise more commonly in adults than in children and show a wide range of clinical behaviors from a low clinical progression, typical of WHO grade II gliomas, to a very short median overall survival.

The most frequent diffuse glioma is GBM (WHO grade IV) that represents 45-50% of all primary intrinsic human brain tumors. GBM is the most aggressive human brain tumor with an annual incidence of 3.1 per 100000 and a median survival of 15 months. GBM is considered incurable notwithstanding aggressive therapies including surgical resection and radiotherapy associated with temozolomide (TMZ) treatment. Many

tumors are resistant to chemotherapy and radiation and for this reason new diagnostic approaches and treatment strategies are needed.

GBM tumors are divided into two distinct classes: primary GBM or "*de novo*", that appears without a known clinical precursor, and secondary GBM, that results from the molecular progression and increased malignancy of pre-existing glioma of WHO grade II or III. However, secondary GBMs are less common than primary GBMs and affect patients prior to the age of 45 years; primary GBMs hit elderly patients [2].

Concerning to histopathologic features, GBM is characterized by necrosis and microvascular proliferation. Other histopathological aspects are anaplasia, high mitotic rates and invasiveness. However, these features are common to both GBM and WHO grade III gliomas.

High-throughput genomic platforms for mRNA expression profiling allowed to identify patterns of gene expression and to convert them into GBM subtypes. Profiling studies have identified molecular signatures of diffuse gliomas and have shown subclasses within GBMs. Four subtypes of GBM were described based on data from *The Cancer Genome Atlas* (TGCA): proneural, neural, classical and mesenchymal. The characterization of these subtypes is important to identify different and specific therapeutic approaches that each subtype may require [3].

1.1.2 Cell biology of GBM

During the last two decades the knowledge about molecular biology of GBM is increased. GBM cells are resistant to many anti-GBM therapies because of the numerous cellular dysfunctions they are exposed to. Some intracellular events cause and sustain GBM (Figure 1) [4]:

- Loss of cell cycle: alteration of at least one component of the $p16^{INK4a}$/cyclin-dependent kinase (CDK)-4/RB (retinoblastoma) 1 pathway that controls the G1-S phase transition occurs in most GBMs.
- Over-expression of growth factors and their receptors: some growth factors are over-expressed in GBM, such as epidermal growth factor receptor (EGFR), platelet-derived growth factor (PDGF), basic fibroblast growth factor (bFGF, FGF-2), transforming growth factor (TGF)-1, and insulin-like growth factor (IGF)-1, and promote growth of neoplastic cells. The best characterized receptors and growth factors in GBM are EGFR and PDGF.
- Angiogenesis: malignant gliomas are vascular tumors and the presence of microvascular proliferation indicates a high grade of malignancy. The vascular endothelial growth factor (VEGF) is the most clearly implicated.
- Invasion and migration: these features cause the infiltration of the surrounding neural net in GBM. Many extracellular matrix molecules and cell surface receptors regulate the signal transduction and influence invasion and migration in GBM.
- Apoptosis: glioma cells grow not only for an increase of proliferation rate but also for a dysregulated apoptosis process. Many molecules involved in the biogenesis of gliomas are also involved in apoptosis, for example p53 and its mutations.
- Genetic instability: this aspect is common to many tumors and promotes genomic damage allowing the selection of malignant clones.

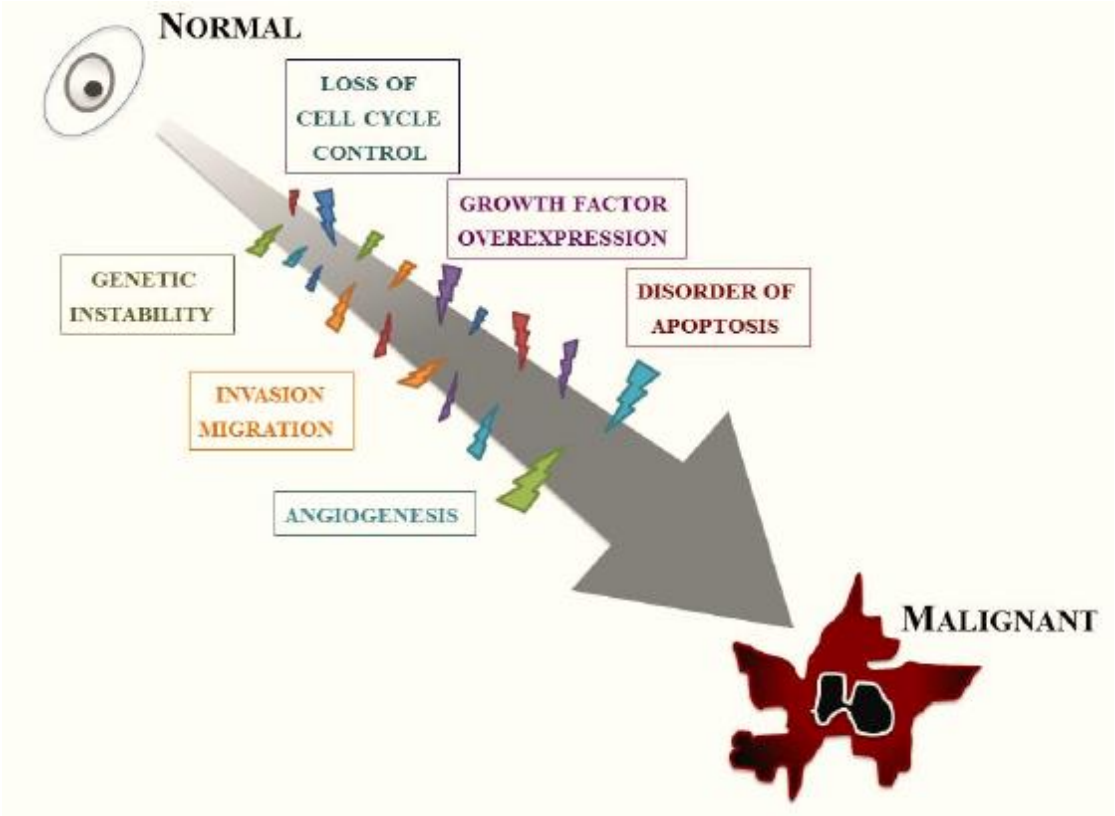

Figure 1. Intracellular altered events that promote GBM (from Nakada M. Cancers. 2011).

1.1.3 Molecular markers of GBM

Promoter methylation of the *MGMT* gene is the most important marker in GBM, in fact it is found in 40% of primary GBM patients. Hypermethylation of the MGMT promoter is used as predictive marker for alkylating chemotherapy in GBM [5].

MGMT is a DNA repair enzyme that restores guanine from O-6-methylguanine, the type of genomic lesion induced by alkylating agents commonly used in chemotherapic treatment of GBM, such as temozolomide

(TMZ). The methylation of MGMT gene promoter is associated with prolonged progression-free survival and overall survival in patients who are treated with alkylating agents [5].

The discovery of mutations of the isocitrate dehydrogenase (IDH) gene has expanded the knowledge of the molecular landscape in GBM. The mutant IDH protein plays a neomorphic enzymatic activity catalyzing the production of the oncometabolite 2-hydroxyglutarate that influences many cellular programs that contribute to the development of GBM. IDH mutations have been identified in secondary GBM and low-grade glioma, while are almost absent in primary GBM [6]. Despite similar histopathologic features, IDH wild-type and mutant glioblastomas show distinct molecular and prognostic features that allow to separately classify them in the classification of brain tumors. IDH mutations are associated with younger age and better outcome; IDH wild-type glioblastoma is associated with older age and poor prognosis. These mutations may have clinical and prognostic importance and may be used to distinguish early secondary GBM from primary GBM [7], [6]. About half of all primary GBMs show amplification of the EGFR gene and the 50% of them with EGFR amplification carry also a mutation in this gene that encodes for EGFRvIII (a variant of EGFR costitutively active) that promotes tumor growth and is associated with a worse clinical outcome [5].

The identification of molecular features of the GBM regulation network may improve the creation of a personalized therapy. To date, the methods used for cancer diagnosis and response evaluations depend on the pathology and the imaging-based technologies. Some methods are invasive or limited to small size tumors. Progress in the molecular characterization of GBM has allowed to identify a plethora of novel therapeutic targets. A deeper knowledge and identification of molecular biomarkers involved in GBM development may

be useful for a better and more sensitive detection. Since GBM shows a wide heterogeneity, a more personalized treatment could be needed.

1.2 Non-coding RNAs

In the late 1990s researchers supposed that human genome comprised about 100,000 protein-coding genes. Over the years, this number rapidly decreased until the recent last version in which the number of protein-coding genes is about 19000 [8]. These data suggest that less than 2% of the whole human genome encodes for proteins and the other 98% represents the keystone of *Homo sapiens* complexity and plays most probably regulatory roles rather than structural ones [9].

In the last decades, two different studies [10], [11] proposed that about 80% of the human genome is dynamically and pervasively transcribed as non-protein-coding RNAs (ncRNAs). Other studies showed that the relative proportion of the proteome-encoding genome differs among evolutionarily distant species. For example, *Saccaromyces cerevisiae* genome is almost entirely comprised of protein coding genes, whereas they represent only 2% of mammalian genomes [12]. These data suggest that ncRNAs are related to the complexity of higher eukaryotes and an alteration of their regulatory functions may promote pathological phenotypes. NcRNAs have been extensively studied because they play important biological roles in the regulation of cellular mechanisms. They are divided into two categories: 1) long non-coding RNAs (lncRNAs), longer than 200 nucleotides, and 2) small non-coding RNAs, 200 nucleotides long or less, such as microRNAs (miRNAs), small interfering RNAs (siRNAs), small nuclear RNAs (snRNAs or U-RNAs), small nucleolar RNAs (snoRNAs), PIWI-interacting RNAs (piRNAs), and tRNAs [13]. Many studies have demonstrated that an

interplay among ncRNAs exists and it influences cell physiology and disease. In addition, ncRNAs can interact with and regulate each other generating a complex network of different species of RNA. They can also compete among each other for binding to mRNAs, acting as competing endogenous RNAs (ceRNAs) [14].

NcRNAs include also a recently discovered class of non-coding RNA molecules, named circular RNAs (circRNAs) characterized by peculiar structure and functions.

1.2.1 Circular RNAs

CircRNAs were first found in RNA viruses in the early 1970s [15]. Few years after they were discovered for the first time in the cytoplasm of eukaryotic cells [16], but at the beginning they were considered artifacts of aberrant mRNA canonical splicing process and lacking biological importance [17]. However, during the last decades researchers showed a growing interest in all biological aspects of these RNA molecules. An important feature of circRNAs is that their expression is not always correlated with the one of their host genes. This aspect could explain the reason why circRNAs are not only by-products of canonical pre-mRNA splicing but they can also arise by a new type of regulated alternative splicing. Another aspect in favor of the importance of circRNAs is that they are evolutionarily conserved among different species [18].

CircRNAs differ from other ncRNAs because they have no free 3' or 5' ends. In fact, they possess a peculiar and unique structure originated through a non-canonical mechanism of splicing, known as "back-splice" or "head-to-tail splice", in which a splice donor is covalently joined to an upstream splice acceptor [18].

This singular circular structure makes them more stable than liner RNA counterpart and resistant to degradation by RNA exonuclease or RNase R [19], [20], [21].

The majority of circRNAs are transferred from the nucleus to the cytoplasm [22]. However, a smaller fraction is localized in the eukaryotic nucleus where they regulate gene expression: this is the case of multiexon-circles with retained introns (termed exon–intron circRNA, or EIciRNA) [23].

CircRNAs mainly originate from exons close to the 5' end of a protein coding gene and may be composed of only a single or multiple exon [19]. Multiple circRNAs can be generated from a single gene (alternative circularization) [24], even though alternative splicing events that modify the back-splice junction have been described [25].

CircRNAs can be classified based on their genomic proximity to a neighboring gene (Figure 2): (1) sense or exonic, derived from one or more exons of the linear transcript of the same strand; (2) intronic, generated from an intron of the linear transcript; their biogenesis depends on a key motif containing a 7-nt GU-rich element close to the 5' splice site and an 11-nt C-rich element near the branch point; (3) antisense, that overlaps one or more exons of the linear transcript on the opposite strand; (4) bidirectional or intragenic, transcribed from the same gene locus of the linear transcript but in close genomic proximity and not classified as "sense" and "intronic"; (5) intergenic, located in the genomic interval between two genes [26].

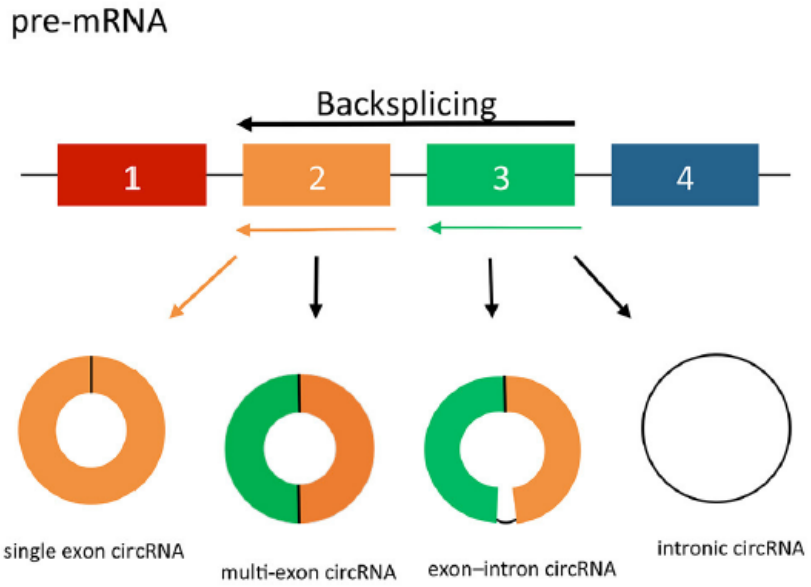

Figure 2. Classification of circRNAs (from Greene J. Front Mol Biosci. 2017).

In addition, novel studies, based on a new tool for circRNAs detection named CIRIexplorer2, allowed the researchers to discover new less conserved exons that are present only in circRNAs and not in linear counterparts [25]. It is not yet known if these novel exons are present exclusively in circRNAs because their incorporation in a linear transcript induces their degradation through a pathway that circRNAs are resistant to, or if they may be comprised specifically in circRNAs due to specific splicing [25].

CircRNAs expression has been widely studied across every domain of life [27], [28], [29], [30]. By analyzing transcriptome sequencing datasets, it has been showed that 5.8% to 23% of actively transcribed human genes generate circRNAs [31].

CircRNAs are generally barely expressed but they can be more abundant than the linear counterpart produced from the same gene [21]. Most of them show an expression that correlates with the one of linear transcript

derived from the same gene, but many genes exhibit different expression regulation of circRNAs and linear RNA variants [32].

Since the expression level at steady-state is related to the synthesis's rate, this different abundance could be determined by a difference in the rate of biogenesis rather than a difference in decay rate [33]. This aspect may indicate that circRNA expression is controlled and the spliceosome must be able to discriminate between canonical splicing that generates linear isoform and back-splicing. However, the mechanism that regulates this discrimination is still not known [34].

1.2.2 Expression and conservation of circRNAs among species

Analyses of transcriptome sequencing datasets have revealed that the expression of circRNAs has been detected in metazoan and in diverse cell types and organisms, ranging from fruit flies [35] to humans [36], [37], [38]. CircRNAs have also been discovered in plants, protists and fungi [35], [39], [40], [41], [27].

Rybak-Wolf et al., 2015, through RNA sequencing and ribosomal- depleted RNA analysis from 29 different types or stages of neural cells and tissues, demonstrated that circRNAs show high, heterogeneous and specific expression in different human brain compartments [32], and, in particular, they are highly enriched in the synapses. This aspect could explain why human circRNAs are more abundant than mouse circRNAs, because synaptic density in the human cerebral cortex may be four times higher than in the mouse brain [42]. It has been shown that circRNA expression is higher during neuronal differentiation, both in cell lines and in primary neuron cultures. The high expression is often associated with the up-regulation of the linear host transcripts,

but exceptions exist such as circStau2a and circStau2b expressed from RNA-binding protein Staufen 2, and circZfp609 [32].

Rybak-Wolf et al. in 2015 observed also that circRNA expression is highly conserved. In fact, most well-expressed circRNAs in mouse are also present as circRNAs in human. Generally, conserved circRNAs are more likely flanked by introns that contain reverse complementary matches than the non-conserved ones, and the length of these introns is also highly conserved during evolution.

Thanks to their stability, circRNAs could act in the mammalian brain as topologically complex platforms to assemble RNP granules or to transport proteins or RNAs. The abundant localization of many circRNAs into the synapses, which often contrasts to the cytoplasmic localization of the corresponding mRNAs, points in this direction. It has been observed that miRNAs can cleave circRNAs [43], and therefore cargo ‘‘release’’ mechanisms are simple to imagine. Finally, due to their high stability, circRNAs might be used by neuronal termini and molecular postsynaptic platforms as synaptic tags to keep a molecular memory.

1.2.3 Biogenesis of circular RNAs

Although many circRNAs have been identified, their biogenesis is still under investigation. As previously described, circRNAs have 3′ and 5′ end covalently joined. Because canonical splice signals flank the junction sites, the spliceosome should be implicated in their generation [44]. The role of spliceosome in circRNA biogenesis is supported by the fact that inhibition of the canonical spliceosome reduces both circRNA levels as well as the levels of the spliced linear transcript [44], [20]. Nevertheless, elements that could be involved in the circularization have been identified. Different mechanism of circRNA biogenesis have been proposed and

they may require the action of *cis*-acting elements, *trans*-acting factors and co- or post-transcriptional processes [21], [45], [44].

Even though biogenesis of circRNAs is still not completely understood different mechanisms of circRNA biogenesis have been proposed.

- **Intron pairing-driven circularization**

This model consists in a base-pairing between complementary motifs contained within the introns flanking the exons involved in the circularization, which leads to the formation of a restricted structure bringing near the splice sites and allowing the formation of circRNAs (Figure 3) [21].

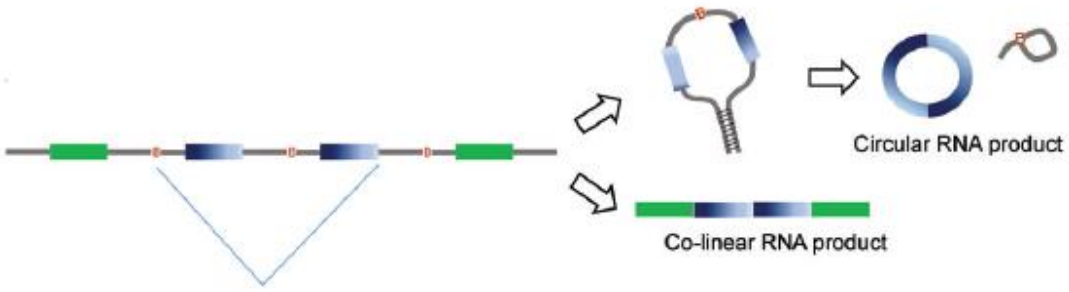

Figure 3. Intro pairing-driven circularization model (from Chen I. Wiley Interdiscip Rev RNA. 2015)

The presence of complementary sequence motifs within flanking introns is one of the principal aspects required for the circularization [24] and it is a prevalent feature of circRNAs expressed in brain and conserved across human, pig and mouse [32]. However, both non-repetitive and repetitive elements may stimulate this mechanism. In humans, repetitive Alu elements are enriched within introns flanking exons involved in the circularization and are the major contributors in the circRNA biogenesis (Figure 4) [21].

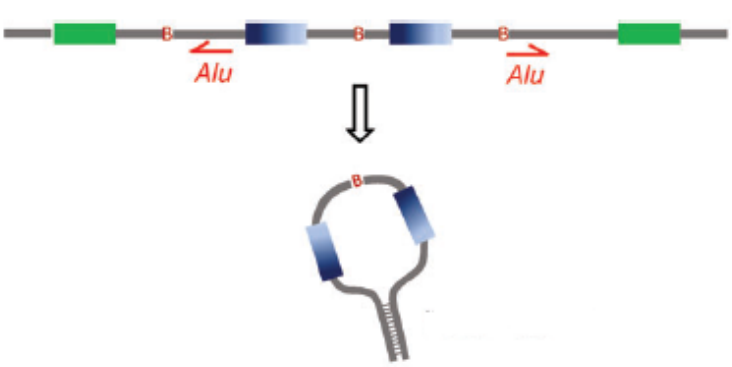

Figure 4. Alu elements involved in the circularization (from Chen I. Wiley Interdiscip Rev RNA. 2015).

Recent studies have clarified the importance of flanking Alu elements in the circularization process [21]. It was suggested that base-pairing between different pairs of Alu repetitive elements affect the linear-to-circular RNA ratio while the presence of two Alu elements within one intron decreased circRNA formation because it leads the formation of an intra-intron pairing [24]. The specific sequence and the stability of the base-pairing stretches are important for the induction of circRNA formation. Nevertheless, circRNA formation is not specifically based on the presence of Alu elements, but mainly requires the formation of an inverted repeat: both Alu elements containing within introns and non-Alu containing complementary regions may enhance circularization [24].

The involvement of complementary sequence motifs in the biogenesis of circRNAs depends on both the stability of the intramolecular interaction between these sequences and the sequence composition of the complementary regions [46]. Additionally, competitive base-pairing between different pairs of complementary

regions as well as the distance from the inverted element to the exon involved in the formation of the circular structure may influence the efficiency of circularization [24].

Intron pairing process may be regulated by RNA editing [47]. RNA editing enzyme adenosine deaminase acting on RNA-1 (ADAR1) binds to double stranded RNA regions and converts adenosines to inosines [48] working as an antagonist of circRNA formation (Figure 5) [32], [36]. To date, it is supposed that nuclear editing performed by ADAR1 before back-splicing may destabilize pairing between complementary motifs within the introns flanking the exons undergoing circularization, preventing the biogenesis of circRNAs based on the base-pairing model. In addition, impaired circRNA biogenesis could be influenced by indirect effects of ADAR1 [32], [36].

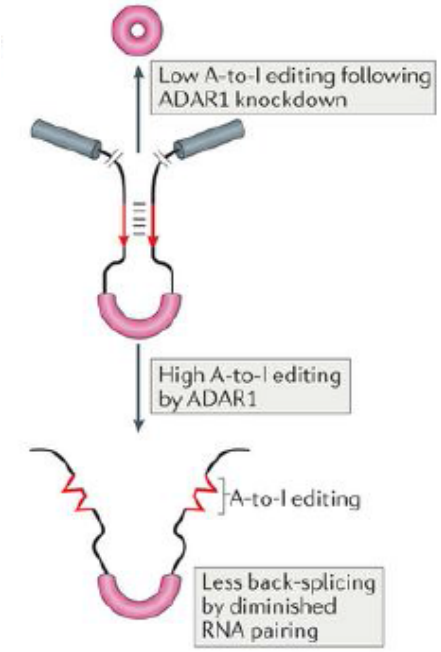

Figure 5. RNA editing and regulation of biogenesis of circRNAs (from Chen LL. Nat Rev Mol Cell Biol. 2016).

- **RNA binding protein pairing driven circularization**

Another potential mechanism of circRNA biogenesis requires RNA binding proteins (RBPs). Their mechanism of action is based on their binding to specific binding sites within introns flanking exons that circularize, bringing them within proximity. This biogenesis model considers the proximity between the splice sites with respect to the direct base-pairing that induces the proximity between complementary motifs. To date, two main RBPs, that act as splicing factors, have been studied: Quaking (QKI) [45] and Muscleblind (MBL) [44] (Figure 6).

More in detail, a strong and direct interaction exists between MBL and circMbl. MBL protein binds to introns flanking circMbl at multiple sites favoring the circularization depending on the MBL expression levels. An increase of the MBL level induces a decrease of the production of its own mRNA by promoting biogenesis of circMbl which in turn sponges out the excess of MBL protein by tethering it [44].

However, binding of RBPs could also promote circularization either by stabilizing complementary sequences or by inhibiting canonical splicing.

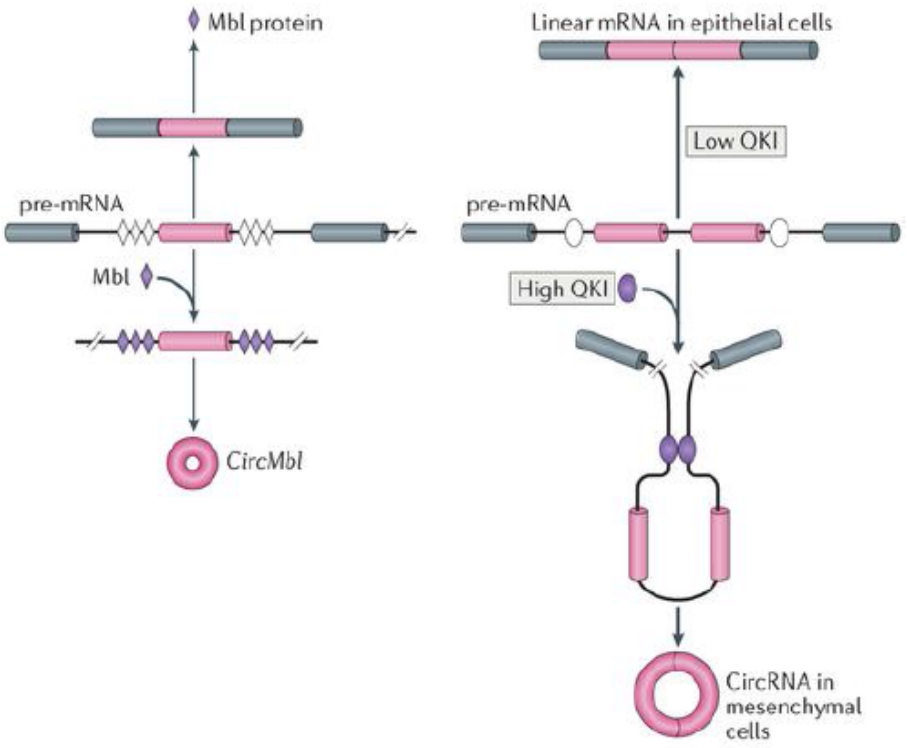

Figure 6. Circularization promoted by *trans*-acting factors (from Chen LL. Nat Rev Mol Cell Biol. 2016).

- **Lariat-driven circularization**

RBPs could determine the formation of a circular structure by inducing exon skipping, in which one or more exons of the transcript are spliced out (skipped), forming an exon containing lariat. In this way, skipped exon(s) within the lariat are in proximity and are recognized and joined by the spliceosome [21]. Although exon skipping depends on *trans*-acting protein factors, the process of circularization itself depends only on intrinsic features of the lariat structure (Figure 7).

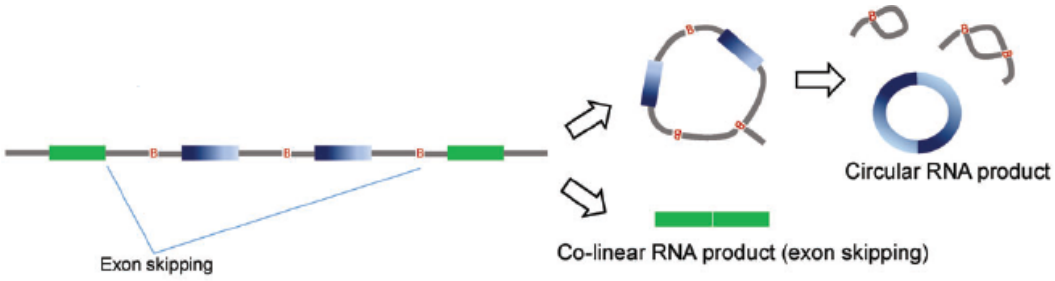

Figure 7. Lariat-driven circularization model (from Chen I. Wiley Interdiscip Rev RNA. 2015).

- **Co- or post-transcriptional biogenesis**

Ashwal-Fluss et al. (2014) showed that circRNAs can be detected in samples of nascent RNA isolated from *Drosophila* fly heads, demonstrating that circRNAs may be produced co-transcriptionally and their production rate depends on their flanking introns [44]. Moreover, canonical pre-mRNA splicing competes with the formation of circRNAs. This competition is tissue-specific and conserved from flies to humans [44]. This hypothesis is also supported by the demonstration that circRNA formation decreased when the efficiency of canonical linear splicing was enhanced using a mutated RNA polymerase II [44]. On the contrary, as demonstrated by the lack of circularization in response to the disruption of poly(A) signal, functional 3′ end processing is necessary for circularization, indicating that circRNA biogenesis may take place post-transcriptionally [46].

CircRNA biogenesis is affected not only by the action of *cis*- and *trans*-acting factors but also by the transcriptional elongation rate. It was observed that circular RNA producing genes are generally longer and are transcribed faster than genes that do not encode circRNAs [33]. This finding suggests that circRNA

formation may compete with formation of canonical linear transcripts and that the rate of transcription may influence which model of biogenesis is favored [44].

If canonical splicing takes place first, a linear RNA with skipped exons and a long intron lariat containing these skipped exons will be generated; these last will be the substrate for the formation of circRNAs by exon skipping model [49]. However, if the back-splicing takes place first, it will directly generate a circRNA together with an exon-intron(s)-exon intermediate, which can be either processed forming a linear RNA with skipped exons or be degraded (direct back-splicing) [49].

These two steps could happen either stochastically or even synergistically [50]. Nevertheless, it is still unknown under which circumstances the spliceosome machinery chooses either canonical splicing or back-splicing to start with the formation of a circRNA.

1.2.4 Nuclear export and degradation of circRNAs

The determination of the localization of circRNAs is important to understand the mechanism through which they act. Little is known about how circRNAs are translocated from the nucleus to the cytoplasm where the majority of circRNAs exert their functions. One of the models by which circRNAs are tagged for export into the cytoplasm may involve the deposition of an exon-junction complex during splicing that may recruit mRNA export factors [51]. Moreover, the mechanism through which ElcircRNAs are localized into the nucleus is due to the intron retention [52].

Some circRNAs show developmentally regulated nucleo-cytoplasmic localization suggesting that an active nuclear export mechanism for circRNAs exists [31].

The mechanism of circRNAs degradation is still not well characterized. CircRNAs could escape the predominant mechanisms of mRNA degradation, which are based on exonucleolytic degradation from either the 3′ or 5′ end. However, since circRNAs appear to accumulate at detectable levels despite a low synthesis rate, it could be possible that the degradation mechanism is not efficient. Endonucleolytic Ago2-miRNA mediated cleavage appears to be one mechanism to initiate degradation [43].

1.2.5 Circular RNA functions

The hypothesis of circRNAs as functional molecules is supported by the fact that circRNAs and their isoforms show often a cell-type, tissue and developmental stage specific expression and some of them are conserved among species [18], [29]. In addition, the sequences of exons forming circRNAs appear to be more conserved at the third codon position, known to be often redundant at protein level with respect to linear exons. This aspect indicates an evolutionary limit at sequence level and suggests potential additional functions apart from encoding protein [18], [53].

The biological importance of the role of circRNAs is still object of debate. However, different mechanisms of action have been proposed (Figure 8).

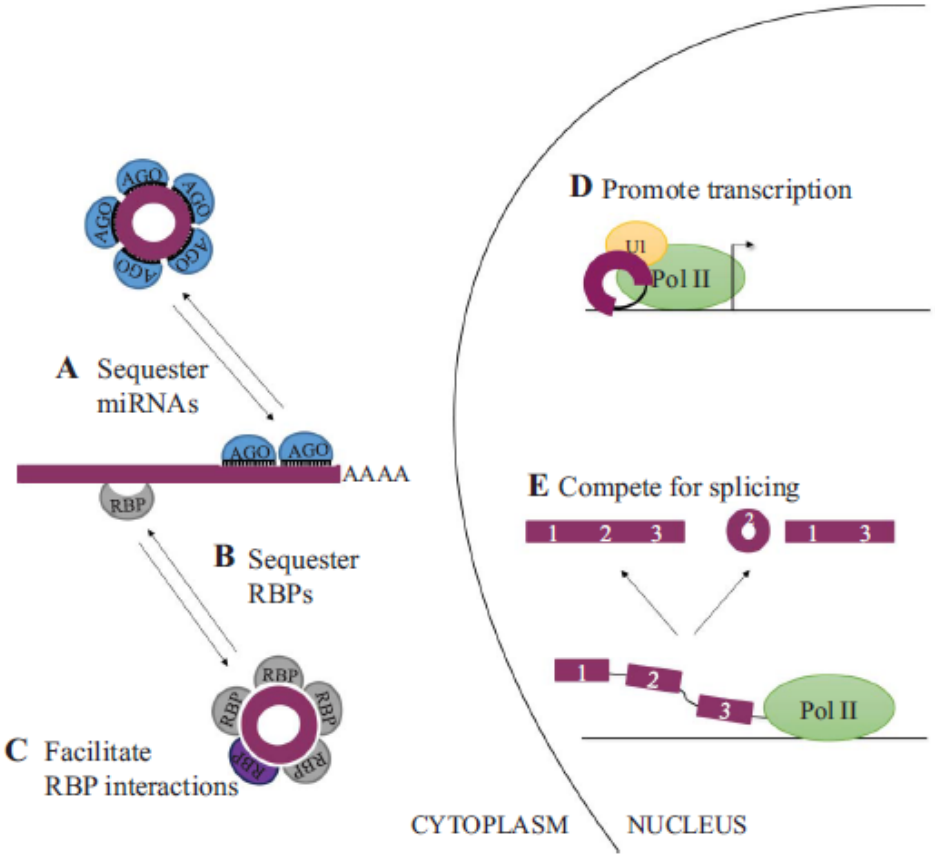

Figure 8. Functions of circRNAs (from Ebbesen KK. RNA Biol. 2017).

- **circRNAs as miRNA sponges**

Recent evidences indicate that circRNAs can function as miRNA sponges or potent competitive endogenous RNA molecules (ceRNAs) [54]. CeRNAs contain shared miRNA response elements (MREs) and can compete for miRNA binding influencing the activities of miRNAs as regulator of gene expression.

It was demonstrated that some circRNAs may act as sponge for miRNAs interacting with the miRNA-Argonaute 2 (Ago2) complex [18], [55], [38] and inhibiting the function of miRNAs for which they possess binding sites (Figure 8 A). Since it is known that miRNAs act as regulators of gene expression by suppressing translation and enhancing exonucleolytic decay of mRNAs [56], the regulation mediated by circRNAs may

influence the expression of miRNA targets. circRNAs may act as efficient miRNA inhibitors because they are able to sequester miRNAs as result of their ability to resist to miRNA mediated exonucleolytic decay due to their no free ends [18], [55]. CDR1As (ciRS-7), as well as *Sry*, have been shown to bind to miRNAs without being degraded: this makes them potential candidates for ceRNAs activity [49].

It was demonstrated that *Sry* circRNA [18], [55] and ciRS-7 [55] possess many miRNA binding sites for one or more specific miRNAs. However, it is not clarified if circRNAs with a small number of binding sites per miRNAs may act as miRNA regulators.

The mouse gene SRY is composed of a single exon and is involved in the determination of the sex in males; Sry is highly expressed in cells of the developing genital ridge, where it exists in the form of linear transcript that is translated into protein, and in adult testes where it exists as a circular product localized into the cytoplasm and is not translated into protein [57], [58]. Hansen et al., 2013 demonstrated that Sry circRNAs can act as an inhibitor of miR-138 activity binding to it in 16 putative binding sites [55].

Cerebellar degeneration-related protein 1 (CDR1) gene produces a natural antisense transcript, named antisense to the cerebellar degeneration-related protein 1 transcript (CDR1as/ciRS-7), highly abundant in the brain of placental mammals, especially in the cerebellum and detectable in other tissues, that interacts with miRNAs and is degraded by miR-671 [43]. ciRS-7/CDR1as contains over 70 binding sites for miR-7 and is bound by Argonautes proteins. ciRS-7 tethering miR-7 provokes a decrease of the activity of miR-7. This aspect suggests that ciRS-7/CDR1as is protected from degradation-miR-7 mediated [55].

To date only circHIPK3 is known to act as a regulator of miR-124 even though it possesses only 2 binding sites for this miRNA [38], indicating that circRNAs may act as miRNA regulators despite a limited number of miRNA binding sites. In addition, circRNAs may interact with multiple miRNAs involved in the same biological function and thereby avoid the need to have many binding sites for a single miRNA, as demonstrated for circHIPK3 which shows 18 binding sites for 9 different miRNAs involved in growth suppression [38]. Other examples are represented by: circ-ITCH that acts as a sponge of miR- 7, miR-17 and miR-124 [59]; circ-Foxo3, which sponges several miRNAs, such as miR-22, miR-136*, miR-138, miR-149*, miR-433, miR-762, miR-3614–5p and miR-3622b–5p [60]; circRNA HRCR, circHIPK3 and has_circ_001569 that act as miRNA sponge binding to miR-223, miR-124 and miR-145 [61], [38], [62].

- **Interaction between circRNAs and RNA binding proteins**

CircRNAs may interact with RBPs and act as a scaffold to facilitate protein interactions, regulate protein functions or sequester the bound proteins (Figure 8 B-C) [44], [63], [64].

An example is given by circ-Foxo3. More in details, CDK2 and p21 proteins could interact with circ-Foxo3 forming of a ternary complex (circ-Foxo3–p21–CDK2), that avoids the formation of cyclin E/CDK2 complex, thus blocking the transition from G1 to S phase. The complex also blocks the inhibitory effect of p21 on cyclin A/CDK2 system, therefore blocking the progression of the cell cycle in S phase and resulting in the arrest of cell cycle in the G1 phase [63].

Holdt et al., 2015 demonstrated that CircANRIL binds to pescadillo homologue 1 (PES1), an essential 60S-pre-ribosomal assembly factor, thereby compromising exonuclease-mediated pre-rRNA processing and

ribosome biogenesis in vascular smooth muscle cells and macrophages. As a result, circANRIL causes nucleolar stress and p53 activation, determining the induction of apoptosis and inhibition of proliferation, which are key cell functions in atherosclerosis [64].

In addition, circRNAs can bind to RBPs that regulate their biogenesis, as showed for the protein MBL, that is directly involved in the circMbl biogenesis [44], and the splicing factor QKI that regulates over one-third of abundant circRNAs biogenesis [45].

- **CircRNAs may regulate parental gene transcription**

CircRNAs with retained introns have been shown to be retained in the nucleus where they promote the transcription of their parental genes (Figure 8 D). The most studied ElciRNAs are circEIF3J and circPAIP2 [23], [23].

Into the nucleus circRNAs interact with the polymerase II (Pol II) machinery and regulate host transcription activity in a *cis*-acting manner [65]. EIciRNAs may bind to factors, such as U1 small nuclear ribonucleoproteins (snRNPs), through RNA-RNA interaction forming the EIciRNA–U1 snRNP complex that may interact with the Pol II transcription complex at the promoters of parental genes and enhance gene expression. Once the transcription of a gene is turned on, the generation of EIciRNA from the gene may further promote the gene transcription, hence generating positive feedback [23].

- **CircRNAs regulate alternative splicing**

The production of circRNAs may regulate linear RNA expression from the same gene, in a self-regulatory manner [22], [44]. This is because most of circRNAs are generated from exon regions of protein coding genes

and because exon(s) comprised into the circRNA would not be a part of any potential linear skipped transcript derived from the same primary transcript. Nonetheless, removal of other exons from the linear transcript during alternative splicing leading to circRNA formation may generate transcript variants that could be degraded by the RNA surveillance apparatus [66] or produce proteins with an altered function (Figure 8 E).

- **Translation of circRNAs**

Although circRNAs are classified as ncRNAs, they have been proposed to be translated *in vitro* and *in vivo* [67]. In eukaryotes, the canonical process of translation starts with the binding of the pre-initiation complex, which contains the small ribosomal subunit [68]. This scans the mRNA until the start codon leading the recruitment of the 60S ribosomal subunit. In addition, ribosomes can be recruited to an internal start codon by a mechanism that depends on the presence of an internal ribosome entry site (IRES). It has been proposed that eukaryotic ribosomes may initiate the translation on circRNAs only if the RNA contains internal ribosome entry site (or IRES) elements [69]. An example of a protein-coding circRNA in eukaryotes is provided by circ-ZNF609, which contains an open reading frame spanning from the start codon, in common with the linear transcript, and terminating at an in-frame STOP signal, created upon circularization. It is associated with heavy polysomes, and it is translated into a protein in a splicing-dependent and cap-independent manner [70].

1.2.6 CircRNAs and disease

Based on the functions of circRNAs, researchers have focused their attention on the role that circRNAs may play in physiological and pathological conditions. It is known that they are associated with autophagy, apoptosis and proliferation, suggesting that circRNAs may function in several diseases through different

mechanisms. Moreover, circRNAs are resistant to degradation by cellular RNA decay machinery and show an extensive distribution, stability, cell type-specific and tissue-specific expression that allow to hypothesize that they could be used as novel and promising biomarkers for the diagnosis, prognosis of human diseases and cancers and therapeutic targets.

Since circRNAs have been shown to be abundant in mammalian brain, their potential involvement in disease of nervous system has been studied. Hansen et al., 2013 showed that ciRS-7 serves as a crucial factor in neuron function and is a good candidate in neurological disorders and brain tumor development [55]. In fact, ciRS-7 acts as a "sponge" of miR-7, which is involved in Parkinson's disease and in various cancer pathways [55]. Other studies showed a mis-regulated miR-7-circRNA system in sporadic Alzheimer's disease (AD), suggesting circRS-7 as an effective target in the treatment of this neurologic disease [71].

Another circRNA involved in AD is circPVT1. It may act as a senescence suppressor in proliferating fibroblasts and appears to sequester let-7 involved in neurodegeneration, a typical feature of AD patients [72].

Xu et al., 2015 showed that ciRS-7 is also involved in diabetes, since it inhibits miR-7 function in islet β cells, which in turn improves insulin secretion [73].

CircMbl could be associated with the initiation and progression of the myotonic dystrophy, a severe degenerative disease. In fact, it is known that circMbl act as a sponge for MBL regulating its production and a MBL aberrant function is involved in this disease [74].

cANRIL is associated with common single-nucleotide polymorphisms (SNPs) that affect cANRIL splicing leading to repression of the INK4A/ARF locus, which is associated with an increased risk of atherosclerosis [75]. In particular, it confers atheroprotection via the induction of apoptosis and inhibition of proliferation [64].

CircRNAs are also involved in vascular disease. Boeckel et al., 2015 demonstrated that cZNF292 possesses proangiogenic activities [76]. In blood vessel diseases it is also possible detect circRNA biomarkers; in fact, hsa_circ_0124644 can function as a diagnostic biomarker of coronary artery disease [77]. Finally, circRNAs play also an important role in the initiation and progression of cardiovascular diseases [78]

1.2.7 CircRNAs and cancer

The increasing interest in understanding circRNA functions, prompted researchers to study the differential expression pattern of circRNAs in order to identify potential biomarkers in cancer diagnosis and investigate their regulatory role in cancer development and progression.

Dis-regulation of circRNAs may influence proliferative signaling, epithelial-to-mesenchymal transition, angiogenesis, apoptosis or drug resistance and, in this manner, may be among the principal causes of cancer development (Figure 9).

CircRNAs are often downregulated in tumor tissues with respect to normal tissue probably due to: (i) errors in the back-splice machinery in malignant tissues; (ii) degradation of circRNAs by deregulated miRNAs in tumor tissue; or (iii) increase of cell proliferation leading to a reduction in circRNA expression [79].

One of the most studied circRNAs is the tumor-suppressor gene Foxo3, which was shown to be involved in the promotion of cancer cell apoptosis by different mechanisms [60], [80]. It is also implicated in the inhibition

of angiogenesis and cell cycle progression [60], [63]. CircFoxo3 was found downregulated in breast cancer and it appears to regulate its progression [81], as well as the circRNAs derived from ABCB10 gene that regulates the proliferation and apoptosis in the same cancer model [82].

Similar to circFoxo3, circZNF292 possesses tumor-suppressor properties: it negatively regulates cell cycle progression [83] and shows also proangiogenic activities [76], as well as circMYLK [84].

Another well characterized circRNA is circITCH, which negatively correlates with cell cycle and proliferation through the inhibition of the Wnt/βCatenin pathway [59], [85].

There are also deregulated circRNAs associated with a late-stage diagnosis of metastases, as circZKSCAN1, circCCDC66, circKCNH1 and circHIAT1; in particular, some of them influence metastasis both *in vitro* and *in vivo* [86].

Zheng et al., 2016 observed that most of circRNAs are upregulated in bladder cancer, unlike the findings in most other cancers [38].

Recent studies have reported that hsa_circ_0000096 can inhibit gastric cancer (GC) cell proliferation and migration [87]. On the contrary, circPVT1 promotes cell proliferation in GC by sponging members of the miR-125 family [88]. Zhang et al., 2017 demonstrated that circ_100269 inhibits cell proliferation by targeting miR-630 and circLARP4 negatively regulates cell growth and tumor invasion in GC [89].

Guo et al., 2016 showed that the knockdown of has_circ_0000069 inhibits cell proliferation, migration and invasion and influences the cell cycle by reducing the G0/G1 phase, proposing this circRNA as a promising target in colorectal cancer (CRC) therapy [90]. A similar role was observed for circCCDC66 and circBANP

[91], [92]. Other studies reported that has_circ_001569 acts as a positive regulator of cell proliferation and invasion in CRC, while hsa_circ_0020397 influences cell viability, apoptosis and invasion in CRC [62], [93]. Several studies showed that ciRS-7 may be considered a potential target in hepatocellular carcinoma (HCC), since it promotes cell proliferation and invasion in HCC [94]. circZKSCAN1 inhibits cell growth in HCC, migration and invasion by mediating many cancer-signaling pathways [95].

The interest in studying of the involvement of circRNAs in cancer is also associated to the fact that many circRNAs act as sponges for miRNAs [96], whose expression could be altered in different types of cancer due to amplification or deletion of miRNA genes, abnormal transcriptional control of miRNAs, dysregulated epigenetic changes and defects in the biogenesis of miRNAs [97], and thus they control their biological functions. The crosstalk between circRNAs and miRNAs is the key to understand the role of circRNAs in carcinogenesis and other diseases [98].

Zheng et al., 2015 showed that circHIPK3 may act as a cell growth modulator in human cells since it binds to multiple miRNAs, as the tumor-suppressor miR-124 [38].

Zhong et al., 2016 showed that a circRNA originated from TCF25 promotes proliferation and migration in bladder cancer by sponging miR-103a-3p and miR-107 [99].

However, there are circRNAs that positively regulate many processes. For example, ciRS-7 positively regulates cell cycle sponging miR-7 [100] and circSLC30A7 promotes cell cycle progression by sponging miR-29 [101].

Figure 9. CircRNAs involved in the regulation of key cancer events (from Kristensen LS. Oncogene. 2018).

1.2.8 CircRNAs as putative biomarkers in cancers and therapeutic targets

Stability and long half-life in cells are the most important features that make circRNAs putative diagnostic and therapeutic biomarkers for cancers. In addition, circRNAs have been shown to be enriched and stable in exosomes and this, together with the correlation between abundance of tumor-derived exosomal circRNAs in serum of xenograft mice and tumor mass, suggests them as promising biomarkers for cancer detection [102]. Moreover, Memczak et al., 2015 observed that circRNAs could be easily detected in clinical standard blood

samples and are expressed at higher levels than the corresponding linear mRNA in human blood, suggesting that they may represent a new class of biomarkers for human disease [103]. Similarly, circRNAs were detected also in cell-free saliva [104]. Given the necessity of non-invasive biomarker detection for many diseases and cancers, circRNAs as biomarkers in human blood, saliva or other body fluids are very promising [26].

The control of the expression of natural circRNAs in specific tissues and cells of the human body might allow to greatly reduce side effects compared with those obtained with synthetic molecules, such as modified chemical drugs and RNA interference constructs, increasing the value of circRNAs. This aspect might open the doors to a new model of future gene therapy. Since one of the important functions of circRNAs is acting as sponge for miRNAs, artificial sponges could be designed and developed by studying endogenous circRNA sponge structures to regulate miRNA function in disease. Another advantage of the progress of circRNAs therapy is their potential low off-target effect that affects miRNAs and siRNAs due to their short lengths and restricts the clinical application of small molecule RNAs [78].

1.2.9 CircRNAs in human brain

As reported by Rybak-Wolf et al., 2015, data from ENCODE project and RNA sequencing of different brain regions, primary neurons, isolated synapses, as well as during neuronal differentiation showed that circRNAs are highly expressed in the brain and their expression is brain region-specific [32]. These researchers suggested also that circRNAs are not homogeneously distributed in the neural compartments, but they are mostly enriched in synapses. This finding, together with the high synaptic density in human cerebral cortex, could explain the higher number of circRNAs in human brain compared to mouse brain regions [32].

It was also observed that circRNA expression increases during neural differentiation, and this aspect often couples to the up-regulation of the linear host gene; however, there are some exception [32].

Surprisingly, circRNA expression is highly conserved in mouse and human. In particular, conserved circRNAs are flanked by introns with reverse complementary matches (RCMs) instead of the non-conserved ones. In addition, neural genes have long introns whose length is also highly conserved during evolution [32].

Song et al., 2016 developed a computational pipeline, named UROBORUS, aiming to identify genome-wide circRNAs based on total RNA-seq data [105]. By this pipeline they obtained the circRNA profile in gliomas. It has been observed a decrease of circRNA amount from normal to oligodendroglioma and GBM, suggesting that the abnormal condition in tumors leads to the failure of the back-splice events required for the formation of circRNAs. In addition, the alternative circularization for some parental gene in glioma tissue decreased with respect to normal tissue, suggesting that the alternative circRNA biogenesis is also altered in tumor conditions [105].

1.2.10 CircRNAs in gliomas

In recent years, many studies have shown that circRNAs are differentially expressed in gliomas and may play an important role in this aggressive cancer. In fact, they can regulate the occurrence, proliferation, migration, invasion and cell cycle progression in glioma, and some of them have been associated with glioma staging, thus they could be used as useful biomarkers for diagnosis and prognosis of gliomas [106]. Below is a list of many studies proposing circRNAs involved in different cellular events of GBM (Figure 10).

Has_circ_0000177 is up-regulated in glioma and may promote cell proliferation and invasion through the activation of Wnt pathway by sponging miR-638 [107]. These cellular processes are also promoted by has_circ_0046701, up-regulated in glioma, that sponges miR-142-3p and regulates the expression of its target ITGB8 [108].

Cell proliferation is also promoted by the has_circ_0007534 that is up-regulated in glioma and enhances ZIC5 expression by miR-761 repression, determining even the increase of cell migration [109], and by has_circ_0012129 [110] and circ-CFH that sponge miR-149 and regulate the AKT1 signaling pathway [111].

CircNFIX, up-regulated in glioma, may promote glioma progression through the up-regulation of NOTCH1 via the Notch signaling pathway by sponging miR-34a-5p [112]. The same pathway is regulated by circHIPK3 sponging miR-654 and, thus, promoting proliferation and invasion [113].

An increase of glioma cell apoptosis, proliferation and migration is caused by the upregulation of circNT5E, which acts as a sponge of miR-422a [114].

Circ-SHKBP1 is upregulated in glioma and it is involved in the regulation of the miR-544a/FOXP1 and miR-379/FOXP2 pathways modulating angiogenesis of U87MG glioma-exposed endothelial cells [115].

Yang et al., 2016 showed that silencing of cZNF292 circRNA inhibits glioma cell proliferation and cell cycle progression and thus, it suppresses tube formation [83].

Knockdown of has_circ_0008344 suppressed the proliferation, migration and invasion of GBM cells and promote tumor cell apoptosis [116].

CircRNA ITCH, down-regulated in glioma, acts as an oncogenic factor sponging miR-214 and regulating ITCH-Wnt/β-catenin pathway in favor of a decrease of proliferation, migration and invasion [117]. These same cellular functions are also performed by circ-TTBK2 that is associated with glioma malignancy and regulates miR-217/HNF1β/Derlin-1 pathway [118].

Barbagallo et al., 2016 demonstrated that CDR1-AS, the unique circRNA targeted and degraded by a miRNA (miR-671-5p), is involved in the miR-671-5p / CDR1-AS / CDR1 /VSNL1 axis which is functionally altered in GBM [119].

Circ-FBXW7 is down-regulated in glioma and encodes FBXW7 protein. The up-regulation of this protein inhibited proliferation and cell cycle acceleration [120]. Another circRNA encoding protein is circ-SHPRH, which encodes for SHPRH-146aa protein and plays a potential role as tumor suppressor [121], [122].

Has_circ_0001649 is down-regulated in glioma and its overexpression causes an inhibition of tumor growth and proliferation and promotes glioma cell apoptosis via Bcl-2/caspase-3 pathway [123].

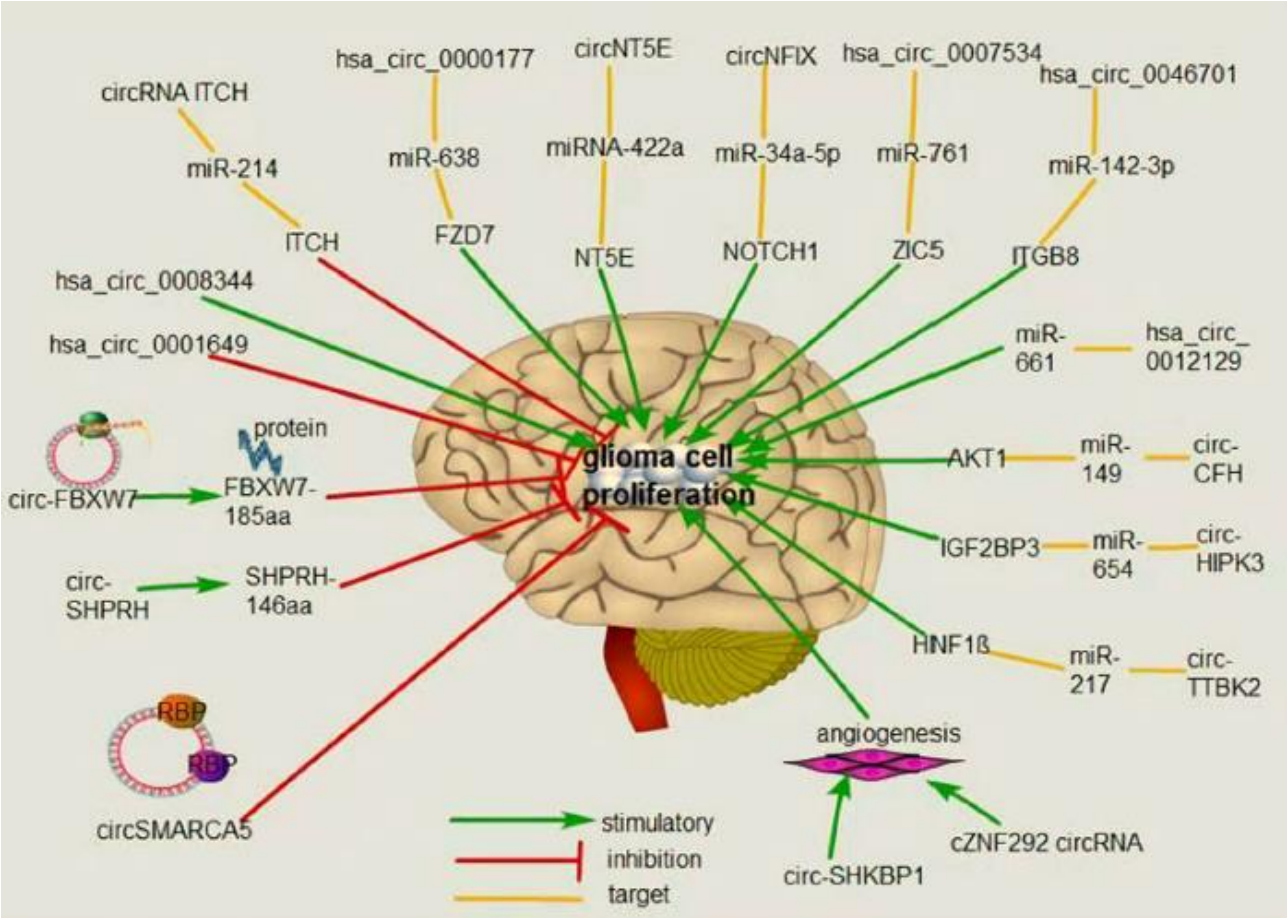

Figure 10. CircRNAs and glioma (from Hao Z. J Mol Neurosci. 2019).

Some circRNAs mentioned above, such as circ-FBXW7 and circ-SHPRH, could be used as prognostic biomarkers.

Since circRNAs have less off-target and side effects with respect to siRNAs [78], they may be considered advantageous targets of molecular therapies in glioma, such as hsa_circ_0001649, cZNF292, hsa_circ_0046701, circNT5E, and circ-TTBK2. In particular circ-SHKBP1 is of large interest in antiangiogenic therapy.

However, further studies will be needed to increase understanding of the molecular mechanisms of circRNAs in glioma pathogenesis and improve the knowledge of the involved regulatory network. Finally, a deeper study of the involvement of circRNAs in glioma pathogenesis could accelerate the clinical application of these molecules in the diagnosis and treatment of this mortal brain tumor [106].

1.3 Alternative splicing

The number of genes in the human genome is considerably lower than the number of known proteins. Gene are transcribed in pre-mRNA which contains exons and introns and is subjected to post-transcriptional modifications. One of these modifications is the pre-mRNA splicing that removes introns joining together the surrounding exons. The resulted mature mRNA can be exported from nucleus into the cytoplasm and translated into a protein. This type of splicing is named constitutive splicing and allows to process the immature transcript in order to obtain only one protein.

Genetic mutations can generate sequence alterations within the transcript and, thus, create new splice sites or enhancer sequences that lead to the recognition of new exons, named cryptic exons, or can alter splicing sites required for the recognition of exons leading to the exclusion of constitutive exons from the transcript. These types of altered splicing generate aberrant transcripts and contribute to disease [124].

However, pre-mRNA can be processed by a different mechanism of splicing, named alternative splicing. This is a post-transcriptional modification by which a single gene can generate multiple transcripts from the same mRNA precursor (Figure 11).

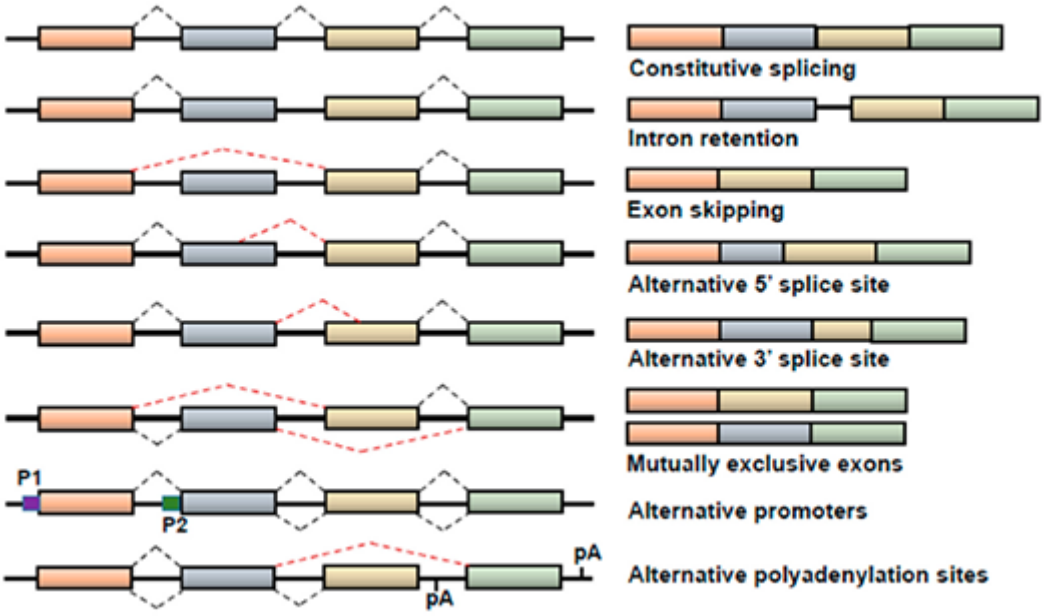

Figure 11. Models of alternative splicing (from Wang BD. Cancers. 2018).

Alternative splicing may be one of the aspects that support the proteome complexity. Alternative splicing allows the production of different protein isoforms which play various and even antagonistic roles. Regulation of alternative splicing depends on the cell type, developmental stage, sex, or external stimuli. Aberrant spliced isoforms are eliminated from the cell by quality control mechanism, such as cytoplasmatic degradation of mRNAs by the nonsense-mediated mRNAs decay (NMD) pathway. In some cases, aberrant spliced isoforms are not removed from cell and they are translated into proteins which may become endogenous antagonist to their normal counterparts, and, in specific conditions, the cause of several disease [125].

In addition, even though alternative splicing contributes to increase the genetic diversity of an organism, some events of disrupted alternative splicing are reported suggesting that it can contribute to disease development

and gravity. Since no mutations in *cis*-acting splicing elements within these genes have been identified, it has been hypothesized that these alterations could be caused by changes in *trans*-acting splicing factors regulation.

1.3.1 Cancer-associated alterations of splicing patterns

The splicing patterns of many genes, such as Ron, Rac1, fibronectin, fibroblast growth factor receptor, CD44, MDM2 and others, have been found to be altered in different tumors.

Ron is the tyrosine kinase receptor for macrophage stimulating protein that regulates a variety of cellular activities involved in the epithelial-to-mesenchymal transition (EMT). An alternatively spliced isoform of Ron (ΔRon) was identified in human gastric, breast and colon carcinomas and induces an invasive phenotype [126], [127].

An alternatively spliced isoform of the Rho-family GTPase Rac1, named Rac1b, is synthesized in an MMP-3-dependent manner leading an increase in cellular reactive oxygen species (ROS) and genomic instability that contribute to tumorigenesis.

MDMD2 and MDMX, regulators of p53, undergo alternative splicing and the resulted isoforms have been identified both in tumors and normal tissues [128], [129].

The characterization of GBM genome and transcriptome allowed the use of bioinformatic approaches in the investigation of alternative splicing in GBM. For example, Yu et al., 2014 identified 617 alternatively spliced genes in GBM using the exon-level expression profile data from the Gene Expression Omnibus (GEO) database, suggesting novel molecular markers for the diagnosis and treatment of GBM [130]. Sadeque et al.

2012 found that 2,477 genes alternative exon usage were significantly associated with patient survival in GBM [131].

The best characterized alterative splicing isoforms that give the major contribution to the GBM pathogenesis are the fibroblast growth factor receptor 1 (FGFR1), the glioma associated oncogene homolog 1 (Gli1), and the epidermal growth factor receptor (EGFR). Increased expression of FGFR1 in GBM is often accompanied by a shift in its splicing pattern, with FGFR1β as the predominant isoform. FGFR1β lacks exon 3 and shows an increased affinity for ligand due to the absence of one of the three extracellular NH2- terminal loops resulting in a cell-growth advantage and contributing to GBM malignancy [132]. The most common mutant form of EGFR associated with GBM is EGFRvIII, although other recurrent non-canonical EGFR transcript forms have been detected. Specifically, the EGFRvIII mutant is predicted to occur through the splice joining of exons 1-8 [133]. Its effects on glioma has been well characterized and it was suggested that it promotes tumorigenesis, stimulates GBM cell invasion, mediates chemo- and radio-therapy resistance in GBM, and contributes to GBM heterogeneity [134].

The glioma-associated oncogene homologue 1 (GLI1), highly upregulated in GBM [135], undergoes alternative splicing resulting in the expression of several different splice variants, including GLI1ΔN and tGLI1 [136]. GLI1ΔN behaves similarly to the full length GLI1 while tGLI1 (lacking exon 3 and part of exon 4) is absent in normal tissue and highly expressed in GBM and other cancers [137]. It was shown that tGLI1 binds to CD24 with a greater affinity than GLI1, increasing the migration and invasion of U87 GBM cells

[138]. In addition, expression of tGLI1 has been directly linked to enhanced tumor growth and vascularity of GBM xenografts [137].

To date, the study of altered spliceosomal mechanism suggests that spliceosomal mutations may offer new therapeutic opportunities. Since splicing factors can act as both oncoproteins and tumour suppressors, distinct therapeutic interventions are needed for treating cancers harboring different spliceosomal mutations. Possible therapeutic strategies may range from the possibility to restore normal splicing to exploit vulnerabilities to specifically target mutant cells [139].

In addition, the finding of cancer-specific alternatively spliced isoforms suggests their potential use as disease biomarkers, both at the mRNA and protein level [140]. Theoretically, a putative spliced form identified exclusively in cancer but not in healthy cells could be a candidate for a diagnostic, prognostic, or predictive biomarker.

1.4 RNA binding proteins

Splicing process can be regulated by *cis* elements (splicing regulatory elements, SREs) and *trans*-acting factors, such as RBPs.

RBPs are involved in all steps of post-transcriptional processes, guiding the fate and function of the transcripts within the cell and providing cellular homeostasis. They can interact with other proteins creating functional complexes named ribonucleoprotein complexes (RNPs) that are involved in the regulation of RNA splicing, polyadenylation, stability, localization, translation and degradation [141].

Changes in the expression levels and activity of RBPs can influence the number of multiple alterations in RNA processing, thus, contributing to the cancer phenotype. In fact, RBPs are involved in several hallmarks of cancer acting by different mechanisms and establishing intricate regulatory networks that regulate multiple cancer aspects. The alteration of these networks is associated with the improving of tumor progression and increased invasiveness [142]. RBPs can be dysregulated in many cancer types affecting the expression and function of oncoproteins and tumor-suppressor proteins.

Galante et al., 2009 studied the expression analysis of more than 300 RBPs in normal *vs*. tumor tissues showing that most of them are upregulated in brain tumors [143]. Kechavarzi and Janga, 2014, using TCGA data, analyzed about 850 RBPs in 16 different tissues from the Human BodyMap 2.0 Project, showing that RBPs are highly expressed with respect to other classes of genes, including regulators, such as transcription factors, suggesting a key role in regulation of gene expression. In addition, they found a set of RBPs strongly upregulated in at least two-thirds of the cancers profiled, related to gene expression, transcriptional deregulation and transport of biomolecules, cellular regulation, and proliferation [144].

One of the major players in RNA processing and cancer development is the polypyrimidine-tract-binding protein (PTB) that regulates both neurogenesis and brain tumor development [145]. PTB is more expressed in brain tumors than in cerebral tissues. In glioma the over expression of PTB alters the regulation of microtubule dynamics through MARK4 by increasing the production of the MARK4L isoform and enhancing cell proliferation [146].

Quaking protein (QKI) is one of the most frequently downregulated splicing factors in lung cancer. In normal conditions, it regulates the splicing of NUMB mRNA promoting the expression of a NUMB isoform that inhibits proliferation and, in addition, it negatively regulates Notch signaling pathway [147]. Likewise, RBM10 is a splicing factor downregulated in lung cancer that affects NUMB mRNA splicing and promotes the same effects mentioned above [148].

RBM4 promotes the pro-apoptotic isoform BCL-X_S of *BCL2L1* and opposes the pro-tumorigenic effects of SRSF1 on mTOR activation, acting as a tumor suppressor [139].

Matrix metalloproteases (MMPs) may be also implicated in splicing regulation. They are generally upregulated in cancers and regulate cell-cell and cell-substratum adhesion, promote tumor cell proliferation, invasion, angiogenesis and metastasis and may influence genomic surveillance, causing genomic instability [149].

However, the most common splicing factors that play an essential role in the splicing process regulation are the serine/arginine SR- rich proteins, named also SR proteins, and the heterogeneous ribonucleoproteins (hRNPs), that promote and repress splicing, respectively, in a sequence-specific manner [150].

HnRNPH is upregulated in gliomas and contributes to invasion, tumor cell survival and tumor growth. In GBM it regulates the switch in splicing of the death-domain adaptor protein insuloma–glucagonoma protein 20 (IG20) with downstream effect of the increase of survival and proliferation [151], [152]. hnRNPH regulates also the splicing of RON tyrosine kinase receptor, promoting the formation of a splicing variant that increases migration and invasion [151], [152]. The splicing factor hnRNPA2, upregulated in GBM cell lines, regulates splicing of several targets leading to the synthesis of anti-apoptotic isoforms [152]. The up-regulation of

hnRNPA1 regulates also the splicing of RON mRNA leading the formation of an oncogenic splicing isoform that is involved in tumor cell invasiveness and motility [152].

A deeper understanding of the functions of RBPs and their effects on their targets could reveal their potential role as targets in cancer therapy. Nevertheless, considering the ability of RBPs to create RNP networks that regulate the expression of transcripts encoding proteins involved in tumor processes, RBPs could be considered among the main actors of carcinogenesis [153].

1.4.1 Serine/arginine (SR)-rich protein family

The SR proteins were first discovered in *Drosophila* [154]. Their sequence characterization allowed the identification of a protein domain rich in arginine/serine (SR) residues. Later, SR proteins were discovered also in human cell lines and it was revealed the presence of an extended RS domain in addition to at least one RNA-binding domain of the RNA recognition motif (RRM)-type [155]. The classification of SR proteins is based on the presence of a phosphoepitope recognized by the monoclonal antibody mAn104 [156], their conservation during evolution and their involvement in splicing [157].

In humans, SR proteins are encoded by nine genes: SFRS1, SFRS2, SFRS3, SFRS4, SFRS5, SFRS6, SFRS7, SFRS9, SFRS11. All the members of human SR protein family, SF2/ASF, SC35, SRp20, SRp40, SRp55, SRp75, SRp30c, 9G8, and SRp54, share a common structure: one or two amino-terminal RNA-binding domain of the RNA recognition motif (RRM) that provide RNA-binding specificity, and a RS domain at the carboxyl terminus, showing a variable length, that participates in protein interactions with other RS-domain-containing

splicing factors [158]. RS domain can also function as a nuclear localization signal by regulating the interaction with the SR protein nuclear import receptor, transportin-SR [159].

1.4.2 SR protein functions

It is known that during alternative splicing *cis*-acting RNA sequence elements (splicing enhancers) allow exon inclusion by recruiting the splicing machinery. They are usually located within the regulated exon and are known as exonic splicing enhancers (ESEs) [160]. One or more SR proteins recognize ESEs and thus the splicing machinery is recruited to the adjacent intron [160]. SR proteins can regulate several steps of the splicing process [161] and need to be phosphorylated for efficient splice-site recognition and dephosphorylated for splicing catalysis [162].

However, some studies report that SR proteins can bind to introns acting as negative regulators of splicing. The best characterized example is shown during the adenovirus infection in which the SR protein SF2/ASF negatively regulates the splicing [163].

SR proteins do not regulate only the splicing, but they are also involved in the regulation of mRNA export thanks to their ability to shuttle continuously between the nucleus and the cytoplasm. To do this they require the phosphorylation of specific residues in the RS domain and the RNA-binding domain [164]. SR proteins can influence the translation in a directly or indirectly manner [165].

1.4.3 SR proteins in disease

Dysregulation of splicing process can promote the formation of protein isoforms that contribute to tumor development and progression and resistance to therapy. It has been demonstrated that a link between altered expression-activity of splicing factors, cancer-associated splicing and transformation exists [166], [167].

In this scenario, SR proteins as well as hnRNPs proteins and others RBPs, can act both as oncoproteins and tumor suppressors.

SR proteins, if overexpressed, can act as oncoproteins. For example, SRSF1 (also known as ASF/SF2) is up-regulated in different cancers, as lung, colon and breast cancers [168], [169]. SRSF1 and SRPK1 have been shown to influence the PI3K/AKT/mTOR and RAS/RAF/MEK/ERK pathways that are the most frequently altered signaling pathways in cancer [170], [171]. In particular, they affect the MAPK pathways activity in colon and breast cancer cells, and SRSF1 affects also the pathway PI3K/AKT/mTOR promoting epithelial cells transformation, motility, and anchorage-independent growth in breast cancer [168].

Another SR protein that acts as an oncoprotein when over-expressed is SRSF3 [172]. Another member of SR protein family is SRSF6: it is known to be a proto-oncogene and frequently over-expressed in human skin cancer [173] and acts as oncoprotein also in lung, colon and breast cancers [174]. SRSF6 is required for both tumor initiation and maintenance of lung and colon cancer cells [174]. It is also highly expressed in basal-cell carcinomas, squamous-cell carcinomas, and malignant melanomas [173].

SRSF10 positively affects cell proliferation and colony formation *in vitro* and increases tumorigenic capacity of colon cancer cells in mice [175].

However, splicing factor dysregulation affects not only the splicing process but also many other cellular processes, including genome integrity, epigenetic regulation, transcription, nuclear export, and translation-dependent mRNA decay [139].

1.4.4 Serine/arginine-rich splicing factor 1 (SRSF1 or ASF/SF2)

Among the above-mentioned SR proteins, the most studied is SRSF1. It was first identified as a splicing regulator and thanks to its ability to bind to different proteins it may regulate several cellular functions. In addition to splicing, SRSF1 regulates nonsense-mediated mRNA decay mechanism (NMD). Its ability to shuttle between nucleus and cytoplasm contributes to the plethora of function that it plays. In the shuttling process, SRSF1 acts as an adaptor that facilitates the export of spliced mRNAs to which it is bound. This mechanism is regulated by phosphorylation and dephosphorylation of SRSF1 [176].

SRSF1 is mainly localized in the cytoplasm where it is involved in the regulation of RNA metabolism, such as translation [177]. SRSF1 promotes also the processing of small non-coding RNAs [178]. It is involved in the regulation of others different biological processes, such as cell-cycle-stage-specific chromatin association and genomic stability maintenance [179]. It participates to the regulation of protein sumoylation [180] and the regulation of nucleolar stress pathway [181].

Despite its pleiotropic function, SRSF1 is the first splicing factor known to be directly involved in cancer: it is over-expressed in many different cancers and acts as a potent proto-oncogene [168].

SRSF1 autoregulates its own expression by a complex process that involves several mechanisms acting at different levels, such as alternative splicing and translation. SRSF1 translation may be negatively regulated at

different steps by different factors. This multi-level regulation probably helps to control the SRSF1 homeostasis. The relative contribution of each mechanism in the regulation of SRSF1 expression might vary in different tissues or physiological states. However, some regulator mechanisms may be altered in different tumors associated with SRSF1 upregulation [168].

It was shown that high levels of SRSF1 affect the alternative splicing pattern of its targets promoting the transformation process [168], such as the putative tumor suppressor BIN1, the transcription factor TEF-1, the kinase MNK2 and the ribosomal-protein kinase S6K1.

The over-expression of SRSF1 is positively regulated by the oncogenic transcription factor MYC and the splicing regulator Sam68 that promote oncogenic phenotypes, such as increased cell-proliferation, anchorage-independent growth, cell motility and invasion, and epithelial-mesenchymal transition (EMT) [182], [183].

The oncogenic potential of SRSF1 is due to its different functions. Its contribution to tumorigenesis is demonstrated by multiple SRSF1-regulated alternative splicing events. SRSF1 overexpression promotes the formation of the non-apoptotic isoforms of three genes encoding apoptosis regulators, such as BIN1, BCL2L11 (BIM) and MCL1 [168], [169], [184]. SRSF1 regulates also cell motility and invasion that promote the development of malignant tumors. For example, SRSF1 promotes the skipping of exon 11 during the splicing of RON producing a protein isoform that induces EMT and enhances cell motility [127]. Moreover, SRSF1 affects alternative splicing of factors involved in cellular signaling pathways, proliferation, and cell-cycle progression, such as *RPS6KB1* encoding the protein S6 kinase 1, a downstream effector in the PI3K/Akt/mTOR signaling pathway, and *MKNK2*, an effector of the MAPK/ERK pathway [185].

SRSF1 plays its oncogenic activity by activating the mTORC1 pathway whose inhibition by rapamycin treatment abolishes SRSF1 ability to transform cells both *in vitro* and *in vivo* [169], [168].

In addition to the changing of proliferation and survival processes that promote the transformation of cancer cells, another important aspect of cancer development is the cellular communication with the surrounding stroma. Cancer cells release angiogenic signals to endothelial cells, such as the vascular endothelial growth factor VEGFA whose expression is regulated by SRSF1 promoting angiogenesis. In fact, VEGFA alternative splicing is regulated by SRSF1 that promotes proximal splice site selection in c-terminal exon 8 of VEGF, forming proangiogenic isoforms [186], [187]. Moreover, concerning angiogenesis, SRSF1-mediated alternative splicing of both RON and TEAD-1 is also associated to increased expression of angiogenic growth factors [188].

The involvement of SRSF1 as well as other SR proteins in a plethora of biological processes and tumorigenesis underlines the importance of splicing in the regulation of gene expression and cellular homeostasis.

A deeper study about the mechanism through which SR proteins affect cellular transformation will be useful to propose new therapeutic strategies for cancer.

1.4.5 Serine/arginine-rich splicing factor 3 (SRSF3 or SRp20)

Serine/arginine-rich splicing factor 3 (SRSF3 or SRp20) is the smallest member of SR family and is involved in the regulation of alternative splicing [189], RNA export, [190], polyadenylation [191], protein translation [190], pri-miRNA processing [192], genome stability [179] and signal pathways [189]. Its overexpression is associated to cancer phenotype; in fact, an increased expression of SRSF3 is important for proliferation and

survival of cancer cells [172]. In addition, it is one of the major regulators in cell reprogramming of induced pluripotent stem cells, suggesting a possible role in the dedifferentiation process of carcinogenesis [193].

To date, only few endogenous RNA targets of SRSF3 have been identified in human cells. SRSF3 shows proto-oncogenic functions and it has been found upregulated in various types of cancer. SRSF3 regulates alternative splicing and gene expression of FoxM1 (forkhead box M1), PLK1 (polo-like kinase 1) and CDC25B (cell division cycle 25B) in osteosarcoma cells, and HPV16 (human papillomavirus type 16) E6 and E7 oncogenes in HPV16-positive cervical cancer cells. Its overexpression promotes cell cycle progression, anchorage-independent cell proliferation, tumor formation in nude mice and aerobic glycolysis and inhibits apoptosis and replicative senescence. Under physiological conditions, SRSF3 regulates the splicing of G6PD (Glucose-6-phosphate dehydrogenase) RNA in hepatocyte differentiation and metabolic function in liver [189]. SRSF3 regulates the expression of the other SR proteins [194] and modulates its own expression [195].

1.5 Angiogenesis

The formation of new blood-vessels from endothelial precursors and hematopoietic stem cells is a physiological event that occurs during embryogenesis and is called vasculogenesis. However, the formation of new blood vessels can occur also in not physiological conditions, and in this case new vessels are formed from pre-existing ones, and the process in known as angiogenesis [196]. These events play an essential role in the formation of a new vascular network that provides nutrients, oxygen and immune cells, and it is also important because it removes waste products.

Angiogenesis derives from an altered of balance between pro-angiogenic and anti-angiogenic factors that leads to the activation of genes that promote the growth of blood vessels, thus promoting angiogenesis [197].

Neovascularization, including tumor angiogenesis, comprises four steps: (1) the basement membrane in tissues is locally injured, with destruction and hypoxia as consequence; (2) endothelial cells are activated by angiogenic factors and migrate; (3) endothelial cells proliferate and stabilize the system; (4) angiogenic factors continue to influence the angiogenic event [198].

Angiogenesis is a fundamental step in the progression of cancer and it is stimulated when tumor cells need nutrients and oxygen. In cancer, it is regulated by both activator and inhibitor factors. However, an increase of activity of angiogenic activators alone is not enough for angiogenesis initiation, but it requires also the decrease of expression of negative regulators or inhibitors of vessel growth [196].

Several different proteins involved in angiogenesis have been identified, such as vascular endothelial growth factor (VEGF), basic fibroblast growth factor (bFGF), angiogenin, transforming growth factor (TGF)-α, TGF-β, tumor necrosis factor (TNF)-α, platelet-derived endothelial growth factor, granulocyte colony-stimulating factor, placental growth factor, interleukin-8, hepatocyte growth factor, and epidermal growth factor.

It has been demonstrated that angiogenic activators play an important role in growth and spread of tumors. Some of them were found to be expressed in several cancers and affect the prognosis of adenocarcinaomas, endometrium, ovary and stomach cancers. These findings suggest that the expression of angiogenic factors reflects the aggressiveness by which tumor cells spread out and it could be used to identify the high-risk patients with poor prognosis [196].

Based on the important role played by angiogenesis in cancer development, the discovery of angiogenic inhibitors could be an important therapeutic approach to reduce the mortality and morbidity from carcinomas.

1.5.1 Vascular endothelial growth factor (VEGF or VEGFA)

The VEGF platelet-derived growth factor (PDGF) family consists of different members: VEGF-A, VEGF-B, VEGF-C and VEGF-E. They act by the binding to their respective receptors and cause proliferation of blood vessels; VEGF-C and VEGFD , are also involved in lymphangiogenesis [198]. The most studied VEGF family member is the vascular endothelial growth factor-A or VEGFA.

VEGFA is a heparin-binding glycoprotein that shows several molecular isoforms which consist of 121, 145, 165, 183, 189, and 206 amino acids and derive from alternative splicing of the pre-mRNA [199]. Most of these isoforms bind to isolated heparin and heparin proteoglycans distributed on cellular surfaces and extracellular matrices and, thus, they may be released from cellular surfaces and extracellular matrices [200].

VEGFA is a specific mitogen for vascular endothelial cells and stimulate all the events involved in angiogenesis. It is also over-expressed in a variety of cancers and diseases and its expression is regulated by different growth factors, such as PDGF, FGF, EGF, TNF, IL-6 [201] and by hypoxia [202]. VEGFA exerts its function by binding to two homologous VEGF receptors, VEGF receptor-1 (Flt-1) and VEGF receptor-2 (KDR), expressed on vascular endothelial cells, leading to their dimerization, and, thus, the activation of signal transduction mediators. Although VEGF receptor-1 is bound by VEGF with high affinity, it modulates availability of VEGF for binding to VEGF receptor-2, that induces an efficient endothelial cell response [203].

In addition to the induction of angiogenesis, VEGF induces also a non-mitogenic response, avoiding the apoptosis of endothelial cells in new-formed vessels and maintaining the viability of immature vasculature [204]. It increases also the vascular permeability in favor of endothelial cell growth [204]. Finally, VEGF induces chemotaxis, and the expression of plasminogen activators and collagenases in endothelial cells. Based on these different functions, it appears clear that VEGF is a key mediator of angiogenesis. However, it can also influence the immune system by several different mechanisms [198].

Since VEGF is important in the normal physiological angiogenesis, alteration of its expression may be involved in important disease processes and cancers. VEGF was identified as the most important tumor angiogenic factor. In fact, the vascular support, especially for the supply of oxygen and nutrients, is fundamental for tumor growth [198].

VEGF plays a central role in tumor angiogenesis, stimulating the formation of new blood vessels from pre-existent capillaries and allowing tumors to get the oxygen and nutrients needed. There are a lot of evidences proving the regulation of VEGF expression by hypoxia inducible factor-1α (HIF-1α) [199].

Several studies have shown that VEGF as well as other members of the family have been identified in different tumor types. VEGF is over-expressed in bladder cancer and a paracrine system, including VEGF and flt-1 receptor, exists between the bladder cancer cells and the adjacent endothelial cells that regulate angiogenesis in this tumor. In addition, the expression of VEGF receptor-2 is correlated with features, such as disease stage and invasive phenotype, that promote the progression of bladder cancer [205], [206].

In breast cancer it was observed that high expression of VEGF and its receptors are associated with a worse outcome and may be considered as prognostic markers in invasive breast carcinoma [207], [208]. Takahashi Y et al., 1995 showed that VEGF is an important angiogenic factor in primary and metastatic human colon cancer; its expression and vessel counts are correlated with vascularity, metastasis, and proliferation of human colon cancer and it may allow to predict risk for metastasis in CRC patients [209]. High expression of VEGF is also associated with the short survival rates in patients with gastric cancer [210] as well as in head and neck squamous cell carcinoma [211].

VEGF and VEGFR expression are associated with a poor prognosis via autocrine and paracrine growth stimulation of non-small-cell lung cancer. Moreover, tumors expressing both flt-1 and KDR VEGF receptors may have greater malignant potential and positively correlate with a poor prognosis [212], [213].

The activation of VEGF-VEGFR system may play a crucial role in the regulation of human malignant mesothelioma growth. VEGF production could be involved in patient survival, not only by promoting angiogenesis but also by directly stimulating tumor growth [214].

VEGF could be used as a prognostic marker in early-stage prostate tumors and the VEGF-Flk-1 system may play a crucial role in this tumor development and progression [215], [216].

1.5.2 VEGFA in GBM

Gliomas show a high degree of vascular proliferation. New-formed blood vessels in brain tumors are characterized by an altered blood-brain barrier that contributes to the pathogenesis of tumor-associated edema.

The microvascular proliferation is one of the features of GBM that allows to distinguish it from other glial tumors; it requires several mechanisms, such as the sprouting of capillaries from pre-existing blood vessels by endothelial proliferation, which depends on the hypoxia, typical of the tumor core. Another aspect that contributes to the new blood-vessel formation is the releasing of angiogenic factors from tumor cells, that recruit cells involved in vessels formation.

It appears clear that angiogenesis plays a fundamental role in gliomas and, recently, evidence is increasing about the important role of the angiogenic factor VEGF in the progression of these brain tumors.

It has been suggested that potential autocrine role of the VEGF-VEGFR2 (KDR) system has a crucial autocrine function that contributes to malignant astrocytoma growth and radioresistance. This hypothesis supports the idea of the use of this signaling cascade as a therapeutic target, possibly in combination with radiotherapy [217]. However, the direct inhibition of VEGFR2 kinase may block the VEGF-VEGFR2-NRP1 pathway and propose a GBM therapeutic strategy to complement the standard approach [218].

Karl H. Plate et al. (1993) suggested that a paracrine mechanism involving VEGF and its receptor, flt-1, is involved in tumor angiogenesis of human gliomas [219]. They also demonstrated that the most important factor that promotes the vascularization in gliomas is VEGF, and hypoxia is the principle cause of VEGF up-regulation in GBM cell *in vivo* models [220].

Human GBM stem-like cells (GBSCs) are important for the initiation, propagation, and recurrence of GBM [221]. Their proliferation is most probably mainly regulated by VEGF in a dose-dependent manner binding to its receptor VEGFR2; in contrast, VEGFR1 decreases the positive effect of VEGF in the proliferation of

GBSCs. In addition, although hypoxia regulates VEGF expression, it affects GBSC proliferation independently on the presence of VEGF [222]. These data are supported by the finding that high levels of VEGF, produced by CD133+ human glioblastoma cells, may be involved in their tumor-initiating capacity [223]. Increased levels of VEGF in GBM accelerate vascular proliferation rate and increase the malignant degree of the disease [224].

Anti-VEGF and VEGFR2 inhibitors are commonly used to target the VEGF-VEGFR2 signaling cascade in glioma patients. However, these two strategies have been disappointing [225], [226].

1.5.3 Anti-angiogenesis therapeutic targets

The importance of VEGF and its receptors in angiogenic events that occur in many solid tumors, such as breast cancer [227], colon cancer [228], hepatoma [229], bladder cancer [230], gastric cancer [231], and prostate cancer [232], provides an interesting chance for the development of new therapeutic approaches, particularly for the most aggressive cancers. These approaches could have the potential to promote regression of the tumor and improve the response to standard chemotherapy and radiation treatments. Inhibition of secretion of endogenous tumor VEGF, neutralization of VEGF in the microcirculation and prevention of VEGF binding and subsequent signal transduction, could be potential therapeutic approaches for blocking VEGF effects.

Several studies aimed to understand how to disrupt tumor angiogenesis and growth by anti-VEGF-A and anti-VEGFR-2 monoclonal antibodies (mAbs) or VEGFRs small molecule tyrosine kinase inhibitors. In fact, molecules that selectively target VEGFR-1 may inhibit tumor vascularization and invasion/metastasis and may produce lower systemic toxicity than agents targeting VEGF-A or VEGFR-2, which cause negative effects

due to inhibition of physiological angiogenesis [233]. For example, devascularization caused by anti-VEGF therapy increases tumor hypoxia, and this hypoxia mediates resistance to antiangiogenic therapy [222].

It has been shown that the inhibition of VEGF may result in the remodeling of the tumor vasculature, leading to decrease in tumor perfusion, microvascular density, vascular volume and interstitial fluid pressure in patients with colorectal cancer [234], allowing the effective delivery of chemotherapy to the tumor. Preclinical studies have shown that anti-VEGF therapy is more efficient in tumor growth inhibition if paired with chemotherapy [234]. Anti-VEGF therapy could have a wide range of application because progression of all solid tumor types is dependent on VEGF, suggesting that VEGF can be an important therapeutic target in the treatment of cancer.

It is known that GBM is characterized by a high degree of vascular proliferation mediated by VEGF, therefore new targeted anti-angiogenic therapies, such as the monoclonal anti-VEGF-A antibody bevacizumab, have proven effects in attenuating tumor (neo)angiogenesis of this aggressive brain cancer [235].

However, anti-VEGF-A treatment effects are transient. In fact, bevacizumab improves progression-free survival of GBM patients, but it has not good effects on overall patient survival because during GBM progression, and tumors in general, patients develop bevacizumab resistance [236], [237].

2. AIM OF THE PROJECT

Considering that circRNAs appear to be very interesting molecules thanks to their peculiar features, derived from their structure and their potential regulatory functions, and given their importance in human brain, this thesis focused on the study of their involvement in GBM cancer.

CircRNA functions are still object of debate, however this project aimed to give a contribution to the understanding of their functional role in the regulation of splicing in GBM and provide a new potential and promising molecular biomarker in this disease.

3. MATERIALS AND METHODS

3.1 Collection of GBM specimens

GBM biopsies and normal brain parenchyma tissues were collected from Azienda Ospedaliero-Universitaria "Policlinico-Vittorio Emanuele", Catania, Italy, thanks to the collaboration with the Department of Neurosurgery and the Department of Pathological Anatomy.

Each fragment obtained during neurosurgery was divided in two portions: one portion was used for fixation and tissue embedded into paraffin, and the other one was collected in sterile tubes on ice, washed in cold sterile PBS to eliminate any blood residue and stored at -80 °C until use.

Only biopsies from patients with a confirmed pathological diagnosis of GBM (according to the 2007 WHO classification) were considered suitable for the study.

Each tumor sample contained more than 90% of cancer tissue. Normal brain parenchyma was obtained, when possible, from a non-eloquent region of the brain adjacent to the tumor that resulted negative to 5-aminolevulinic acid (5-ALA) fluorescence during surgery. In addition, microscopy analysis confirmed the absence of infiltration of cancer cells within normal brain parenchyma.

Commercially available FirstChoice® Human Brain Reference RNA (Ambion, Austin, TX, USA) and Human Astrocyte Total RNA (ScienCell Research Laboratories®, San Diego, CA, USA) were used as healthy tissues.

Age, sex and clinical features of the analyzed samples of the two different cohorts used in the studies are reported in Table 1.

Type of Samples	N	Mean Age (Years-StdDev)	Sex M	Sex F	Mean OS (Months-StdDev)	Mean PFS (Months-StdDev)
Training set (Fresh-frozen biopsies)	10	60.5 ± 12.1	5	5	19.1 ± 7.2	
Test set (FFPE biopsies)	56	62 ± 12.7	33	23	17 ± 14.2	
FFPE Normal Brain Parenchyma	7	60.4 ± 11.1	2	5		
Fresh-frozen GBM biopsies	31	63.6 ± 10.9	15	16	15 ± 8.2	13.8 ± 8.7
Fresh-frozen unaffected brain parenchyma	20	64 ± 10.3	8	12		
FirstChoice® Human Brain Reference Total RNA	1 (commercially available)	68.3 ± 15	13	10		

Table 1. Features of samples included in the study.

3.2 GBM cell lines

A172 human glioblastoma cells were grown in DMEM with 4.5 g/L glucose with the addition of 10% FBS, 2 mM L-Glutamine, 1 mM sodium pyruvate; CAS-1 and SNB-19 cells were grown in DMEM with 1 g/L glucose supplemented with 10% FBS, 2 mM L-Glutamine; DBTRG cells were grown in RPMI 1640 with L-Glutamine, supplemented with 10% FBS; U87-MG cells were grown in DMEM with 1 g/L glucose supplemented with 10% FBS, 1% non-essential amino acids 1 mM sodium pyruvate.

3.3 Immunohistochemistry: percentage of GFAP+ cells in GBM biopsies

Sections were dewaxed in xylene, hydrated using graded ethanols and incubated for 30 min in 0.3% H2O2/methanol to quench endogenous peroxidase activity, then rinsed for 20 min with PBS. The sections were heated (5 min x 3) in capped polypropylene slide-holders with citrate buffer (10 mM citric acid, 0.05% Tween 20, pH 6.0), using a microwave oven (750 W) to unmask antigenic sites. The blocking step was

performed before application of the primary antibody with 5% BSA in PBS for 1 h in a humid chamber. BSA was used as a blocking agent to prevent non-specific binding of the antibody. Then, the sections were incubated overnight at 4 °C with rabbit polyclonal anti-GFAP antibody (DAKO, Glostrup, Denmark), diluted 1:7000 in PBS. The secondary antibody, biotinylated anti-rabbit antibody, was applied for 30 min at *25*°C, followed by the avidin–biotin–peroxidase complex (Vector Laboratories, Burlingame, CA, USA) for a further 30 min at room temperature. The immunoreaction was visualized by incubating the sections for 4 min in a 0.1% 3,3′-diaminobenzidine (DAB) and 0.02% hydrogen peroxide solution (DAB substrate kit, Vector Laboratories, CA, USA). The sections were lightly counterstained with Mayer's hematoxylin (Histolab Products AB, Göteborg, Sweden) mounted in GVA mountant (Zymed Laboratories, San Francisco, CA, USA) and observed with a Zeiss Axioplan light microscope (Carl Zeiss, Oberkochen, Germany) [238].

GFAP-positive (GFAP+) cells percentage was evaluated in the highest immunoreactivity fields. It was determined by dividing the number of positive staining cells by 1000 cells. Cells were considered positive if there was any cytoplasmic staining present [238].

3.4 Circular RNA selection

After a detailed review of literature, circRNAs were selected based on their association with at least one of the following biological processes: (i) regulation of neuronal differentiation; (ii) epithelial-to-mesenchymal transition (EMT); and (iii) cell proliferation. All selected circRNA transcripts had to be expressed and enriched in human brain, according to RNA Seq data deposited in circBase (*http://www.circbase.org/*) (Table 2).

#	Candidate circRNA (circBase ID)	Parental Gene Symbol	Known modulation or function of circRNA expression in specific cell context	Source (PMID)
1	hsa_circ_0028270	ATXN2	Upregulated during EMT. This circRNA is also highly expressed in several SNC districts (see PMID: 25921068)	25768908
2	hsa_circ_0008702	GNB1	Downregulated during EMT. This circRNA is also highly expressed in several SNC districts (see PMID: 25921068)	25768908
3	hsa_circ_0000284	HIPK3	Involved in cell growth. Highly expressed in normal Brain	27050392
4	hsa_circ_0008002	POLE2	Upregulated during EMT. This circRNA is also highly expressed in several SNC districts (see PMID: 25921068)	25768908
5	hsa_circ_0132250	RIMS1	Downregulated in GBM vs Normal Brain (other dataset)	26873924
6	hsa_circ_0099634	Rmst	LncRNA Rmst (host gene of the same name circ_Rmst) regulates neuronal differentiation in mouse	25921068
7	hsa_circ_0054598	RTN4	Upregulated during neuronal differentiation both in humans and mice	25921068
8	hsa_circ_0001649	SHPRH	Upregulated during EMT. This circRNA is also highly expressed in several SNC districts (see PMID: 25921068).	25768908
9	hsa_circ_0003694	SMAD2	Upregulated during EMT. This circRNA is also highly expressed in several SNC districts (see PMID: 25921068)	25768908
10	hsa_circ_0001445	SMARCA 5	Upregulated during EMT. This circRNA is also highly expressed in several SNC districts (see PMID: 25921068)	25768908
11	hsa_circ_0073237	VCAN	Upregulated in GBM vs Normal Brain (other dataset)	26873924
12	hsa_circ_0004383	ZNF292	Upregulated in HUVEC under hypoxia. Its silencing reduces endothelial cell proliferation and suppresses tube formation by inhibiting glioma cell proliferation and cell cycle progression in human glioma U87MG and U251 cells	26377962; 27613831

Table 2. List of the candidate circular RNAs (from Barbagallo D. Int J Mol Sci. 2018)

3.5 Primer design for the detection of circRNAs and their linear counterparts

Primer design was performed by using NCBI primer blast tool (*https://www.ncbi.nlm.nih.gov/tools/primer-blast/*). For the detection of linear isoforms convergent primers were designed; divergent primers were used for the detection of circRNAs (Table 3). Primer pairs were tested *in silico* and all those primer pairs that recognized more than one circular isoform produced by the same host gene were discarded.

Primer ID	Sequence
GAPDH Fw	GTCAGCCGCATCTTCTTTTG
GAPDH Rev	GCGCCCAATACGACCAAATC
hsa_circ_ATXN2 Fw	TCAGACTTTGTTGTGGTACAGT
hsa_circ_ATXN2 Rev	TTGGAGCCCTCTTTTTGCAT
hsa_circ_GNB1 Fw	GGGCACAGACTCCAGACAAAT
hsa_circ_GNB1 Rev	TGTGAGATCTTAATTCAGAAGGGC
hsa_circ_HIPK3 Fw	GGTCGGCCAGTCATGTATCA
hsa_circ_HIPK3 Rev	AGGCCATACCTGTAGTACCGA
hsa_circ_POLE2 Fw	AGTACTACTAGAGAGCACGTTTTCA
hsa_circ_POLE2 Rev	CTGAATTGTACACAAAGCGTGGA
hsa_circ_RIMS1 Fw	AGCCTTAGTGCCAAAGTGGT
hsa_circ_RIMS1 Rev	TAAGCTTGCTGTTTGACTAAGCTG
hsa_circ_RMST Fw	GGGCTAGTTGAGGAATGGCT
hsa_circ_RMST Rev	ACTCACTCCATCATCCTGAGA
hsa_circ_RTN4 Fw	TGAGTAAAACTTCAGATGAGACCCT
hsa_circ_RTN4 Rev	GCAGAGGAGCGTATCACAGG
hsa_circ_SHPRH Fw	AAACTGCTGAGAGAAGGGCAG
hsa_circ_SHPRH Rev	TCATCAGAGTTCTGACCACAGC
hsa_circ_SMAD2 Fw	TGAAGATGGAGAAACAAGTGACC
hsa_circ_SMAD2 Rev	AGAGCAAGTGCTGTGTCCATA
hsa_circ_SMARCA5 Fw	ACAATGGATACAGAGTCAAGTGTT
hsa_circ_SMARCA5 Rev	CCACAAGCCTCCCTTTTGTTTT
hsa_circ_VCAN Fw	TGAAACAGATTTCCTGATTGGCA
hsa_circ_VCAN Rev	TCATTCGACCTGGTAAATAGATTGC
hsa_circ_ZNF292 Fw	GGGTGTGGAAAAACCCGGTA
hsa_circ_ZNF292 Rev	TCTGGGGCAAGCCTTTATCC
Linear_SMARCA5 Fw	ATGGGTACCAACACTTAGATCTGT
Linear_SMARCA5 Rev	AACGTCTCTGACAAAAGCAGC
SMARCA5 Probe	TGCAGTCTTCTTTGCACCTCTTTCCAAAATACCATCG ATATCTTCATCAGTGATCTCACT

SRSF3 Ex4 (NR_036610.1) Fw	TCGTCGCCCTCGAGATGAT
SRSF3 Ex4 (NR_036610.1) Rev	GTGGTGAGAAGAGACATGATGGT
SRSF3 No Ex4 (NM_003017.4) Fw	CGTCGCAGATCTCCAAGAAGG
SRSF3 No Ex4 (NM_003017.4) Rev	CCTATCTCTAGAAAGGGACCTGC
TBP Fw	ACTTGACCTAAAGACCATTGCA
TBP Rev	GGCTCTCTTATCCTCATGATTACC

Table 3. Primer sequences (from Barbagallo D. Int J Mol Sci. 2018).

3.6 RNA isolation and purification

Total RNA from fresh-frozen and FFPE biopsies was extracted by using TRIzol® and RecoverAll® kits (Thermo Fisher Scientific), respectively. Briefly, after homogenizing the fresh-frozen sample mixed with TRIzol® Reagent, chloroform was added to allow the separation of the homogenate into a clear upper aqueous layer (containing RNA), an interphase, and a lower organic layer (containing DNA and proteins). Isopropanol allowed the precipitation of RNA from the aqueous layer. The precipitated RNA was washed to remove impurities and then resuspended to be used in downstream experiments.

FFPE samples were incubated in xylene at elevated temperatures to solubilize and remove paraffin from the tissue, then washed in alcohol solutions to remove the xylene. The deparaffinized samples were subjected to a protease treatment to digest proteins covalently bound to RNA. Finally, RNA was purified by capture on a glass-fiber filter, washed and eluted.

Total RNA was quantified both through spectrophotometer and Qubit™ fluorometer (Thermo Fisher Scientific).

3.7 Vector construction

pcDNA3_circSMARCA5 vector was constructed by the insertion of a PCR amplified fragment of the human genome 1450 bp long into the pcDNA3 backbone. It consisted of SMARCA5's exons 15 and 16 (the two exons that circularizing generate circSMARCA5), the intron between them and 440 bp upstream and 546 bp downstream exons 15 and 16, respectively. BamHI and ApaI were used to perform the digestion of both PCR product and vector (Figure 12)

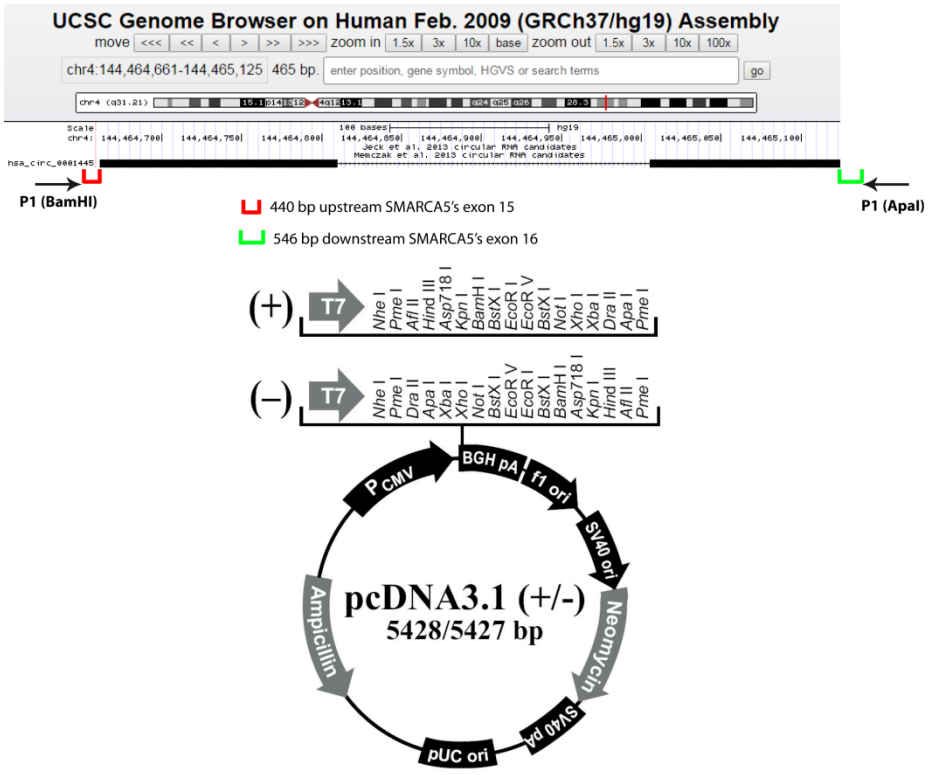

Figure 12. Schema of circSMARCA5's cloning into the pcDNA3 expression vector (from Barbagallo D. Int J Mol Sci. 2018).

3.8 Transfection of GBM cell line

U87-MG cell lines were seeded at a density of 6 x 10^5 per well in 6 wells plate and cultured for 24 hours. Cells were transfected with Lipofectamine 2000 (Thermo Fisher Scientific, Waltham, MA, USA), according to supplier's protocol. Transfection efficiencies of more than 80% were achieved.

3.9 Northern Analysis

Ten micrograms of total RNA were loaded on a 1.2% denaturing agarose gel. RNA was transferred to Amersham hybond-N+ membranes (GE Healthcare). The membrane was hybridized with (32P)-labelled probes in Church buffer (0.5 M NaPO4, 7% SDS, 1 mM EDTA, 1% BSA, pH 7.5) at 55°C and washed in 2x SSC (300 mM NaCl, 30 mM Na-citrate, pH 7.0) with 0.1% SDS at 50°C. The membrane was exposed on phosphorimager screens and analyzed using Quantity One or Image Lab software (Bio Rad). SMARCA5 probe sequence used in northern blot assay is reported in Table 3.

3.10 qRT PCR

Total RNA was reverse-transcribed in cDNA and amplified by using gene-specific primers either in two steps, by MLV-RT (Thermo Fisher Scientific) using random hexamer primers and LightCycler® 480 SYBR Green I Master (Roche Molecular Systems, Inc., Pleasanton, CA, USA), or in one step, using RNA-to-Ct™ 1-Step Kit (Thermo Fisher Scientific). Quantitative PCR was performed on either 7900HT Fast Real-Time PCR System (Thermo Fisher Scientific) or LightCycler 480 (Roche Molecular Systems, Inc.). TBP and GAPDH were used as endogenous control genes. The relative amount of gene expression and the fold change for each transcript were calculated using the 2^-DDCt method.

3.11 Cell migration and viability assay

Cell migration was assessed using Oris™ Cell Migration Assay (Platypus Technologies, Madison, WI, USA). Cells were seeded at a density of 3.5 x 10^4 per well in 96-well plates with the detection mask attached at the bottom and the stoppers placed. Twenty-four hours after seeding, cells were transfected and grown for other 24 h in a serum free medium. After this time, the stoppers were removed, and migration rate was revealed in the detection zone after 24 h by staining the cells with Hoechst® 33342 at a final concentration of 5 µg/mL. Migrated cells were quantified through ImageJ software (*https://imagej.nih.gov/ij/index.html*).

Cell viability was measured using MTT (3(4,5-dimethylthiazol-2-yl)2,5-diphenyl-tetrazoliumbromide. Cells were seeded at a density of 2.4 x 10^4 per well in a 96 wells plate, grown for 24 h and then transfected for other 24 h. Viability was assessed reading absorbance at 580 nm 24 h, 48 h, 72 h and 96 h after transfection.

3.12 Prediction analysis of circSMARCA5 interactions

circInteractome (*https://circinteractome.nia.nih.gov/index.html*) and starBase (*http://starbase.sysu.edu.cn/*) online tools were used to predict interactions between circSMARCA5 and miRNAs.

circSMARCA5 FASTA sequence was given as input to RBPMap [239], ATTRACT (*https://attract.cnic.es/index*) and *cat*Rapid (*http://service.tartaglialab.com/page/catrapid_group*) online tools, in order to carry out the prediction analysis of the RBPs that potentially bind to circSMARCA5 sequence. Based on the results of the prediction analysis of RBPs-circSMARCA5 binding, a literature review allowed to select known targets of the candidate RBPs, and the target with the highest clinical interest in GBM was chosen for further analyses.

3.13 Primer sequence design to detect VEGFA transcripts

VEGFA was selected among the targets of the predicted RBP interacting with circSMARCA5. To test the expression of VEGFA and its splicing variants, primer sequences were designed. Primers which were common to all the human VEGFA isoforms annotated in Gene NCBI database (*https://www.ncbi.nlm.nih.gov/gene/7422*) were used to amplify VEGFAtot. More in detail, forward and reverse primer were designed on exons 2 and 3, respectively. To amplify VEGFA splicing variants (Iso8a or Iso8b) a common forward primer recognized both isoforms was used, while specific reverse primers to each isoform were designed (Table 4).

Transcript	Fw primer	Rev primer
SRSF1	CCATCCAGGCGGTCTGAAAA	ACCTGCTTCACGCATGTGAT
SRSF3	TCGTCGCCCTCGAGATGAT	GTGGTGAGAAGAGACATGATGGT
VEGFA Iso8A	TTCCTGCAAAAACACAGACTCGC	TCACCGCCTCGGCTTGTCACAT
VEGFA Iso8B	TTCCTGCAAAAACACAGACTCGC	TCAGTCTTTCCTGGTGAGAGATCTGCA
VEGFAtot	GCACCCATGGCAGAAGG	CTCGATTGGATGGCAGTAGCT
GAPDH	GTCAGCCGCATCTTCTTTTG	GCGCCCAATACGACCAAATC

Table 4. Primer sequences (from Barbagallo D. Cancers. 2019).

3.14 RNA Immunoprecipitation (RIP)

Cells were seeded in 10 cm dishes at a density of 3.6 x 10^6 and cultured for 72 hours. Twenty microliters of Dynabeads™ Protein A/G (ThermoFischer Scientific) were firstly equilibrated with lysis buffer and then incubated with 5 µg of mouse monoclonal IgG2b antibody against SRSF1 (Santa Cruz Biotechnology, Inc., Heidelberg, Germany) or isotype control IgG from mouse (negative control) (Santa Cruz Biotechnology, Inc.)

for 2 h at 4°C. Ten percent of the volume of U87-MG lysate supernatant was collected before immunoprecipitation and used as Input for RNA and protein analyses, respectively. The remaining supernatant was divided in two aliquots that were incubated either with monoclonal IgG2b antibody against SRSF1 or isotype control IgG for 2 h at 4°C. After washing, ten percent of the beads were used for western analysis of either SRSF1 or IgG pulled-down. The remaining beads were resuspended in 1 mL of Trizol for RNA extraction. Western analysis was performed on Input, SRSF1- and IgG-IPed samples in order to verify the specificity of immunoprecipitation.

3.15 Protein Extraction

Proteins were extracted from biopsies by using RIPA buffer (Abcam, Cambridge, UK) with the addition of protease and phosphatase inhibitors. Lysis was supported by mechanical pressure using a steel pestle and ultrasounds using a sonicator. Proteins extracted were quantified by Qubit™ fluorometer (ThermoFisher Scientific).

Human Brain Cerebral Cortex Protein Medley (Takara Clontech®, Mountain View, CA, USA) was used as further unaffected control

3.16 Immunoblotting

After quantification through Qubit™ fluorometer (Thermo Fisher Scientific), proteins were subjected to SDS-PAGE. 30 ug of protein lysate were added with 10 ul LDS Sample Buffer 4X, 4 ul of 10x Sample Reducing Agent (Thermo Fisher Scientific) and water up to a final volume of 40 ul. Samples were boiled at 95°C for five minutes to allow protein denaturation. Denatured samples and ladder (SeeBlue™ Plus2 Pre-stained

Protein Standard, Life Technologies) were loaded in a precast polyacrylamide gel (Bolt 4-12% Bis-Tris Plus, Thermo Fisher Scientific). Resolved proteins were transferred, through a transfer system (iBlot® Gel Transfer Device, Thermo Fisher Scientific), to a nitrocellulose membrane and immunoblotted with primary antibodies against SRSF1 (mouse monoclonal antibody from Santa Cruz Biotechnology, Inc., Cat. n. sc-73026) or ACTB (rabbit polyclonal antibody from Abcam, Cat. n. ab16039). Secondary antibodies HRP-conjugated anti-mouse (for SRSF1) or anti-rabbit (for ACTB) (Santa Cruz Biotechnology, Inc, Cat. n. sc-516102 and sc-2004, respectively) were used for chemiluminescent detection with the ECL method (Pierce™ ECL Western Blotting Substrate, Thermo Fisher Scientific). ImageJ software (*https://imagej.nih.gov/ij/index.html*) was used to quantify gel bands.

3.17 Immunostaining for CD31

For each case, all Hematoxylin and Eosin (H&E) stained sections were assessed by two pathologists and one representative sample was identified. Slides were cut at 4-5 µm, dried, deparaffinized and rehydrated. Then, sections were incubated for 30 min at 4°C with mouse monoclonal anti-Human CD31, Endothelial Cell antibody (JC70A, Dako Corporation, Glostrup, Denmark), diluted 1/40 in PBS (Sigma, Milan, Italy). The biotinylated anti-rabbit secondary antibody was applied for 30 min at 20°C, followed by the avidin-biotin-peroxidase complex (Vector Laboratories, Burlin1701519 game, CA, USA) for a further 30 min at 20°C. The immunoreaction was visualized by incubating the sections for 4 min in a diaminobenzidine (DAB) and 0.02% hydrogen peroxide solution (DAB substrate kit, Vector Laboratories, CA, USA).

3.18 Assessment of blood vascular microvessel density (MVD)

Immunohistochemical sections were observed with a Zeiss Axioplan light microscope (CarlZeiss, Oberkochen, Germany). In order to perform MVD assessment, vascular hotspots were identified on CD31 sections by a light microscope at 4x and 10x magnifications. MVD was evaluated as the total number of vessels per mm^2 with a conversion factor of 1 mm^2 equaling 4 high power fields (HPFs) at 40x magnification of highest vascular densities. Areas with ≥50 of viable tumor cells were counted; tissues with extensive necrosis, hemorrhage and desmoplasia were excluded. Every single stained endothelial cell and each lumen for long branched vessels and glomeruloid tufts were counted. Moreover, small clusters of ≥2 staining endothelial cells within the same vessel was counted as one vascular structure.

3.19 Identification of inverted sequences within introns flanking circSMARCA5's exons 15 and 16 by *in silico* analysis

To investigate if circSMARCA5 biogenesis may be regulated by a base-pairing mechanism, its sequence was scanned for the intronic sequences flanking both exons 15 and 16. Briefly, human circSMARCA5 genomic sequence was obtained from UCSC Genome Browser (*https://genome.ucsc.edu/*). A window of 1 kb upstream and 1 kb downstream exons 15 and 16, respectively, was given as input to EMBOSS einverted tool (*http://emboss.bioinformatics.nl/ cgi-bin/emboss/einverted*) together with circSMARCA5 genomic sequence.

3.20 Conservation analysis among species of circSMARCA5's inverted sequences

To evaluate if inverted sequences flanking exons 15 and 16 of circSMARCA5 are conserved among species, UCSC and ClustalW2 (*http://www.genome.jp/tools-bin/clustalw*) were applied.

More in detail, SMARCA5 genomic and spliced sequences of twenty species, Homo sapiens included, were obtained from NCBI Gene (*https://www.ncbi.nlm.nih.gov/gene*). To verify the position of human SMARCA5's exons 15 and 16 in the genomic sequence of other species with respect to Homo sapiens, Blast2seq (*https://blast.ncbi.nlm.nih.gov/Blast.cgi*) was used and the alignment between human exon 15 and 16 sequences and the ones of each specie was performed.

After getting the positions of exons 15 and 16 of all the considered species, their FASTA sequences were downloaded. These sequences, added of 300 nt upstream and downstream exons 15 and 16, respectively, were given as input to Einverted in order to verify the presence of inverted sequences in the considered species as well as in Homo sapiens.

ClustalW2 was used to assess the presence of conserved nucleotides by a multiple alignment of the inverted sequences among twelve primates retrieved in UCSC.

3.21 eCLIP analysis

Bam-files (accessions ENCFF913MGS, ENCFF374XWQ, and ENCFF833PXB) were downloaded from *http://www.encodeproject.org* and indexed with samtools. Read densities were visualized using the IGV browser and analyzed using the pysam module in python.

3.22 TCGA data

TCGA GBM RNA-seq data were retrieved from Cancer RNA-Seq Nexus database (*http://syslab4.nchu.edu.tw/*).

3.23 Statistical Analyses

Significance tests were assessed by two-tailed student's *t*-test and Mann–Whitney test. Correlation tests were performed by using Spearman's correlation test and ANOVA Dunn's multiple comparisons test. *P*-values lower than 0.05 were considered significant.

Student *t*-test, Mann-Whitney test, Spearman's correlation test, ANOVA Dunn's multiple comparisons test, Kaplan-Meier overall survival (OS) and progression-free survival (PFS) curves were assessed by SPSS v. 23 software. MetaboAnalyst (*https://www.metaboanalyst.ca/*) was used to perform logistic regression and Receiver Operating Characteristic (ROC) curves.

4. RESULTS

4.1 Expression profile of selected circRNAs

The expression of the selected circRNAs was assessed in a training set of ten fresh-frozen GBM samples paired with adjacent non-tumor tissues (NORM). It was observed a significant downregulation of circSHPRH (hsa_circ_0001649) and circSMARCA5 (hsa_circ_0001445) (*p*-value = 0.015, *p*-value = 0.017, n = 5, Student's *t*-test) in GBM biopsies with respect to non-tumor tissues (Figure 13).

CircSMARCA5 was chosen for further downstream studies thanks to its abundance in several brain regions as well as in GBM biopsies with respect to circSHPRH, as reported by circBase and by Song et al. 2016 [105].

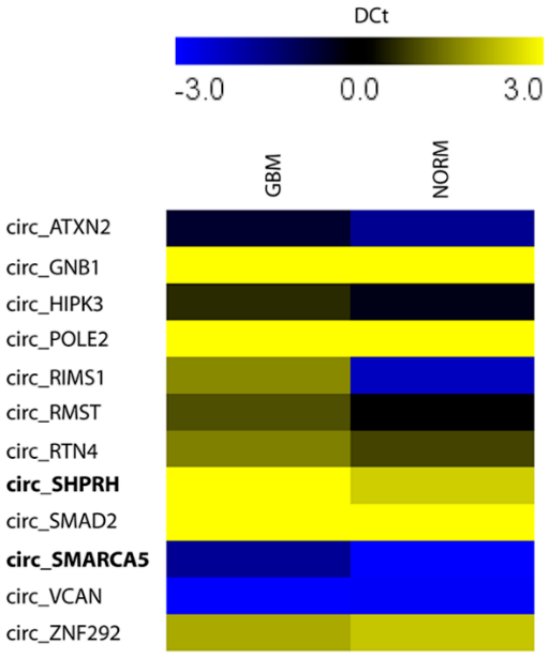

Figure 13. Expression profile of candidate circRNAs in the training set. Expression values shown as DCt values higher and lower than the controls are shown in yellow and blue, respectively. The significant downregulation of circSHPRH and circSMARCA5 is shown in bold (from Barbagallo D. Int J Mol Sci. 2018).

The expression of circSMARCA5 was further evaluated in a test set of sixty-three FFPE biopsies (fifty-six GBM samples and seven unaffected controls). The result confirmed the downregulation of circSMARCA5 in GBM biopsies previously observed in the training set (*p*-value < 0.00001, nGBM = 56, nNORM = 7, Student's *t*-test) (Figure 14). On the contrary, the expression of the linear isoform counterpart did not vary, suggesting a specific dysregulation of the circular isoform (Figure 14). In addition, circSMARCA5 downregulation was also observed in five GBM cell lines with respect to healthy astrocytes (Figure 15A). Moreover, the evaluation of percentage of GFAP+ cells in GBM biopsies and normal brain parenchyma showed that astrocytes may be considered the most representative cell type in GBM biopsies with respect to the controls (Figure 15B).

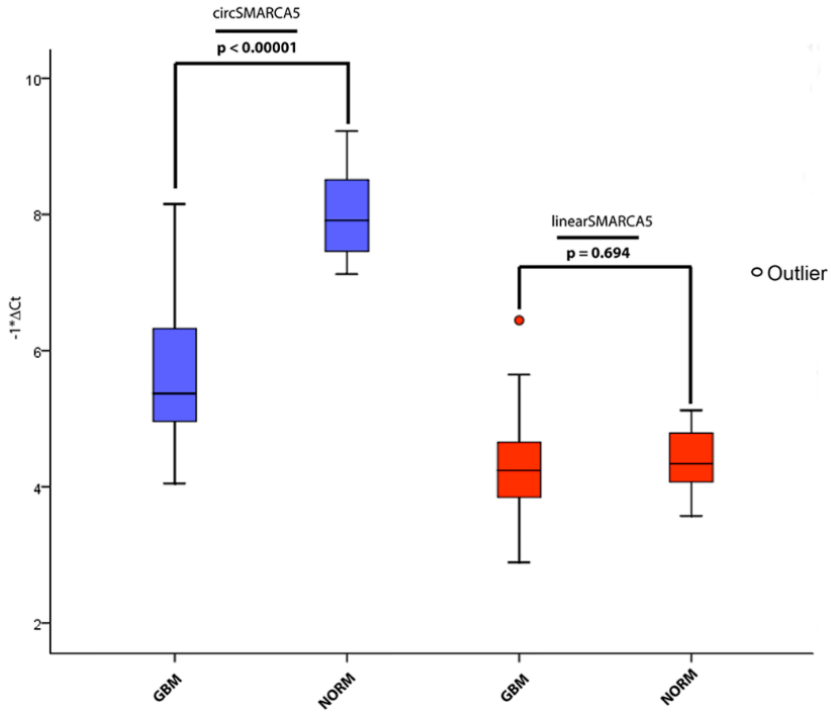

Figure 14. Expression of circSMARCA5 and linear SMARCA5 in the test set. Expression values are shown as -DCt relative to (mRNA) TBP (from Barbagallo D. Int J Mol Sci. 2018).

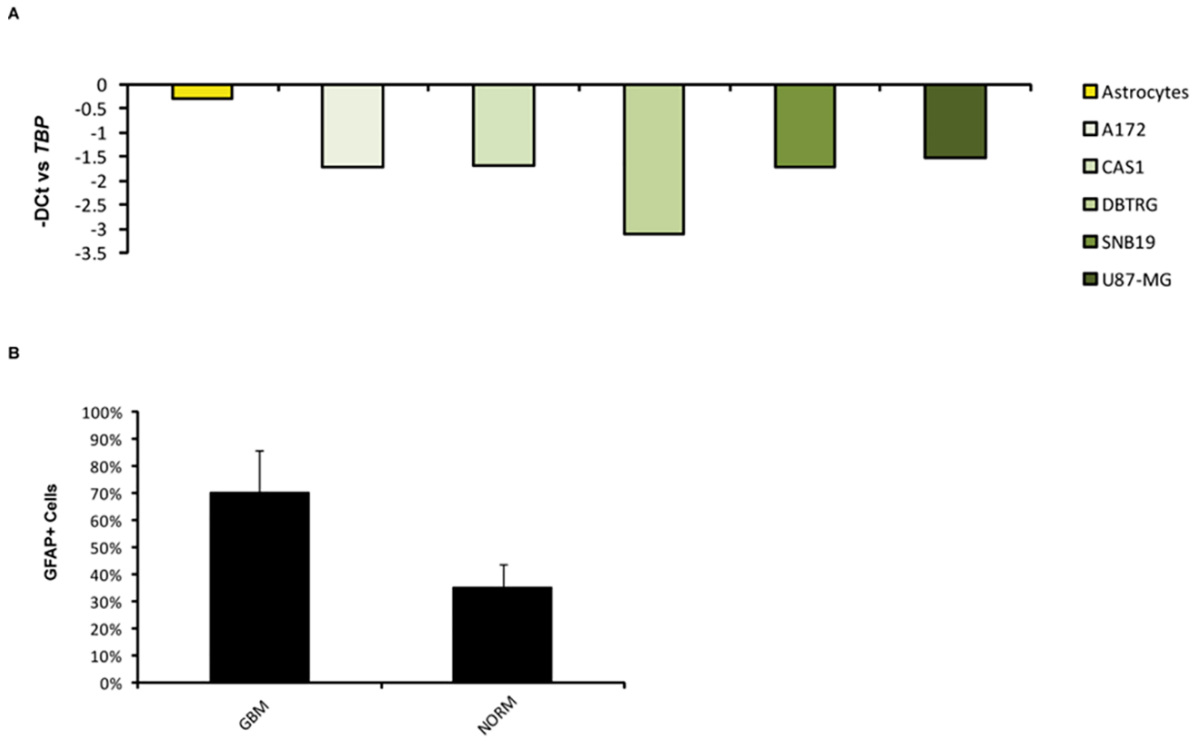

Figure 15. (A) Expression profile of circSMARCA5 in human astrocytes and GBM cell lines A172, CAS1, DBTRG, SNB19, U87-MG. Expression values are reported as –DCt relative to TBP; **(B)** percentage of GFAP+ cells in GBM (GBM) and normal brain parenchyma (NORM) biopsies. Data are reported as mean ± SD (nGBM = 56, nNORM = 7) (from Barbagallo D. Int J Mol Sci. 2018).

4.2 Expression of circSMARCA5 correlates with glioma grade malignancy

Downregulation of circSMARCA5 was also observed in the analysis of an independent dataset consisting of twenty GBM, three grade III glioma, four grade II glioma, thirteen normal brain cortex and six normal brain (*p*- value= < 0.05, ANOVA test) [105]. This analysis revealed that a decreased expression of circSMARCA5 was associated with an increase of glioma grade malignancy (Figure 16).

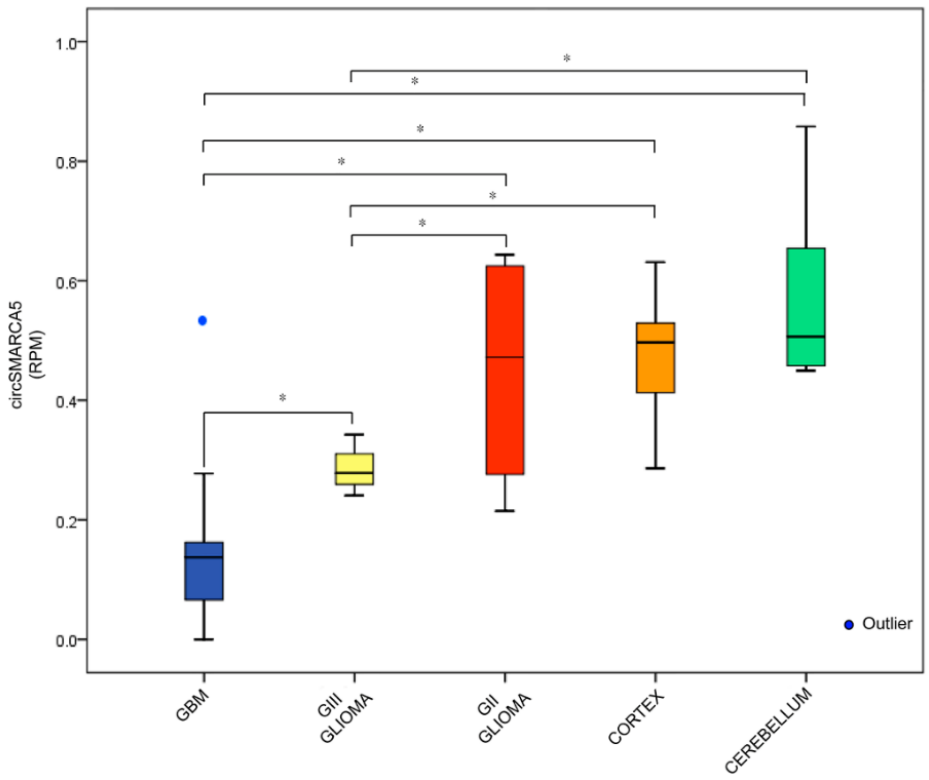

Figure 16. CircSMARCA5 expression in three grade tumor groups (GBM, Grade III—GIII- and Grade II—GII-gliomas) and two different control groups (Cortex and Cerebellum). Expression values are reported as reads per million mapped reads (RPM) (from Barbagallo D. Int J Mol Sci. 2018).

4.3 Cloning of circSMARCA5 in GBM cell line

U87-MG cells were transfected with pcDNA3_circSMARCA5 and, according to northern blotting and expression analysis, they produced and overexpressed the circular isoform of SMARCA5 (Figure 17).

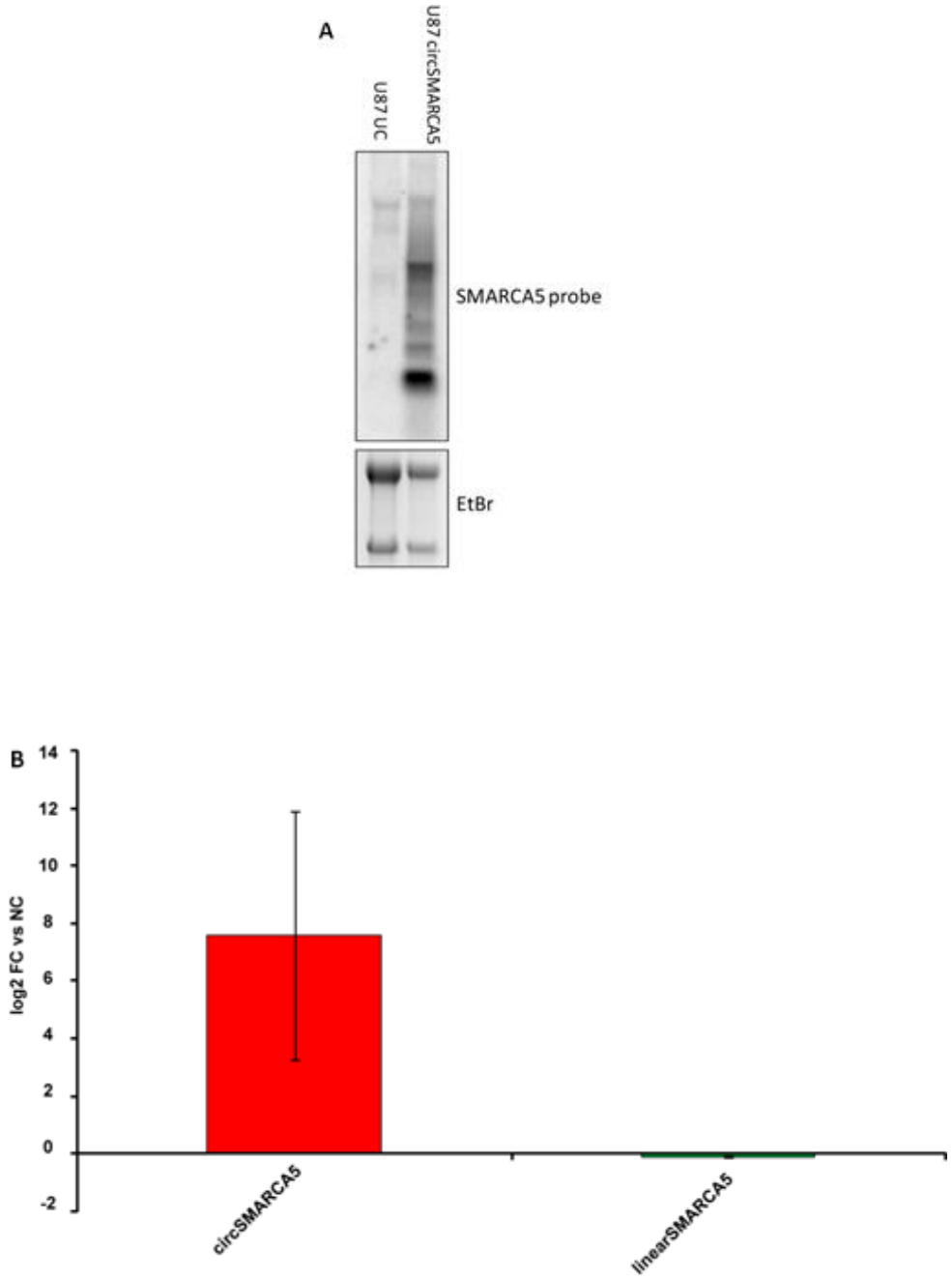

Figure 17. (**A**) Northern blot of untransfected (UC) and circSMARCA5-transfected U87-MG total RNA with a probe for SMARCA5 (from Barbagallo D. et al., Int J Mol Sci. 2018) (**B**) Expression of circSMARCA5 and linear SMARCA5 in U87-MG transfected with pcDNA3-circSMARCA5 vector with respect to NC (U87-MG transfected with the empty vector). Data are reported as log2 fold change (FC) vs NC (from Barbagallo D. et al., Cancers 2019).

Scanning for sequence of introns flanking circSMARCA5's exons 15 and 16 by using EMBOSS einverted, revealed that these sequences contain a 132 nucleotides long inverted repeat (cloned within pcDNA3_circSMARCA5 vector) showing a 77% of complementarity (Figure 18A). The inverted repeats

resulted to be conserved among primates. This result suggested that these sequences could be involved in circSMARCA5 biogenesis (Figure 18B).

In fact, analysis of conservation during evolution of the inverted repeats showed that they appeared for the first time as a very small sequence (30 nucleotides long), probably not functional, in genomes of lagomorpha and rodentia, whereas a longer, most probably functional, inverted repeat emerged in primate genomes (Table 5). Since circSMARCA5 has not been annotated in mouse according to CircBase, this result suggested that circSMARCA5 is primate specific and its biogenesis may depend on the long-inverted sequence.

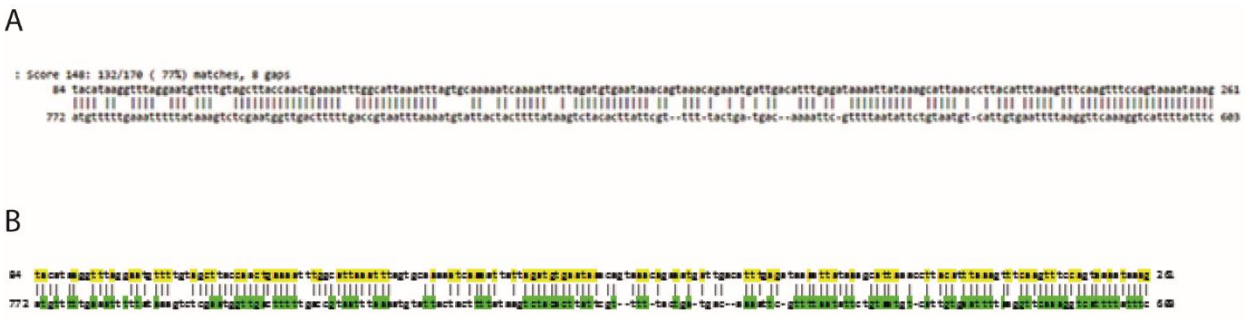

Figure 18. (A) Inverted repeat identified by Einverted within the sequence of introns flanking human circSMARCA5 exons. **(B)** Conserved nucleotides within inverted repeat flanking circSMARCA5 sequence. Conservation was assessed by aligning the sequences from twelve primates retrieved in UCSC, through ClustalW. Nucleotides highlighted in yellow and green represent conserved nucleotides within the inverted repeat upstream and downstream circSMARCA5 (from Barbagallo D. et al., Int J Mol Sci. 2018).

Class	Infraclass	Order	Species	Inverted Repeat
Mammalia	Eutheria	Primata	*Homo sapiens* (Hsa)	✓
			Pan troglodytes (Ptr)	✓
			Gorilla gorilla (Ggo)	✓
			Macaca mulatta (Mcc)	✓
		Lagomorpha	*Ochotona princeps*	X
			Oryctolagus cuniculus (Ocu)	✓
		Rodentia	*Castor canadensis* (Ccan)	✓
			Mus musculus (Mmu)	X
			Cricetulus griseus (Cge)	X

			Rattus norvegicus (Rno)	X
	Metatheria	Monotremata	*Ornithorhynchus anatinus* (Oaa)	X
		Didelphimorphia	*Monodelphis domestica* (Mdo)	X
		Diprotodontia	*Phascolarctos cinereus*	X
		Dasyuromorphia	*Sarcophilus harrisii* (Shr)	X
Amphibia		Anura	*Xenopus leavis* (Xla)	X
			Nanorana parkeri (Npr)	X
			Xenopus tropicalis (Xtr)	X
Reptilia		Testudines	*Pelodiscus sinensis* (Pss))	X
		Ophidae	*Python bivittatus* (Pbi)	X
		Squamata	*Gekko japonicus* (Gja)	X

Table 5. Inverted repeats identified within the introns flanking circSMARCA5 sequences in various species (from Barbagallo D. et al, Int J Mol Sci. 2018).

4.4 CircSMARCA5 regulates GBM cell migration

Functional analyses revealed that U87-MG cells overexpressing pcDNA3_circSMARCA5 showed a significant decreased migration rate with respect to U87-MG transfected with pcDNA3, used as negative control (p-value = 0.015, n = 3, Student's t-test) (Figure 19). However, viability of U87-MG appeared not to be affected under the same experimental conditions (Figure 20).

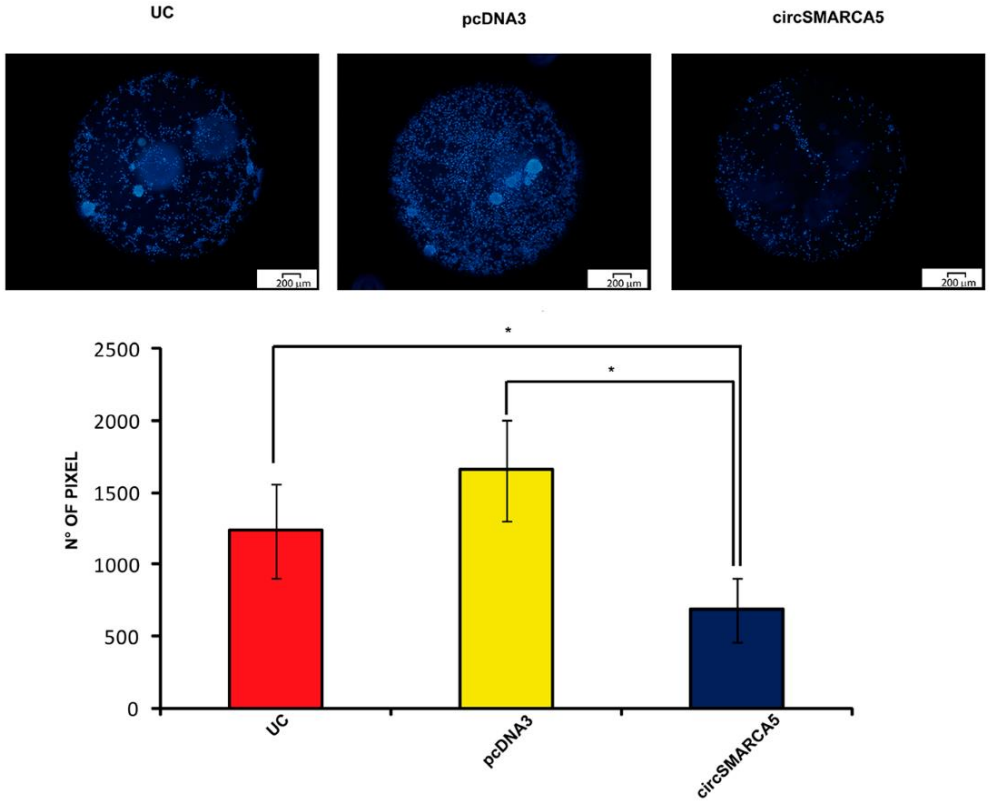

Figure 19. Migration of untransfected (UC), pcDNA3 and pcDNA3_circSMARCA5 (circSMARCA5) transfected U87-MG cells. Cells were stained with Hoechst® 33342 at a final concentration of 5 µg/mL (upper panel). Quantitative data are reported as the number of pixels within the detection area (lower panel) (from Barbagallo D. Int J Mol Sci. 2018).

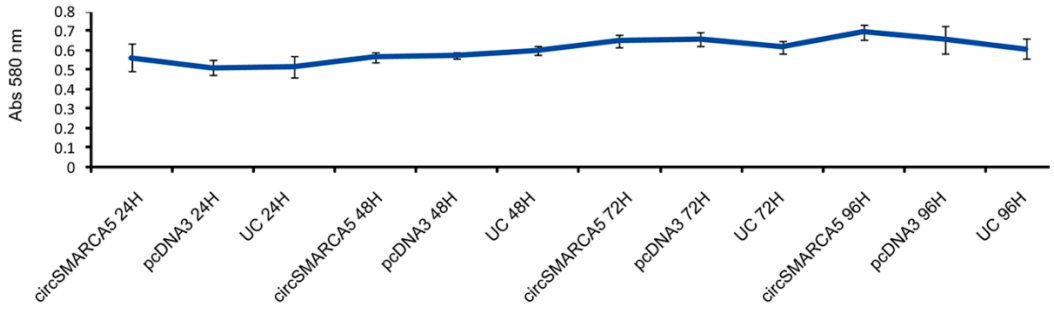

Figure 20. Viability of untransfected (UC), pcDNA3 and pcDNA3_circSMARCA5 (circSMARCA5) transfected U87-MG cells. Data are reported as baseline-corrected absorbance at 580 nm (n = 6) (from Barbagallo D. et al., Int J Mol Sci. 2018).

4.5 Prediction analysis of interaction between circSMARCA5 and miRNAs or RBPs

To investigate the mechanism through which circSMARCA5 may exert its function, a prediction analysis of the interaction between circSMARCA5 and both miRNAs and RBPs was performed.

StarBase and circInteractome predictions showed a not significant enrichment of miRNA binding sites within circSMARCA5 sequence, probably due to its short length of only 269 nucleotides. However, circSMARCA5 appeared to be enriched in RBP binding sites as revealed by all the applied tools (RBPMap, ATTRACT and *cat*Rapid) (Table 6). In particular, circSMARCA5 is predicted to be bound by SRSF1 at multiple sites by all the three consulted tools. This prediction is also supported by enhanced UV crosslinking and immunoprecipitation (eCLIP) data on K562, available in Encyclopedia of DNA Elements (ENCODE) (Figure 21).

RBP	**ATTRACT**	**RBPMAP**	***cat*RAPID**
SRSF1	√	√	√
TARDBP	√	√	X
CELF1	√	X	√
CELF2	√	X	√
CELF4	√	X	√
CELF5	√	X	√
CMTR1	√	X	X
CPEB4	√	X	√
DAZAP1	√	X	X
DDX58	√	X	X
ELAVL1	√	X	X
ELAVL2	√	X	X
ELAVL4	√	X	X
ESRP2	√	X	√
F2	√	X	X
FUS	√	X	√
GRSF1	√	X	√
HNRNPA0	√	X	X
HNRNPA1	√	X	X
HNRNPA2B1	√	X	X
HNRNPC	√	X	X

HNRNPD	√	X	X
HNRNPDL	√	X	X
HNRNPF	√	X	X
HNRNPH1	√	X	X
HNRNPH2	√	X	X
HNRNPH3	√	X	X
HNRNPL	√	X	X
IGF2BP2	√	X	X
IGF2BP3	√	X	X
KHDRBS1	√	X	X
KHSRP	√	X	X
LIN28A	√	X	X
MBNL1	√	X	√
NOVA1	√	X	√
NOVA2	√	X	√
NXF1	√	X	√
OAS1	√	X	√
PABPC1	√	X	X
PABPC3	√	X	X
PABPN1	√	X	X
PHAX	√	X	√
PIWIL1	√	X	X
PPIE	√	X	√
PTBP1	√	X	√
RBM3	√	X	√
RBM46	√	X	√
RBM5	√	X	X
RBMS3	√	X	√
RBMX	√	X	√
RNASEL	√	X	X
SART3	√	X	X
SFPQ	√	X	√
SRP14	√	X	√
SRP19	√	X	√
SRP54	√	X	√
SRP68	√	X	√
SRSF10	√	X	X
SRSF11	√	X	X
SRSF2	√	X	√
SRSF3	√	X	√
SRSF5	√	X	√
SRSF6	√	X	√
SRSF9	√	X	√
SSB	√	X	X
TIA1	√	X	√

TIAL1	√	X	X
TRA2A	√	X	√
TRA2B	√	X	√
XPO5	√	X	X
YBX1	√	X	X
YTHDC1	√	X	X
ZFP36	√	X	X
ANKHD1	X	√	X
BRUNOL4	X	√	X
BRUNOL5	X	√	X
CNOT4	X	√	√
CUG-BP	X	√	X
ESRP2	X	√	√
FXR1	X	√	√
G3BP2	X	√	√
HNRNPC	X	√	X
HNRNPF	X	√	X
HNRNPH1	X	√	X
HuR	X	√	X
KHDRBS1	X	√	X
KHDRBS2	X	√	X
KHDRBS3	X	√	X
LIN28A	X	√	X
MBNL1	X	√	√
PABPC3	X	√	X
PABPC5	X	√	X
PABPN1	X	√	X
PTBP1	X	√	√
PUM2	X	√	X
RBM24	X	√	√
RBM3	X	√	√
RBM41	X	√	√
RBM46	X	√	√
RBM5	X	√	X
RBMS1	X	√	√
RBMS3	X	√	√
SNRNP70	X	√	X
SRSF10	X	√	X
SRSF2	X	√	√
SRSF3	X	√	√
SRSF5	X	√	√
SRSF7	X	√	√
TRA2B	X	√	√
TUT1	X	√	X

Table 6. RBPs predicted to bind circSMARCA5 (from Barbagallo D. Int J Mol Sci. 2018).

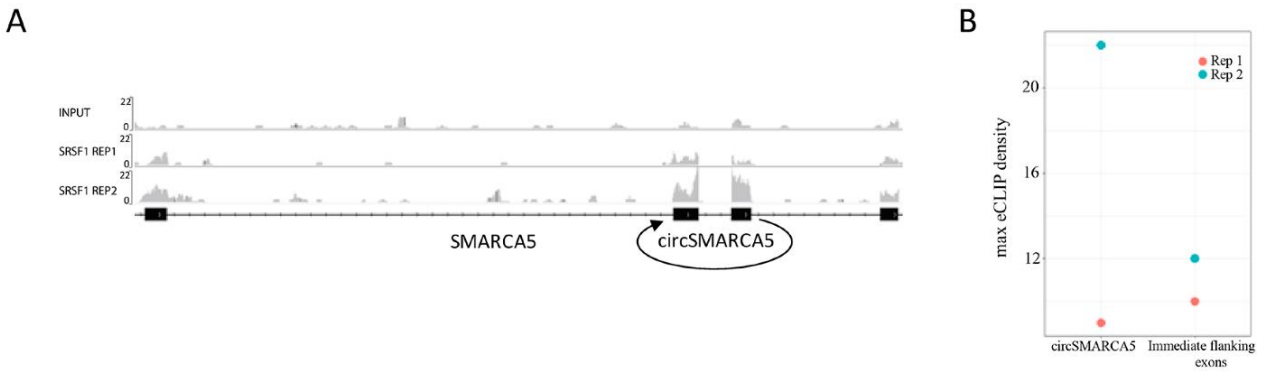

Figure 21. SRFS1 eCLIP data from ENCODE on K562 cells. (**A**) eCLIP read density within the SMARCA5 gene locus (chr4:144461450-144466050, hg19), containing the circSMARCA5 and the immediate flanking exons, visualized by the Integrative Genomics Viewer (IGV). (**B**) Max read density obtained on circSMARCA5 and in the immediate flanking exons (as shown in a) from SRSF1 eCLIP replicates 1 and 2 (from Barbagallo D. Int J Mol Sci. 2018).

4.6 CircSMARCA5 regulates the splicing of SRSF3 pre-mRNA

It is known that SRSF1 is a splicing factor involved in many biomolecular functions and acts as oncoprotein in several cancers. It is also involved in the regulation of the pre-mRNA SRSF3 splicing inducing the inclusion of exon 4 [195]. It is also upregulated in GBM biopsies with respect to normal tissues as reported by TCGA data (Figure 22).

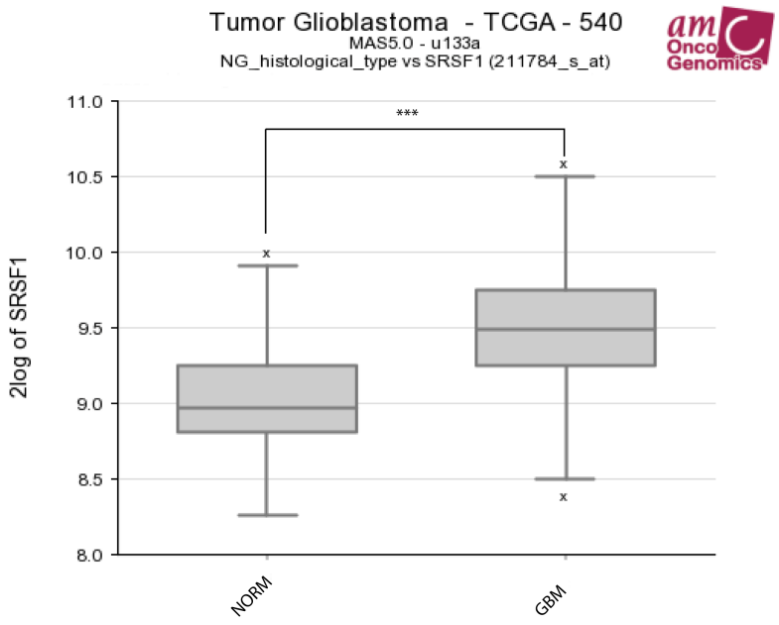

Figure 22. Box-plot of the expression of (mRNA) *SRSF1* in GBM and control (NORM) samples (data from Tumor Glioblastoma - TCGA - 540 - MAS5.0 - u133a, analyzed and visualized through R2 platform) (***p-value < 0.001) (from Barbagallo D. Int J Mol Sci. 2018).

Based on this knowledge and in order to investigate the possible functional role of circSMARCA5 as a regulator of splicing, U87-MG cells were transfected with pcDNA3_circSMARCA5 vector and the expression of two isoforms of SRSF3 mRNA with or without exon 4 (SRSF3 No Ex4 and SRSF3 Ex4, respectively) was tested.

SRSF3 Ex 4 mRNA, whose expression levels are normally low within cells (Figure 23), increased in U87-MG overexpressing circSMARCA5 (p-value < 0.01, n = 3, Student's t-test) (Figure 24).

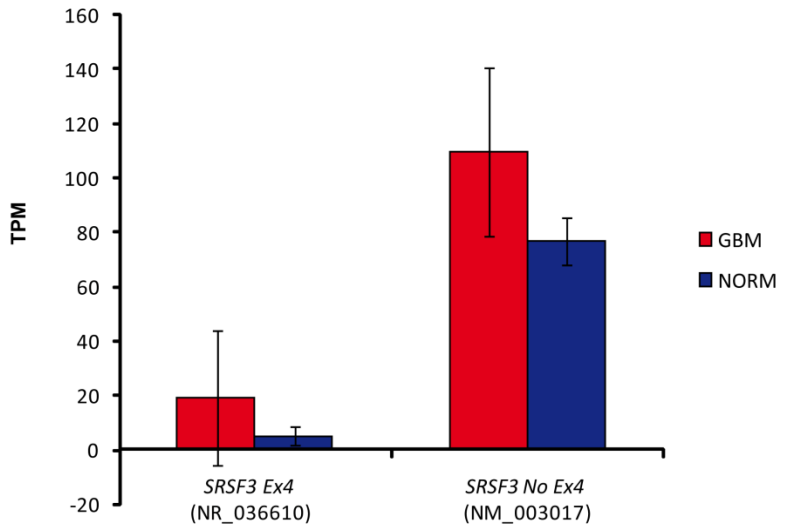

Figure 23. Expression of (mRNA) *SRSF3* isoforms in GBM and control samples (data from TCGA). Expression values are reported as Transcripts per Million (TPM) and data are represented as mean ± SD (n_{GBM} = 156, n_{NORM} = 5) (from Barbagallo D. et al., Int J Mol Sci. 2018).

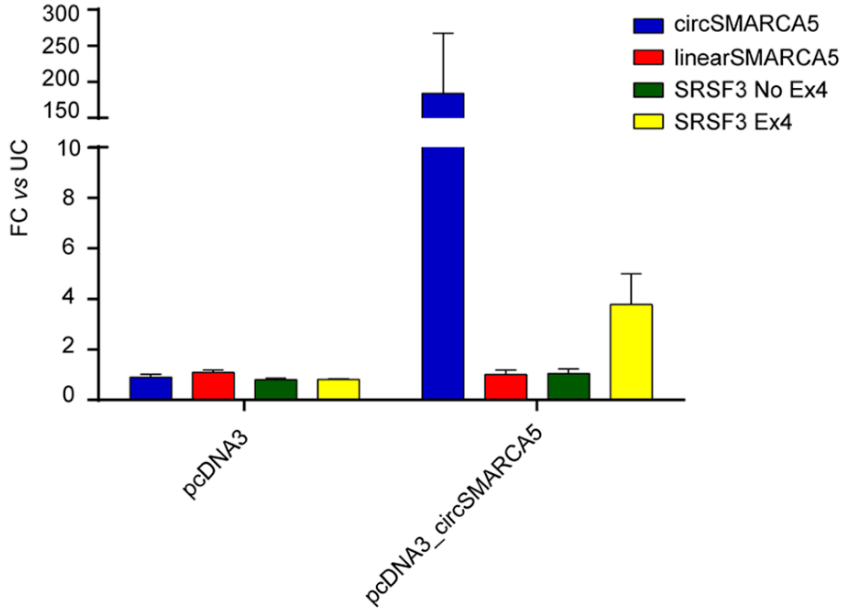

Figure 24. Expression of circSMARCA5, linearSMARCA5, SRSF3 No Ex4 and SRSF3 Ex4 in U87-MG overexpressing circSMARCA5. Data are reported as fold-change (FC) versus untransfected cells (UC) (from Barbagallo D. et al, Int J Mol Sci. 2018).

As expected, it was also observed a significant upregulation of SRSF3 No Ex4 mRNA in the same cohort of GBM biopsies (p-value < 0.05, nGBM = 56, nNORM = 7, Student's t-test), in which circSMARCA5 was

significantly downregulated (Figure 25). Surprisingly, SRSF3 Ex4 mRNA was also upregulated in GBM biopsies (p-value < 0.01, nGBM = 56, nNORM = 7, Student's t-test) (Figure 25). However, consistently with data obtained in U87-MG cells overexpressing circSMARCA5, the SRSF3 Ex4/SRSF3 No Ex4 ratio positively correlated with the downregulation of circSMARCA5 in GBM biopsies (r-value = 0.36, p-value = 0.004, Spearman's correlation test) (Figure 26).

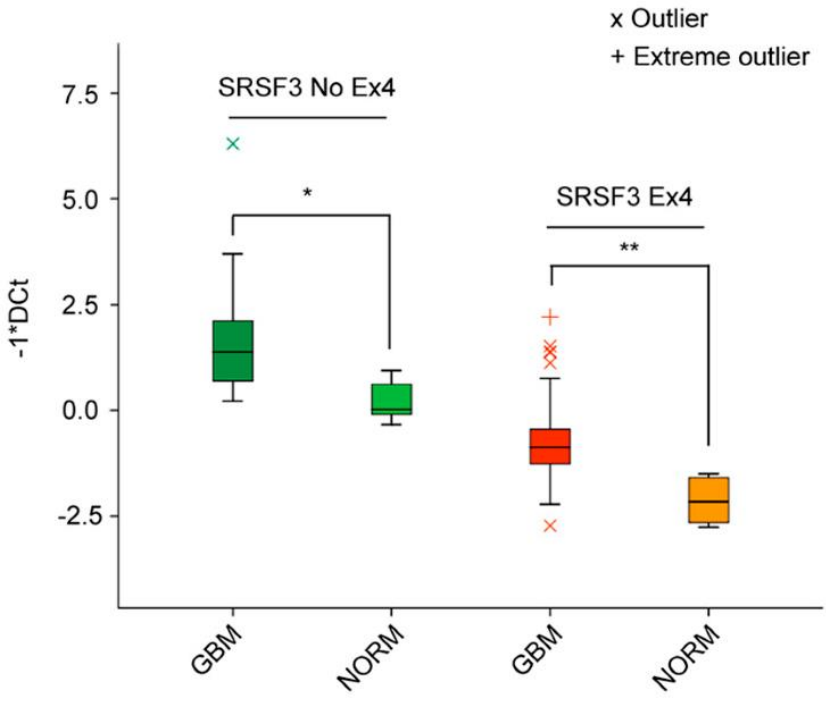

Figure 25. Expression of SRSF3 No Ex4 and SRSF3 Ex4 in GBM biopsies (GBM) with respect to normal brain parenchyma (NORM). Expression values are reported as -DCt relative to (mRNA) TBP (from Barbagallo D. Int J Mol Sci. 2018).

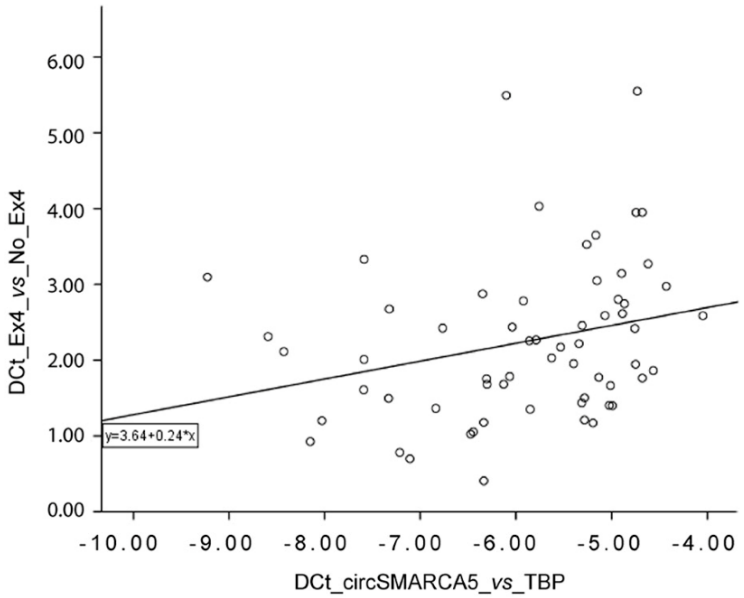

Figure 26. Correlation between SRSF3 Ex4/SRSF3 No Ex4 ratio and circSMARCA5. Data are represented as DCt relative to (mRNA) TBP in a scatter plot (from Barbagallo D. Int J Mol Sci. 2018).

4.7 Receiver Operating Characteristic (ROC) curve analysis

The analysis of ROC curves revealed that circSMARCA5 could be considered a promising biomarker in GBM

(Figure 27).

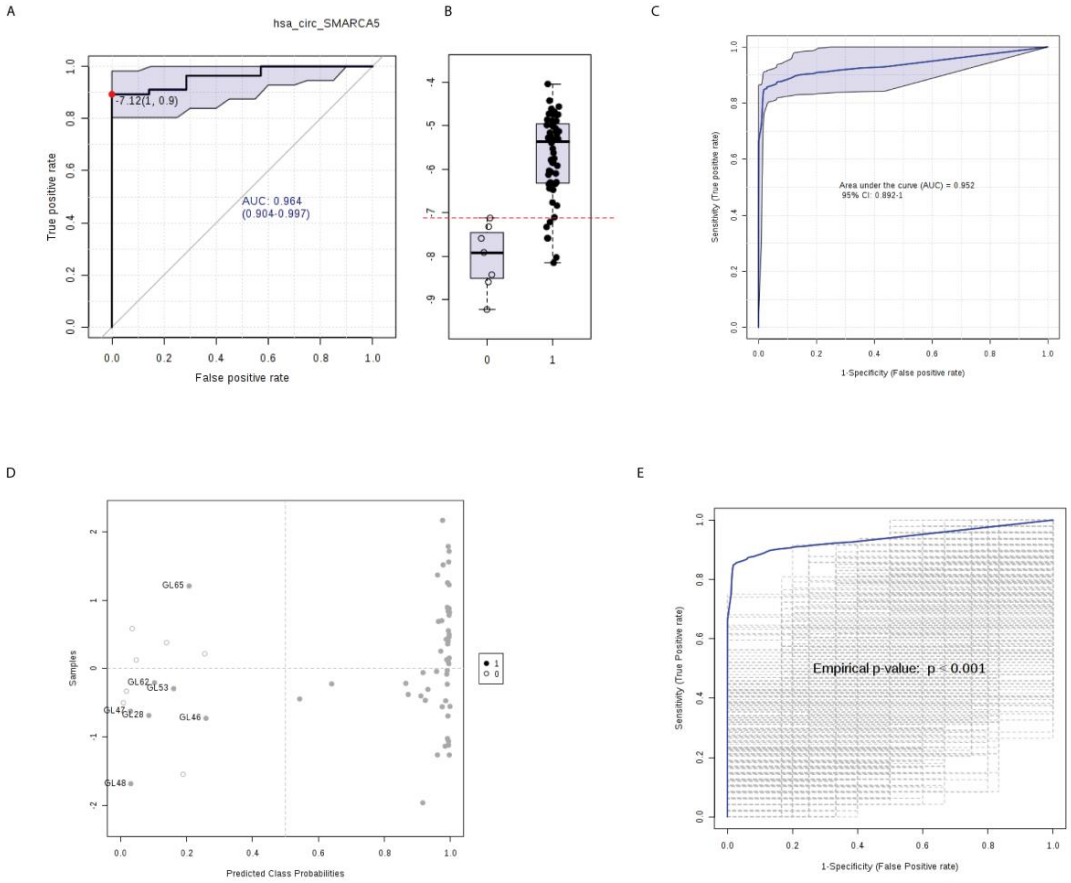

Figure 27. ROC curve analysis of circSMARCA5. (**A, B**) The 95% confidence interval is calculated using 500 bootstrappings. Optimal cutoff is showed using farthest to diagonal line (Youden) method; (**C**) Biomarker model. 100 cross validation (CV) were performed and the results were averaged to generate the plot. 95% confidence band is shown. Logistic regression algorithm has been used to generate the curve; (**D**) Average of predicted class probabilities of each sample across the 100 cross-validations. The classification boundary is located at the center (x = 0.5, the dotted line); (**e**) AUROC based on 1000 permutation (from Barbagallo D. et al., Int J Mol Sci. 2018).

4.8 CircSMARCA5 physically interacts with SRSF1

SRSF1 binds to circSMARCA5 in at least seven different binding sites that are conserved among primates, including Homo sapiens (Figure 28A).

SRSF1 RIP assay allowed to validate the predicted interaction between circSMARCA5 and this splicing factor. Both circSMARCA5 and SRSF3 mRNA, a known splicing target of SRSF1 used as a positive control, were significantly enriched (* *p*-value < 0.05; ** *p*-value < 0.01, N = 4, two-samples *t*-test) in immunoprecipitated

U87-MG cell lysate with respect to GAPDH used as a negative control (Figure 28B). Western analysis confirmed the specificity of the RIP assay (Figure 28C).

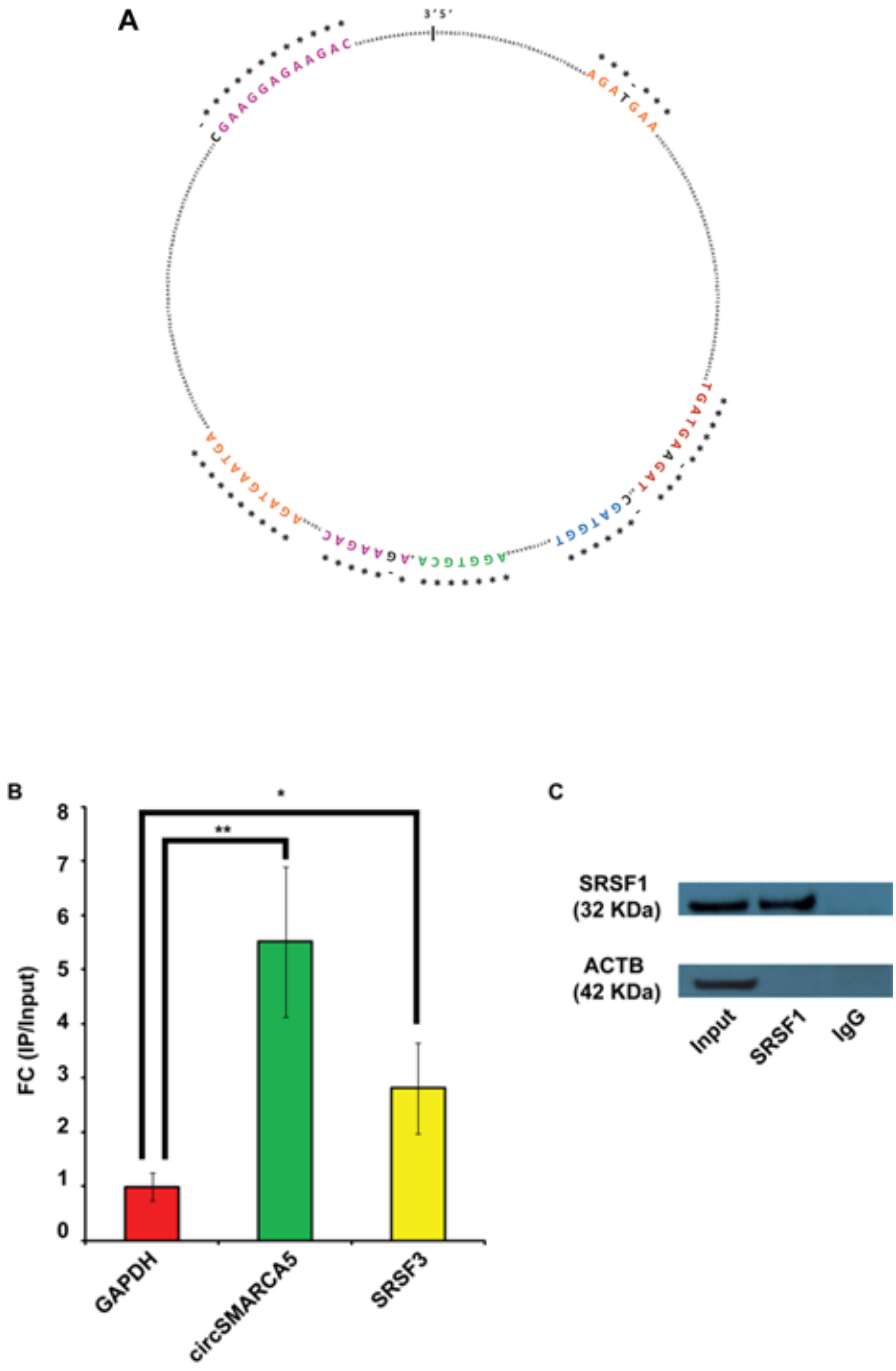

Figure 28. (A) SRSF1 binding sites on circSMARCA5 sequence predicted by RBPMap database. * indicates sequence conservation among primates including H*omo sapiens*. **(B)** Fold enrichment (FC) of circSMARCA5, SRSF3 and GAPDH in Iped U87-MG lysate with respect to input. **(C)** Western blot of U87-MG Input, SRSF1 and normal IgG RIPed samples (from Barbagallo D. Cancers. 2019).

4.9 SRSF1, VEGFA and circSMARCA5 expression in GBM biopsies

SRSF1 mRNA was upregulated in GBM biopsies with respect to unaffected controls (UC) (p-value = 0.0009, N(GBM) = 31, N (UC) = 20, Mann–Whitney test) (Figure 29A) as well as SRSF1 protein (p-value = 0.022, N(GBM) = 14, N(UC) = 8, two-sample t-test) (Figure 29B-C).

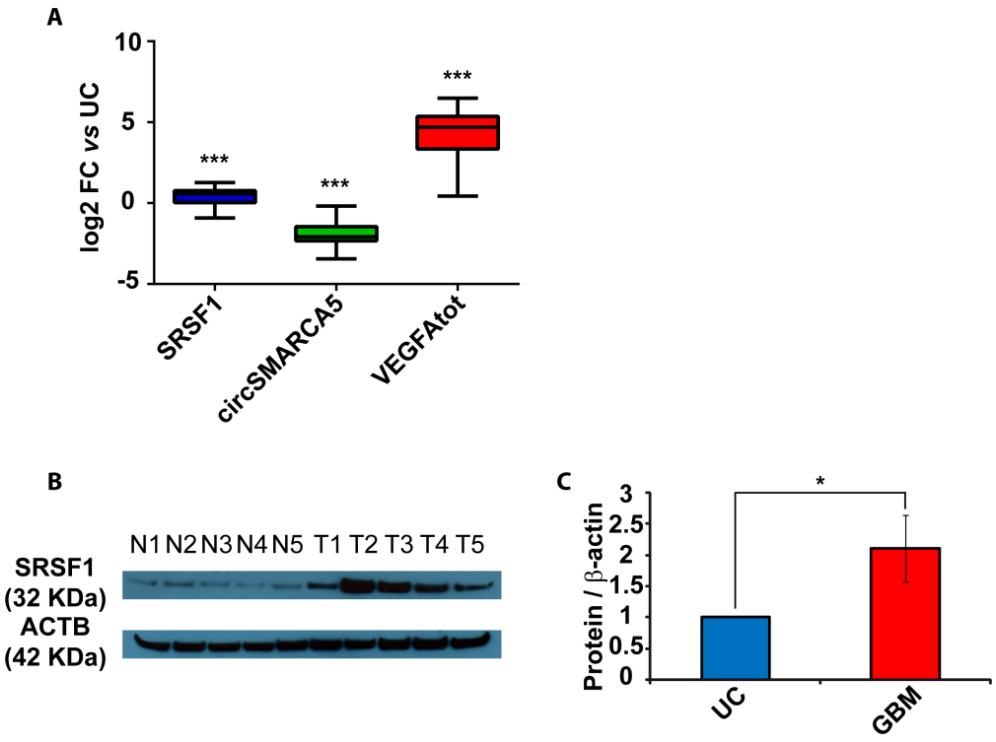

Figure 29. (A) Expression of SRSF1, circSMARCA5 and total VEGFA RNA in GBM biopsies. Data are represented as log2 fold change (FC) values versus UC. **(B)** Western blot of SRSF1 in a selection of UC (N) and GBM (T) samples. ACTB was used as a loading control. **(C)** Densitometric quantification of SRSF1. Data, shown as mean ± standard deviation, represent fold change versus UC (from Barbagallo D. et al., Cancers. 2019).

After a literature review of SRSF1's splicing targets, the attention was focused on VEGFA (Table 7) whose pre-mRNA can be alternatively spliced by SRSF1 generating both pro and anti-angiogenic isoforms [240], [241], [242].

Total VEGFA mRNA (VEGFAtot) was upregulated in GBM with respect to UC in the same cohort (*p*-value < 0.00001, N(GBM) = 31, N (UC) = 20, Mann–Whitney test), while circSMARCA5 was downregulated (*p*-value < 0.00001, N(GBM) = 31, N (UC) = 20, Mann–Whitney test) (Figure 29A), confirming data obtained in the independent cohort shown in Figure 14.

SRSF1 target's Official Gene Symbol	**Reference (PMID or DOI)**
ADD1	17310252
AKT	26273603
AKT1	26431027
ANXA7	24550987
BCL2	28315432
BCL2A1	28315432
BCL2L1	26273603
BCL2L11	22245967
BCL2L2	28315432
BIN1	17310252
BIRC5	24550987
CASP2	24807918
CASP2	17310252
CASP8	28315432
CASP9	26273603
CCND1	23592547
CD247	24807918
CD44	24807918
CDK4	18841201
CDKN1A	25993413
CEBPA	28315432
CFLAR	28315432
CLK1	24842991
CRADD	28315432
CTNNB1	23592547
DFFA	26273603
DIABLO	28315432
EGFR	DOI: 10.18103/mra.v0i1.11
ENG	24807918
ENSA	18841201

FAS	28315432
FGFR	DOI: 10.18103/mra.v0i1.11
FN1	21615404
FOXO4	26431027
HIPK2	28315432
HNRNPA2B1	17310252
IGF1R	18841201
MADD	28315432
MAPK3	18841201
MAPT	24807918
MAX	DOI: 10.18103/mra.v0i1.11
MCL1	24550987
MIR505	29120871
MKNK2	17310252
MNK2B	26273603
MST1R	16364913
MYC	28315432
NETO2	18841201
PABPC1	18841201
PDCD4	28315432
PKM	24842991
PRKCD	26431027
PRKDC	28315432
RAC1	19602482
RPS6KB	17310252
RPS6KB1	25776557
RTN4	DOI: 10.18103/mra.v0i1.11
SFRS1	18841201
SLC39A14	24807918
SRSF3	9305649
TEAD1	26273603
TEAD1	17310252
TMPO	28315432
TNFRSF19	28315432
TNFRSF9	28315432
TNFSF10	28315432
TP53	28315432
TPM1	DOI: 10.18103/mra.v0i1.11
TSC2	17310252; 26431027
VEGFA	**26273603**

Table 7. SRSF1's splicing targets retrieved by literature (from Barbagallo D. Int J Mol Sci. 2018).

4.10 Expression of SRSF1 and VEGFA transcripts in REMBRANDT and TCGA databases

REpository for Molecular BRAin Neoplasia DaTa (REMBRANDT) (Figure 30) [243] and The Cancer Genome Atlas (TCGA) (Figure 31) [244] databases were examined to test the expression of both SRSF1 and VEGFA mRNAs in an independent cohort of GBM biopsies. More in detail, SRSF1 mRNA was significantly upregulated in all glioma grades with respect to normal brain (*p*-value < 0.0001, ANOVA Dunn's multiple comparisons test) (Figure 30A), while VEGFA was significantly upregulated specifically in GBM (*p*-value < 0.0001, ANOVA Dunn's multiple comparisons test) (Figure 30B). It was also observed a positive correlation between SRSF1 and VEGFA expression in GBM samples (Figure 30C).

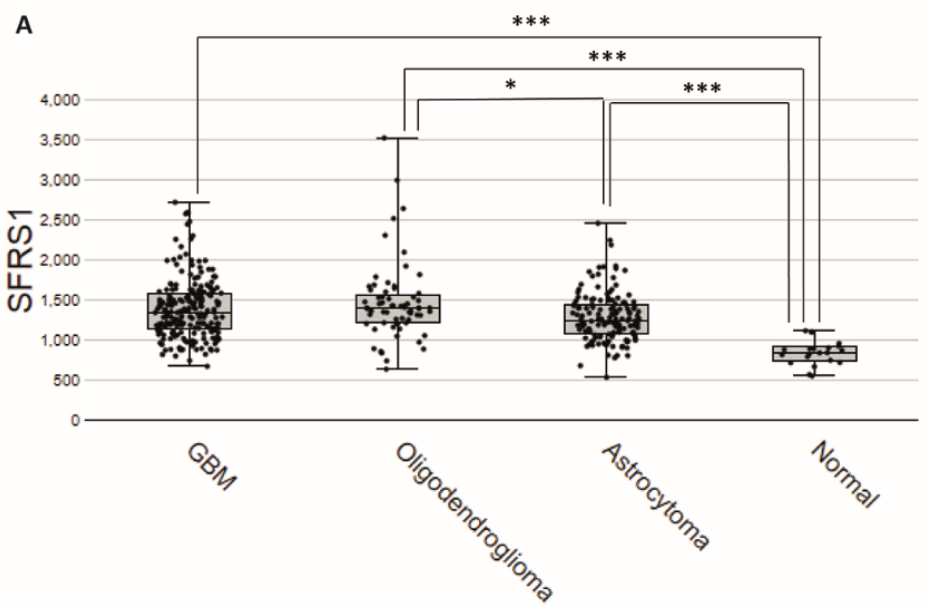

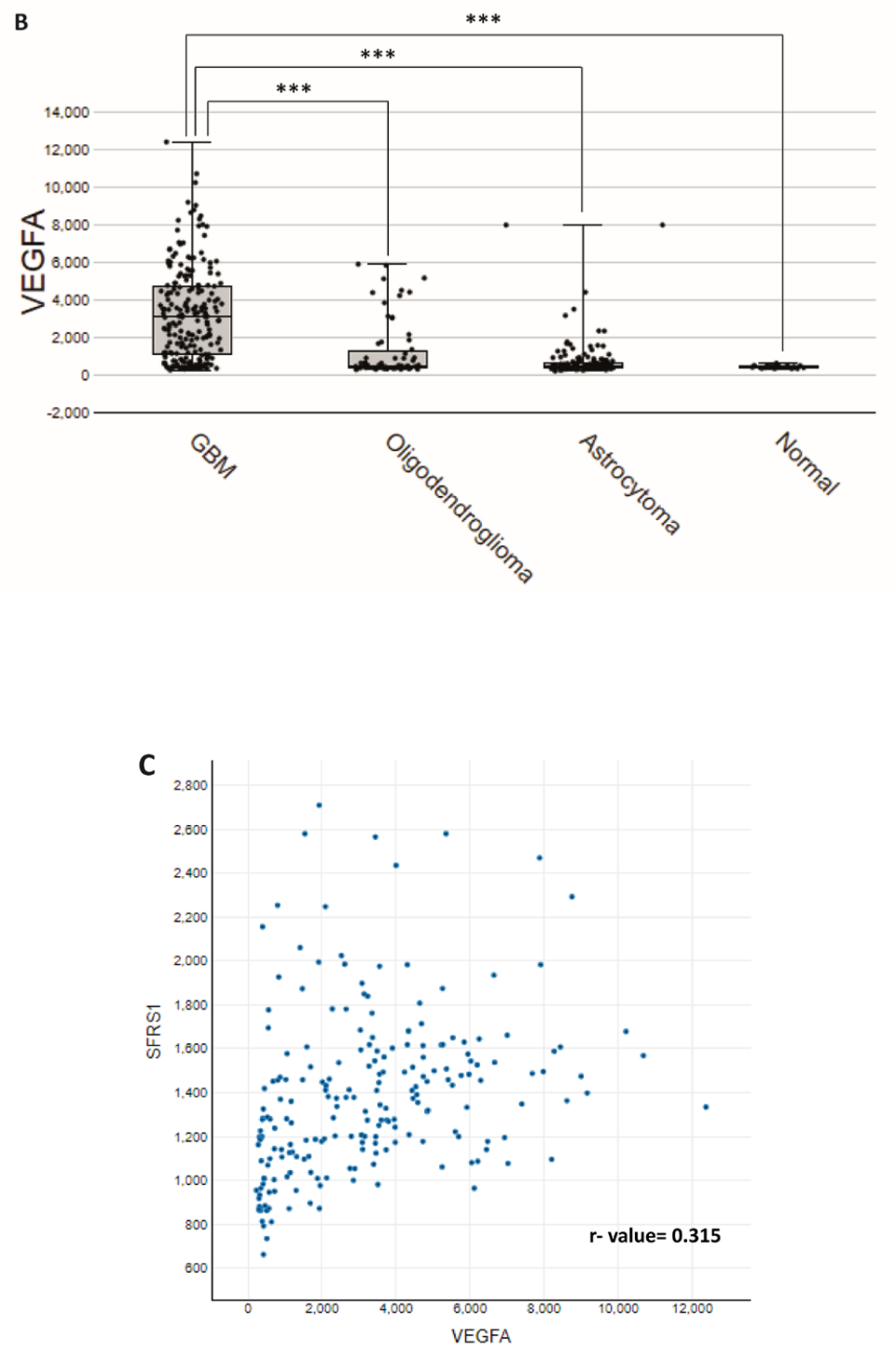

Figure 30. (A) Expression of SRSF1 (Affymetrix HG U133 v2.0 Plus) (* p-value < 0.05; *** p-value < 0.001, ANOVA Dunn's multiple comparisons test). **(B)** Expression of VEGFA (Affymetrix HG U133 v2.0 Plus) (*** p-value < 0.001, ANOVA Dunn's multiple comparisons test). **(C)** Correlation between SRSF1 and VEGFA expression in GBM samples (from Barbagallo D. Cancers. 2019).

In addition, SRSF1 and VEGFA mRNAs were both significantly upregulated in all GBM subtypes, but not in the neural subtype, with respect to unaffected brain samples (ANOVA Dunn's multiple comparisons test; significant *p*-values are shown in the figure 31).

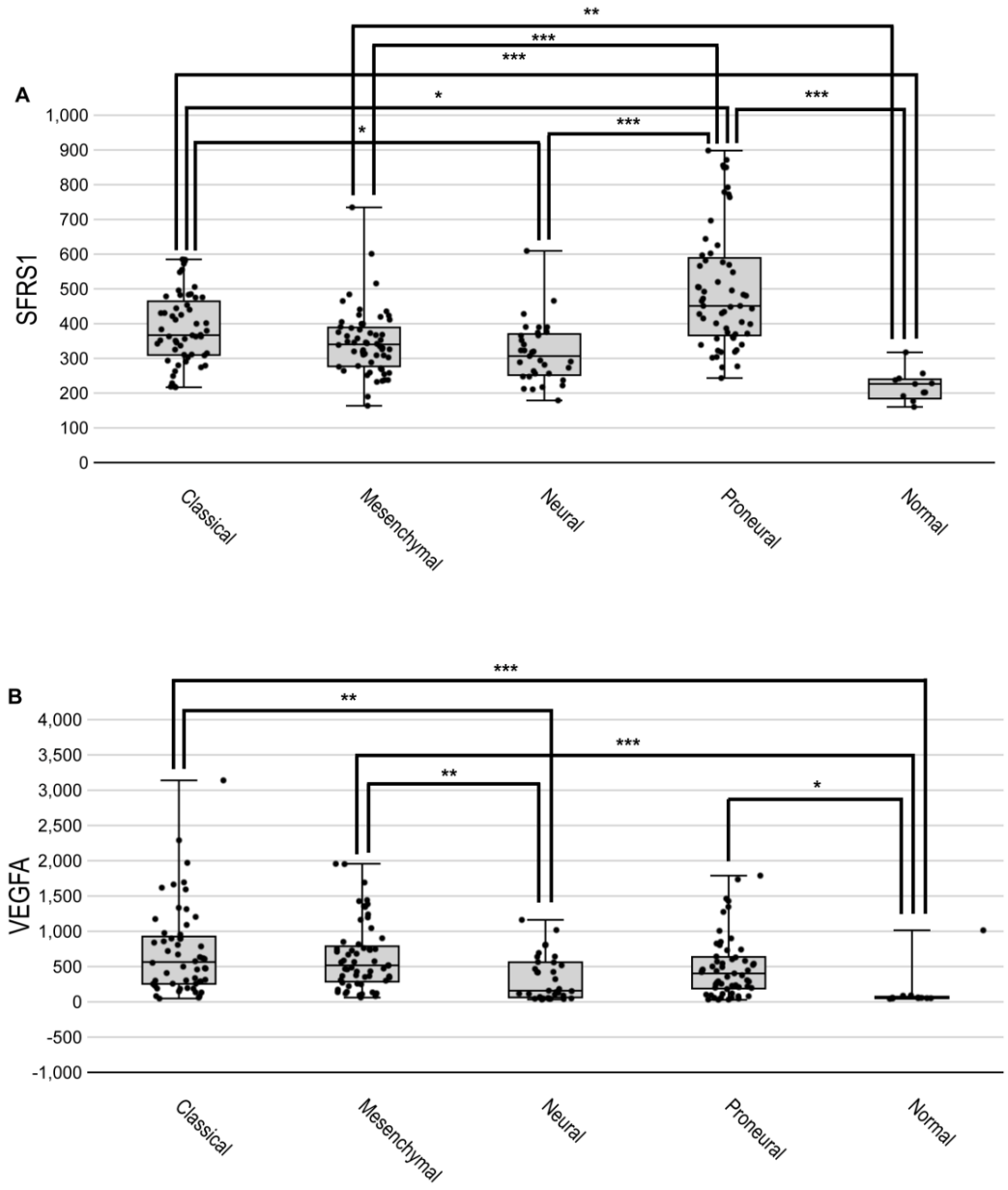

Figure 31. (A) Expression of SRSF1 (Affymetrix HT HG U133A) (* p-value < 0.05; ** p-value < 0.01; *** p-value < 0.001, ANOVA Dunn's multiple comparisons test). **(B)** Expression of VEGFA (Affymetrix HT HG U133A) (* p-value < 0.05; ** p-value < 0.01; *** p-value < 0.001, ANOVA Dunn's multiple comparisons test) (from Barbagallo D. et al, Cancers. 2019).

4.11 Ratio of pro- to anti-angiogenic VEGFA mRNA isoforms in GBM biopsies and in U87-MG cells overexpressing circSMARCA5

To investigate if circSMARCA5 may act as a regulator of VEGFA pre-mRNA splicing, the expression of VEGFAtot, pro- and anti-angiogenic VEGFA mRNA isoforms (Iso8a and Iso8b, respectively) were evaluated in the GBM cohort. The Iso8a-to-Iso8b ratio was significantly higher in GBM biopsies with respect to UC (*p*-value < 0.00001, N = 27, Mann–Whitney test) (Figure 32A; Figure 33A).

In the same cohort, the expression of circSMARCA5 was negatively correlated with that of SRSF1 mRNA (*r*-value = -0.36, *p*-value = 0.011, Spearman correlation test) and with the Iso8a-to-Iso8b ratio (*r*-value = -0.47, *p*-value = 0.006, Spearman correlation test) (Figure 32B). The Iso8a-to-Iso8b ratio was also higher in three GBM cell lines (A172, CAS-1 and U87-MG) with respect to healthy brain (Figure 34).

U87-MG overexpressing circSMARCA5 showed a significant decrease in the Iso8a-to-Iso8b ratio with respect to the same cells transfected with the empty vector (negative control, NC) (*p*-value = 0.0055, N=3, two-sample *t*-test) (Figure 32C and Figure 33B).

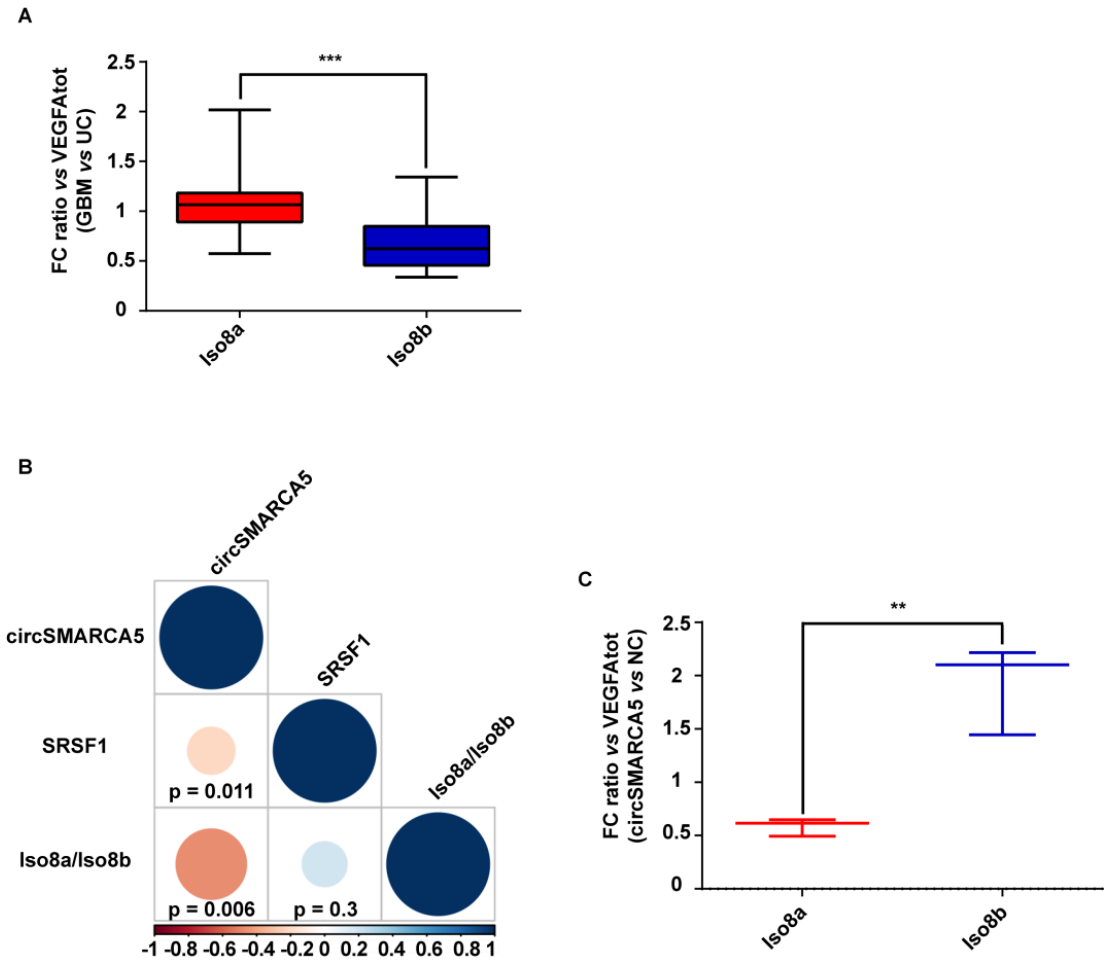

Figure 32. (A) Ratios between fold changes of Iso8a and total VEGFA (VEGFAtot) and Iso8b and VEGFAtot in GBM compared to UC. **(B)** Correlation matrix among the expression of circSMARCA5 and SRSF1 and Iso8a-to-Iso8b ratio. **(C)** Ratios between fold changes of Iso8a and VEGFAtot and Iso8b and VEGFAtot in U87-MG overexpressing circSMARCA5 with respect to U87-MG transfected with the empty vector (NC) (from Barbagallo D. Cancers. 2019).

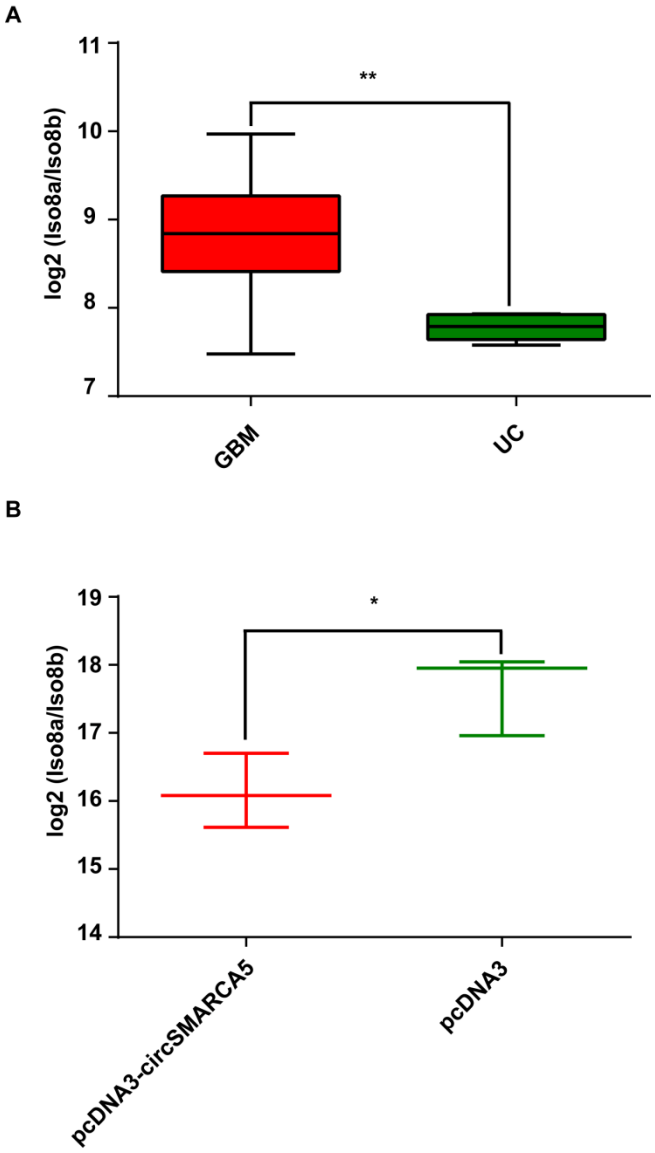

Figure 33. Iso8a/Iso8b ratio in GBM and UC **(A)** and in U87-MG overexpressing circSMARCA5 (pcDNA3-circSMARCA5) and NC (pcDNA3) **(B)**. Data are shown as log2 (2^-DCt(Iso8a)/2^-DCt(Iso8b)). (** p-value < 0.01, N(GBM) = 27, N(UC) = 5, Mann-Whitney Test (A); (* p-value < 0.05, N = 3, two sample t-test (B)) (from Barbagallo D. et al., Cancers. 2019).

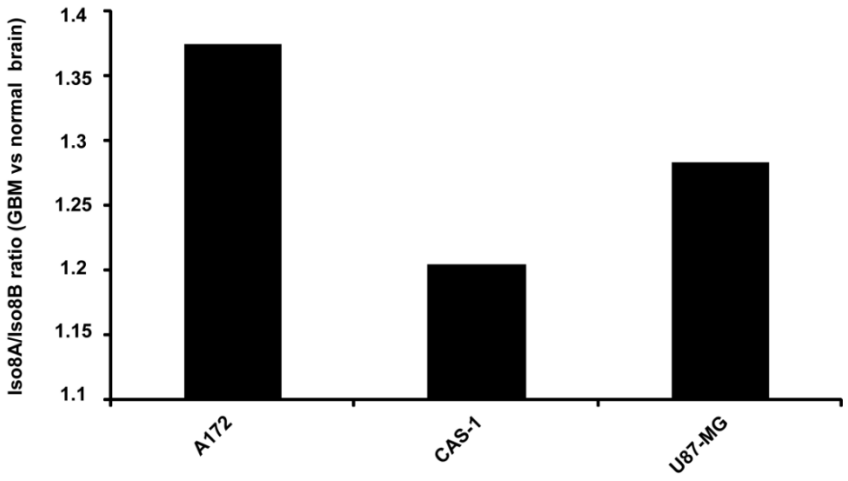

Figure 34. Iso8A vs Iso8B ratio in three different GBM cell lines. Total VEGFA was used as endogenous control; normal brain from Ambion was used as calibrator tissue (from Barbagallo D. et al., Cancers. 2019).

4.12 Correlation between circSMARCA5/SRSF1/VEGFA expression and blood vascular microvessel density

Blood vascular microvessel density (MVD) evaluated in the GBM cohort was significantly higher in GBM samples than in unaffected controls (p-value < 0.00001, N(GBM) = 31, N(UC) = 18, two sample t-test) (Figure 35A-B). This result was not unexpected, but surprisingly MVD positively correlated with SRSF1 mRNA expression and the Iso8a-to-Iso8b ratio (r-values = 0.38, and 0.41, respectively; p-values = 0.00663, and 0.026, respectively, Spearman correlation test), while negatively correlated with circSMARCA5 expression (r-value = -0.59, p-value = 0.00001, Spearman correlation test) (Figure 35C).

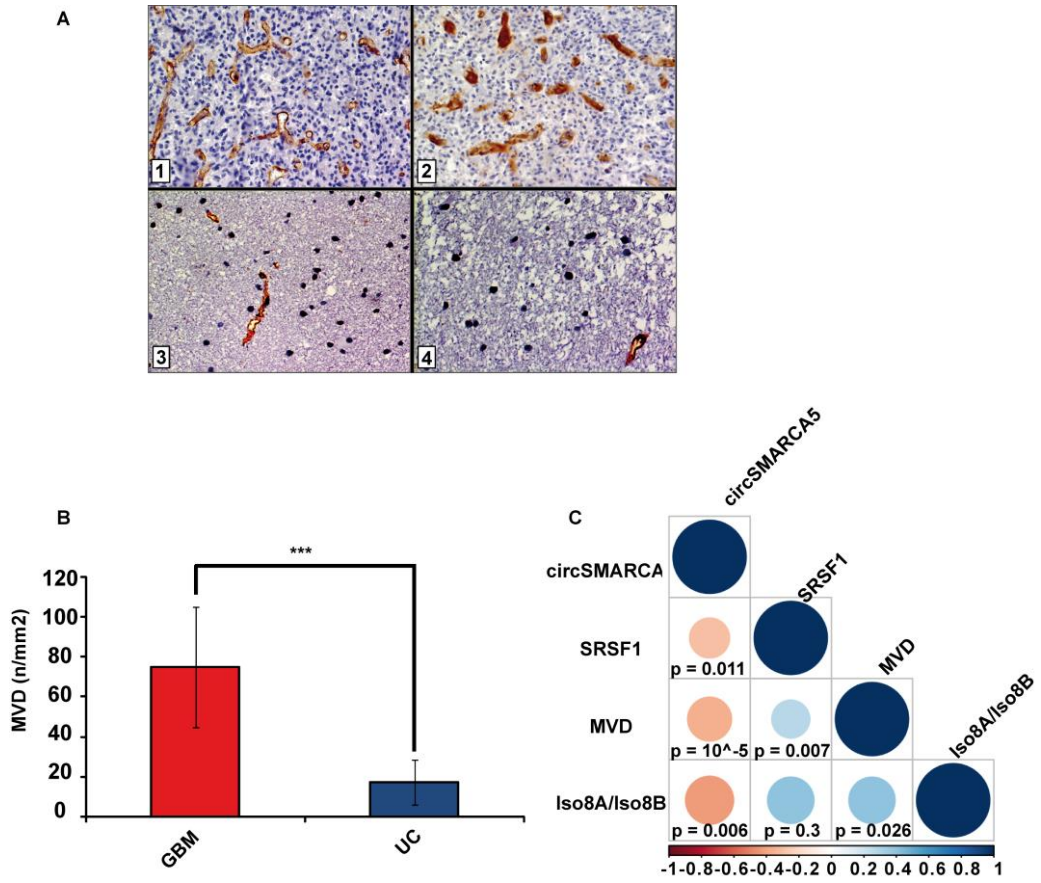

Figure 35. (A) Representative immunohistochemical staining for CD31 showing areas of high MVD with multiple branching vessels in glioblastoma tissue (1 and 2) and a lower MVD in unaffected brain tissue (3 and 4). Immunoperoxidase staining; 400× magnification **(B)** Bar graph representing the mean MVD in GBM and UC samples. Data are represented as mean ± standard deviation. **(C)** Correlation matrix among MVD, circSMARCA5 and SRSF1 expression and Iso8a to Iso8b ratio. Positive and negative correlations are displayed in blue and red color, respectively. Color scale bar indicates *r* values. Color intensity and the size of the circle are proportional to the correlation coefficients into the correlogram (from Barbagallo D. Cancers. 2019).

4.13 CircSMARCA5 expression and GBM Patients' Overall Survival (OS) and Progression-Free Survival (PFS)

Analysis of Kaplan Meier curves showed that circSMARCA5 downregulation was associated with poorer OS and PFS in GBM (*p*-values = 0.033, and 0.012, respectively, logrank test) (Figure 36).

The same analysis was performed on TCGA data showing a negative correlation between mesenchymal GBM patients' OS and SRSF1 expression (p-value = 0.0172, logrank test) (Figure 37).

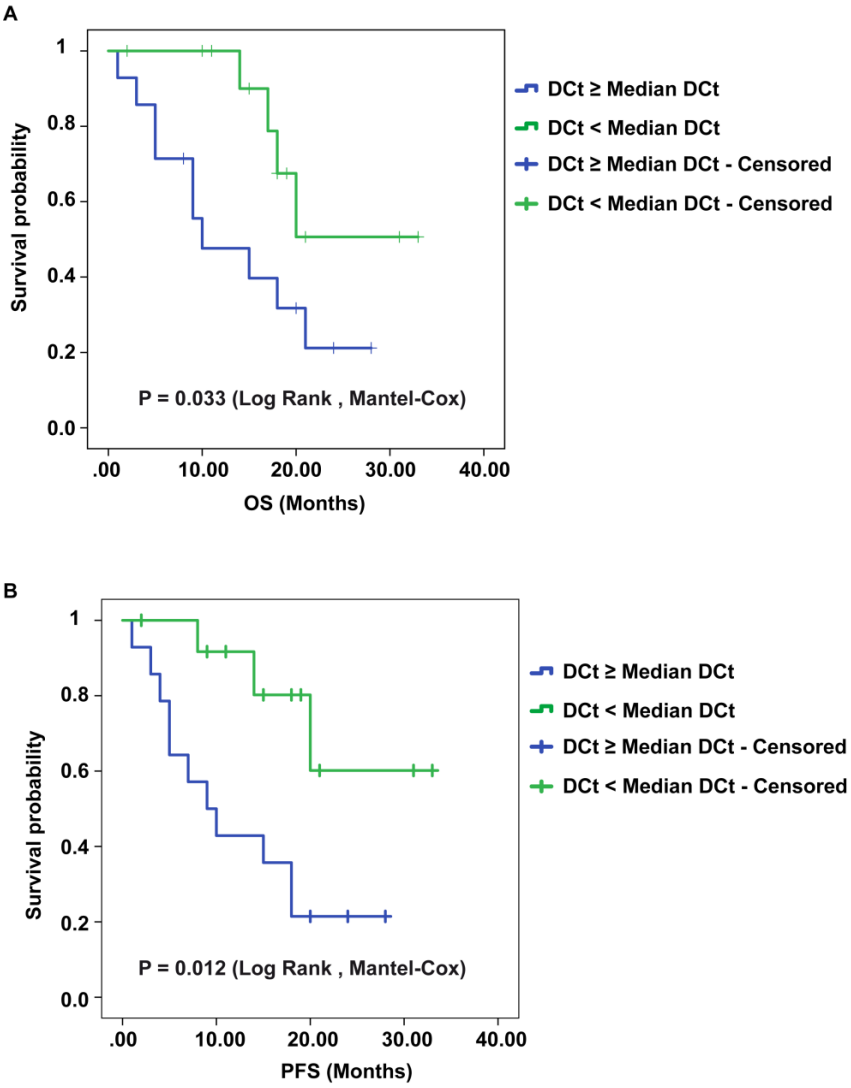

Figure 36. Kaplan–Meier overall survival (OS) **(A)** and progression-free survival (PFS) **(B)** curves of GBM patients, based on the expression of circSMARCA5 (from Barbagallo D. et al, Cancers. 2019).

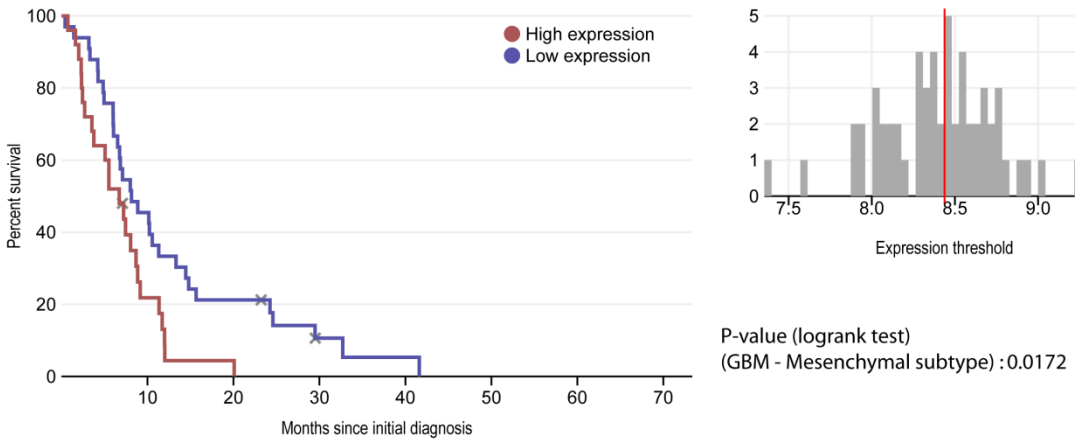

Figure 37. Kaplan-Meier overall survival curves of mesenchymal GBM patients, based on the expression of SRSF1. Patients having a higher expression of SRFS1 survive less than patients with a lower expression of SRSF1 (from Barbagallo D. et al., Cancers. 2019).

5. DISCUSSION

This thesis is focused on circSMARCA5, an exonic 269-nucleotide-long circRNA, highly enriched in human brain, as reported in circBase.

It has been shown that circSMARCA5 expression was decreased in GBM biopsies with respect to normal brain parenchyma, contrary to its linear counterpart that did not vary. Moreover, its expression decreased also in GBM cell lines with respect to normal brain. Astrocytes were the most representative cell type in GBM cohort and seemed to give the main contribute to the altered expression of circSMARCA5 in GBM. Despite this result, it is not possible exclude that other cell types, as Tumor Associated Macrophages (TAMs), may influence the expression of circSMARCA5 in GBM.

This result, according to a previously described increase of circular to linear transcript ratios during differentiation of cardiomyocytes [245] and, together with the inverse relationship between circSMARCA5 expression and glioma grade malignancy, suggested a functional involvement of circSMARCA5 in GBM.

To characterize the effects of the expression of this circRNA, its sequence was cloned into an expression vector, together with a segment of the introns upstream and downstream the circSMARCA5's 15 and 16 exons (these exons generate circSMARCA5 by circularization), respectively.

The scanning for flanking intronic sequences revealed that they include an inverted sequence 132 nucleotides long showing 77% complementarity. This result suggested that these sequences may be responsible for the biogenesis of circSMARCA5. In addition, the analysis of conservation during evolution of the inverted

sequences showed that they are conserved among primates and, since circSMARCA5 is not annotated in mouse, as reported in circBase, it may hypothesize that it has a primate-specific expression.

In vitro functional analysis showed that circSMARCA5 negatively regulated GBM cell migration but did not influence cell viability.

To analyze the mechanism through which circSMARCA5 may exert its function, a prediction analysis of the interaction between circSMARCA5 and miRNAs and/or RBPs was performed. *In silico* analysis revealed that circSMARCA5 is predicted to be bound by SRSF1 at multiple sites; on the contrary, predicted binding sites for miRNAs were not observed, probably due to the short sequence of circSMARCA5.

The predicted interaction between circSMARCA5 and SRSF1, in addition to *in vitro* analysis, allowed to propose that circSMARCA5 may exert its function by altering splicing in GBM cells, specifically by modulating the SRSF1 splicing factor, known to be involved in many biomolecular functions: (i) splicing; (ii) regulation of RNA metabolism; (iii) mRNA translation; (iv) miRNA processing; (v) protein sumoylation; (vi) stress response [246]. SRSF1 is also upregulated and acts as oncoprotein in several cancers [247], [248].

The hypothesis of the role of circSMARCA5 as a splicing regulator was supported by eCLIP data from ENCODE [249] as well as by the expression analysis of SRSF3 splicing isoforms in U87-MG overexpressing circSMARCA5 and data on GBM biopsies. More in detail, SRSF3 Ex4 mRNA increased in U87-MG overexpressing circSMARCA5 and SRSF3 No Ex4 mRNA was significantly upregulated in the same cohort of GBM biopsies. Unexpectedly, SRSF3 Ex4 mRNA was also upregulated in GBM. However, consistently

with data obtained in U87-MG cells overexpressing circSMARCA5, the SRSF3 Ex4/SRSF3 No Ex4 ratio positively correlated with the expression of circSMARCA5 in GBM biopsies.

Based on these data about circSMARCA5 modulation and according to Jumaa et al. and Jihua et al. [195], [250], it was possible to hypothesize that circSMARCA5 downregulation in GBM biopsies, associated with upregulation of SRSF1, may promote the skipping of exon 4 in SRSF3 pre-mRNA. At the same time, increased levels of functional SRSF3 protein may determine the increased expression of SRSF3 Ex4 mRNA (which results in a non-productive non-sense mediated decay (NMD) substrate [251], [252], in a self-regulatory manner.

Despite the increased expression of both SRSF3 mRNA isoforms in GBM biopsies compared to normal brain parenchyma, it was observed a significant positive correlation between SRSF3 Ex4/SRSF3 No Ex4 ratio and circSMARCA5 expression. These data supported the hypothesis that circSMARCA5 may indirectly regulate the expression of SRSF3 mRNA isoforms, by tethering SRSF1, and, in turn, the functional SRSF3 protein (synthesized from SRSF3 No Ex4) may positively regulate the expression of SRSF3 Ex4 mRNA, which is normally expressed at very low levels within cells. However, it is not possible exclude that other regulator molecules (in addition to circSMARCA5) may contribute in regulating the expression of SRSF3 mRNA isoforms within GBM cells. Interestingly, SRSF1, in addition to the known biological functions that it regulates, including splicing, [246] is also involved in a self-regulatory network comprising several splicing factors, as PTBP1 and SRSF3 that act as known oncoproteins in different types of cancer [139]. Most

specifically, the splicing pattern of SRSF3 mRNA is defined by SRSF1 and SRSF3 itself regulates the expression of PTBP1 whose overexpression is known to positively regulate GBM cells migration [253].

The predicted physical interaction between circSMARCA5 and SRSFS1 was validated by RIP analysis in U87-MG cell lysate. In order to study if the interaction between circSMARCA5 and SRSF1 may be involved in the regulation of the splicing pattern of SRSF1's targets, VEGFA has been chosen as a known and validated target of SRSF1 and an interesting clinical molecule in GBM.

It is known that VEGFA pre-mRNA can be alternatively spliced generating both pro and anti-angiogenic isoforms (VEGF-Axxxa and VEGF-Axxxb, respectively) depending on the recognition by SRSF1 of a proximal splicing site (PSS) within the eighth exon of VEGFA pre-mRNA. In detail, the higher the amount of SRSF1 binding the PSS, the higher the retention of full-length eighth exon is, improving the synthesis of VEGF-Axxxa isoforms [240], [241], [242]. Aberrant splicing of VEGFA, leading to an alteration in the pro/anti-angiogenic ratio, was described in human colon cancer [237].

Data on GBM biopsies and U87-MG cell line showed that the Iso8a-to-Iso8b ratio was significantly higher in GBM biopsies with respect to unaffected controls and it was also higher in three GBM cell lines (A172, CAS1 and U87-MG). Interestingly, U87-MG overexpressing circSMARCA5 showed a significant decrease in the Iso8a-to-Iso8b ratio with respect to the same cells transfected with the empty vector.

Taken together these data supported the hypothesis that circSMARCA5 performs a trans-acting splicing function within GBM cells by tethering SRSF1 and, thus, affecting angiogenesis in GBM.

Moreover, based on *in silico* analyses by using REMBRANDT and TCGA databases, this pathway seemed to be specifically dysregulated in GBM with respect to the other glioma grades.

The hypothesis of a functional involvement of circSMARCA5 in the regulation of angiogenesis was also supported by the correlations observed among the circSMARCA5/SRSF1/VEGFA expression and the blood microvascular vessel density.

The control of the pro- to anti-angiogenic switch may represent a valid alternative to the therapy based on monoclonal anti-VEGFA antibodies that did not reach the expected results to date [254]. Finally, even if on a limited cohort of patients, the perspective use of circSMARCA5 as a prognostic biomarker and a therapeutic target [241], [255], [256] in GBM cells appears to be promising.

6. BIBLIOGRAPHY

1. Louis, D.N., et al., *The 2016 World Health Organization Classification of Tumors of the Central Nervous System: a summary.* Acta Neuropathol, 2016. **131**(6): p. 803-20.
2. Ohgaki, H. and P. Kleihues, *Genetic pathways to primary and secondary glioblastoma.* Am J Pathol, 2007. **170**(5): p. 1445-53.
3. Verhaak, R.G., et al., *Integrated genomic analysis identifies clinically relevant subtypes of glioblastoma characterized by abnormalities in PDGFRA, IDH1, EGFR, and NF1.* Cancer Cell, 2010. **17**(1): p. 98-110.
4. Nakada, M., et al., *Aberrant signaling pathways in glioma.* Cancers (Basel), 2011. **3**(3): p. 3242-78.
5. Aldape, K., et al., *Glioblastoma: pathology, molecular mechanisms and markers.* Acta Neuropathol, 2015. **129**(6): p. 829-48.
6. Liu, A., et al., *Genetics and Epigenetics of Glioblastoma: Applications and Overall Incidence of IDH1 Mutation.* Front Oncol, 2016. **6**: p. 16.
7. Parsons, D.W., et al., *An integrated genomic analysis of human glioblastoma multiforme.* Science, 2008. **321**(5897): p. 1807-12.
8. Esteller, M., *Non-coding RNAs in human disease.* Nat Rev Genet, 2011. **12**(12): p. 861-74.
9. Ragusa, M., et al., *Molecular Crosstalking among Noncoding RNAs: A New Network Layer of Genome Regulation in Cancer.* Int J Genomics, 2017. **2017**: p. 4723193.
10. Consortium, E.P., et al., *Identification and analysis of functional elements in 1% of the human genome by the ENCODE pilot project.* Nature, 2007. **447**(7146): p. 799-816.
11. Bernstein, B.E., et al., *The NIH Roadmap Epigenomics Mapping Consortium.* Nat Biotechnol, 2010. **28**(10): p. 1045-8.
12. Sana, J., et al., *Novel classes of non-coding RNAs and cancer.* J Transl Med, 2012. **10**: p. 103.
13. Ragusa, M., et al., *Non-coding landscapes of colorectal cancer.* World J Gastroenterol, 2015. **21**(41): p. 11709-39.
14. Kartha, R.V. and S. Subramanian, *Competing endogenous RNAs (ceRNAs): new entrants to the intricacies of gene regulation.* Front Genet, 2014. **5**: p. 8.
15. Sanger, H.L., et al., *Viroids are single-stranded covalently closed circular RNA molecules existing as highly base-paired rod-like structures.* Proc Natl Acad Sci U S A, 1976. **73**(11): p. 3852-6.
16. Hsu, M.T. and M. Coca-Prados, *Electron microscopic evidence for the circular form of RNA in the cytoplasm of eukaryotic cells.* Nature, 1979. **280**(5720): p. 339-40.
17. Cocquerelle, C., et al., *Mis-splicing yields circular RNA molecules.* FASEB J, 1993. **7**(1): p. 155-60.
18. Memczak, S., et al., *Circular RNAs are a large class of animal RNAs with regulatory potency.* Nature, 2013. **495**(7441): p. 333-8.
19. Guo, J.U., et al., *Expanded identification and characterization of mammalian circular RNAs.* Genome Biol, 2014. **15**(7): p. 409.
20. Starke, S., et al., *Exon circularization requires canonical splice signals.* Cell Rep, 2015. **10**(1): p. 103-11.
21. Jeck, W.R., et al., *Circular RNAs are abundant, conserved, and associated with ALU repeats.* RNA, 2013. **19**(2): p. 141-57.
22. Lasda, E. and R. Parker, *Circular RNAs: diversity of form and function.* RNA, 2014. **20**(12): p. 1829-42.
23. Li, Z., et al., *Exon-intron circular RNAs regulate transcription in the nucleus.* Nat Struct Mol Biol, 2015. **22**(3): p. 256-64.
24. Zhang, X.O., et al., *Complementary sequence-mediated exon circularization.* Cell, 2014. **159**(1): p. 134-147.
25. Zhang, X.O., et al., *Diverse alternative back-splicing and alternative splicing landscape of circular RNAs.* Genome Res, 2016. **26**(9): p. 1277-87.
26. Qu, S., et al., *The emerging landscape of circular RNA in life processes.* RNA Biol, 2017. **14**(8): p. 992-999.
27. Wang, P.L., et al., *Circular RNA is expressed across the eukaryotic tree of life.* PLoS One, 2014. **9**(6): p. e90859.
28. Salzman, J., et al., *Circular RNAs are the predominant transcript isoform from hundreds of human genes in diverse cell types.* PLoS One, 2012. **7**(2): p. e30733.
29. Salzman, J., et al., *Cell-type specific features of circular RNA expression.* PLoS Genet, 2013. **9**(9): p. e1003777.
30. Danan, M., et al., *Transcriptome-wide discovery of circular RNAs in Archaea.* Nucleic Acids Res, 2012. **40**(7): p. 3131-42.
31. Veno, M.T., et al., *Spatio-temporal regulation of circular RNA expression during porcine embryonic brain development.* Genome Biol, 2015. **16**: p. 245.

32. Rybak-Wolf, A., et al., *Circular RNAs in the Mammalian Brain Are Highly Abundant, Conserved, and Dynamically Expressed.* Mol Cell, 2015. **58**(5): p. 870-85.
33. Zhang, Y., et al., *The Biogenesis of Nascent Circular RNAs.* Cell Rep, 2016. **15**(3): p. 611-624.
34. Ebbesen, K.K., J. Kjems, and T.B. Hansen, *Circular RNAs: Identification, biogenesis and function.* Biochim Biophys Acta, 2016. **1859**(1): p. 163-8.
35. Lu, T., et al., *Transcriptome-wide investigation of circular RNAs in rice.* RNA, 2015. **21**(12): p. 2076-87.
36. Ivanov, A., et al., *Analysis of intron sequences reveals hallmarks of circular RNA biogenesis in animals.* Cell Rep, 2015. **10**(2): p. 170-7.
37. Westholm, J.O., et al., *Genome-wide analysis of drosophila circular RNAs reveals their structural and sequence properties and age-dependent neural accumulation.* Cell Rep, 2014. **9**(5): p. 1966-1980.
38. Zheng, Q., et al., *Circular RNA profiling reveals an abundant circHIPK3 that regulates cell growth by sponging multiple miRNAs.* Nat Commun, 2016. **7**: p. 11215.
39. Sun, X., et al., *Integrative analysis of Arabidopsis thaliana transcriptomics reveals intuitive splicing mechanism for circular RNA.* FEBS Lett, 2016. **590**(20): p. 3510-3516.
40. Ye, C.Y., et al., *Widespread noncoding circular RNAs in plants.* New Phytol, 2015. **208**(1): p. 88-95.
41. Broadbent, K.M., et al., *Strand-specific RNA sequencing in Plasmodium falciparum malaria identifies developmentally regulated long non-coding RNA and circular RNA.* BMC Genomics, 2015. **16**: p. 454.
42. Herculano-Houzel, S., *The human brain in numbers: a linearly scaled-up primate brain.* Front Hum Neurosci, 2009. **3**: p. 31.
43. Hansen, T.B., et al., *miRNA-dependent gene silencing involving Ago2-mediated cleavage of a circular antisense RNA.* EMBO J, 2011. **30**(21): p. 4414-22.
44. Ashwal-Fluss, R., et al., *circRNA biogenesis competes with pre-mRNA splicing.* Mol Cell, 2014. **56**(1): p. 55-66.
45. Conn, S.J., et al., *The RNA binding protein quaking regulates formation of circRNAs.* Cell, 2015. **160**(6): p. 1125-34.
46. Liang, D. and J.E. Wilusz, *Short intronic repeat sequences facilitate circular RNA production.* Genes Dev, 2014. **28**(20): p. 2233-47.
47. Ebbesen, K.K., T.B. Hansen, and J. Kjems, *Insights into circular RNA biology.* RNA Biol, 2017. **14**(8): p. 1035-1045.
48. Nishikura, K., *Functions and regulation of RNA editing by ADAR deaminases.* Annu Rev Biochem, 2010. **79**: p. 321-49.
49. Jeck, W.R. and N.E. Sharpless, *Detecting and characterizing circular RNAs.* Nat Biotechnol, 2014. **32**(5): p. 453-61.
50. Chen, L.L. and L. Yang, *Regulation of circRNA biogenesis.* RNA Biol, 2015. **12**(4): p. 381-8.
51. Le Hir, H., et al., *The exon-exon junction complex provides a binding platform for factors involved in mRNA export and nonsense-mediated mRNA decay.* EMBO J, 2001. **20**(17): p. 4987-97.
52. Yap, K., et al., *Coordinated regulation of neuronal mRNA steady-state levels through developmentally controlled intron retention.* Genes Dev, 2012. **26**(11): p. 1209-23.
53. Guo, J., *Transcription: the epicenter of gene expression.* J Zhejiang Univ Sci B, 2014. **15**(5): p. 409-11.
54. Taulli, R., C. Loretelli, and P.P. Pandolfi, *From pseudo-ceRNAs to circ-ceRNAs: a tale of cross-talk and competition.* Nat Struct Mol Biol, 2013. **20**(5): p. 541-3.
55. Hansen, T.B., et al., *Natural RNA circles function as efficient microRNA sponges.* Nature, 2013. **495**(7441): p. 384-8.
56. Pasquinelli, A.E., *MicroRNAs and their targets: recognition, regulation and an emerging reciprocal relationship.* Nat Rev Genet, 2012. **13**(4): p. 271-82.
57. Capel, B., et al., *Circular transcripts of the testis-determining gene Sry in adult mouse testis.* Cell, 1993. **73**(5): p. 1019-30.
58. Hacker, A., et al., *Expression of Sry, the mouse sex determining gene.* Development, 1995. **121**(6): p. 1603-14.
59. Li, F., et al., *Circular RNA ITCH has inhibitory effect on ESCC by suppressing the Wnt/beta-catenin pathway.* Oncotarget, 2015. **6**(8): p. 6001-13.
60. Yang, W., et al., *Foxo3 activity promoted by non-coding effects of circular RNA and Foxo3 pseudogene in the inhibition of tumor growth and angiogenesis.* Oncogene, 2016. **35**(30): p. 3919-31.
61. Wang, K., et al., *A circular RNA protects the heart from pathological hypertrophy and heart failure by targeting miR-223.* Eur Heart J, 2016. **37**(33): p. 2602-11.
62. Xie, H., et al., *Emerging roles of circRNA_001569 targeting miR-145 in the proliferation and invasion of colorectal cancer.* Oncotarget, 2016. **7**(18): p. 26680-91.
63. Du, W.W., et al., *Foxo3 circular RNA retards cell cycle progression via forming ternary complexes with p21 and CDK2.* Nucleic Acids Res, 2016. **44**(6): p. 2846-58.
64. Holdt, L.M., et al., *Circular non-coding RNA ANRIL modulates ribosomal RNA maturation and atherosclerosis in humans.* Nat Commun, 2016. **7**: p. 12429.

65. Zhang, Y., et al., *Circular intronic long noncoding RNAs.* Mol Cell, 2013. **51**(6): p. 792-806.
66. Lykke-Andersen, J. and E.J. Bennett, *Protecting the proteome: Eukaryotic cotranslational quality control pathways.* J Cell Biol, 2014. **204**(4): p. 467-76.
67. Abe, N., et al., *Rolling Circle Translation of Circular RNA in Living Human Cells.* Sci Rep, 2015. **5**: p. 16435.
68. Aitken, C.E. and J.R. Lorsch, *A mechanistic overview of translation initiation in eukaryotes.* Nat Struct Mol Biol, 2012. **19**(6): p. 568-76.
69. Chen, C.Y. and P. Sarnow, *Initiation of protein synthesis by the eukaryotic translational apparatus on circular RNAs.* Science, 1995. **268**(5209): p. 415-7.
70. Legnini, I., et al., *Circ-ZNF609 Is a Circular RNA that Can Be Translated and Functions in Myogenesis.* Mol Cell, 2017. **66**(1): p. 22-37 e9.
71. Zhao, Y., et al., *Deficiency in the Ubiquitin Conjugating Enzyme UBE2A in Alzheimer's Disease (AD) is Linked to Deficits in a Natural Circular miRNA-7 Sponge (circRNA; ciRS-7).* Genes (Basel), 2016. **7**(12).
72. Panda, A.C., et al., *Identification of senescence-associated circular RNAs (SAC-RNAs) reveals senescence suppressor CircPVT1.* Nucleic Acids Res, 2017. **45**(7): p. 4021-4035.
73. Xu, H., et al., *The circular RNA Cdr1as, via miR-7 and its targets, regulates insulin transcription and secretion in islet cells.* Sci Rep, 2015. **5**: p. 12453.
74. Qu, S., et al., *Circular RNA: A new star of noncoding RNAs.* Cancer Lett, 2015. **365**(2): p. 141-8.
75. Burd, C.E., et al., *Expression of linear and novel circular forms of an INK4/ARF-associated non-coding RNA correlates with atherosclerosis risk.* PLoS Genet, 2010. **6**(12): p. e1001233.
76. Boeckel, J.N., et al., *Identification and Characterization of Hypoxia-Regulated Endothelial Circular RNA.* Circ Res, 2015. **117**(10): p. 884-90.
77. Zhao, Z., et al., *Peripheral blood circular RNA hsa_circ_0124644 can be used as a diagnostic biomarker of coronary artery disease.* Sci Rep, 2017. **7**: p. 39918.
78. Han, B., J. Chao, and H. Yao, *Circular RNA and its mechanisms in disease: From the bench to the clinic.* Pharmacol Ther, 2018. **187**: p. 31-44.
79. Scotti, M.M. and M.S. Swanson, *RNA mis-splicing in disease.* Nat Rev Genet, 2016. **17**(1): p. 19-32.
80. Du, W.W., et al., *Induction of tumor apoptosis through a circular RNA enhancing Foxo3 activity.* Cell Death Differ, 2017. **24**(2): p. 357-370.
81. Lu, W.Y., *Roles of the circular RNA circ-Foxo3 in breast cancer progression.* Cell Cycle, 2017. **16**(7): p. 589-590.
82. Liang, H.F., et al., *Circular RNA circ-ABCB10 promotes breast cancer proliferation and progression through sponging miR-1271.* Am J Cancer Res, 2017. **7**(7): p. 1566-1576.
83. Yang, P., et al., *Silencing of cZNF292 circular RNA suppresses human glioma tube formation via the Wnt/beta-catenin signaling pathway.* Oncotarget, 2016. **7**(39): p. 63449-63455.
84. Zhong, Z., et al., *Circular RNA MYLK as a competing endogenous RNA promotes bladder cancer progression through modulating VEGFA/VEGFR2 signaling pathway.* Cancer Lett, 2017. **403**: p. 305-317.
85. Wan, L., et al., *Circular RNA-ITCH Suppresses Lung Cancer Proliferation via Inhibiting the Wnt/beta-Catenin Pathway.* Biomed Res Int, 2016. **2016**: p. 1579490.
86. Kristensen, L.S., et al., *Circular RNAs in cancer: opportunities and challenges in the field.* Oncogene, 2018. **37**(5): p. 555-565.
87. Li, P., et al., *Circular RNA 0000096 affects cell growth and migration in gastric cancer.* Br J Cancer, 2017. **116**(5): p. 626-633.
88. Chen, J., et al., *Circular RNA profile identifies circPVT1 as a proliferative factor and prognostic marker in gastric cancer.* Cancer Lett, 2017. **388**: p. 208-219.
89. Zhang, Y., et al., *CircRNA_100269 is downregulated in gastric cancer and suppresses tumor cell growth by targeting miR-630.* Aging (Albany NY), 2017. **9**(6): p. 1585-1594.
90. Guo, J.N., et al., *Comprehensive profile of differentially expressed circular RNAs reveals that hsa_circ_0000069 is upregulated and promotes cell proliferation, migration, and invasion in colorectal cancer.* Onco Targets Ther, 2016. **9**: p. 7451-7458.
91. Hsiao, K.Y., et al., *Noncoding Effects of Circular RNA CCDC66 Promote Colon Cancer Growth and Metastasis.* Cancer Res, 2017. **77**(9): p. 2339-2350.
92. Zhu, M., et al., *Circular BANP, an upregulated circular RNA that modulates cell proliferation in colorectal cancer.* Biomed Pharmacother, 2017. **88**: p. 138-144.
93. Zhang, X.L., L.L. Xu, and F. Wang, *Hsa_circ_0020397 regulates colorectal cancer cell viability, apoptosis and invasion by promoting the expression of the miR-138 targets TERT and PD-L1.* Cell Biol Int, 2017. **41**(9): p. 1056-1064.
94. Yu, L., et al., *The Circular RNA Cdr1as Act as an Oncogene in Hepatocellular Carcinoma through Targeting miR-7 Expression.* PLoS One, 2016. **11**(7): p. e0158347.

95. Yao, Z., et al., *ZKSCAN1 gene and its related circular RNA (circZKSCAN1) both inhibit hepatocellular carcinoma cell growth, migration, and invasion but through different signaling pathways.* Mol Oncol, 2017. **11**(4): p. 422-437.
96. Kent, O.A. and J.T. Mendell, *A small piece in the cancer puzzle: microRNAs as tumor suppressors and oncogenes.* Oncogene, 2006. **25**(46): p. 6188-96.
97. Peng, Y. and C.M. Croce, *The role of MicroRNAs in human cancer.* Signal Transduct Target Ther, 2016. **1**: p. 15004.
98. Ghosal, S., et al., *Circ2Traits: a comprehensive database for circular RNA potentially associated with disease and traits.* Front Genet, 2013. **4**: p. 283.
99. Zhong, Z., M. Lv, and J. Chen, *Screening differential circular RNA expression profiles reveals the regulatory role of circTCF25-miR-103a-3p/miR-107-CDK6 pathway in bladder carcinoma.* Sci Rep, 2016. **6**: p. 30919.
100. Weng, W., et al., *Circular RNA ciRS-7-A Promising Prognostic Biomarker and a Potential Therapeutic Target in Colorectal Cancer.* Clin Cancer Res, 2017. **23**(14): p. 3918-3928.
101. Chen, L., et al., *circRNA_100290 plays a role in oral cancer by functioning as a sponge of the miR-29 family.* Oncogene, 2017. **36**(32): p. 4551-4561.
102. Li, Y., et al., *Circular RNA is enriched and stable in exosomes: a promising biomarker for cancer diagnosis.* Cell Res, 2015. **25**(8): p. 981-4.
103. Memczak, S., et al., *Identification and Characterization of Circular RNAs As a New Class of Putative Biomarkers in Human Blood.* PLoS One, 2015. **10**(10): p. e0141214.
104. Bahn, J.H., et al., *The landscape of microRNA, Piwi-interacting RNA, and circular RNA in human saliva.* Clin Chem, 2015. **61**(1): p. 221-30.
105. Song, X., et al., *Circular RNA profile in gliomas revealed by identification tool UROBORUS.* Nucleic Acids Res, 2016. **44**(9): p. e87.
106. Hao, Z., et al., *Circular RNAs: Functions and Prospects in Glioma.* J Mol Neurosci, 2019. **67**(1): p. 72-81.
107. Chen, Z. and X. Duan, *hsa_circ_0000177-miR-638-FZD7-Wnt Signaling Cascade Contributes to the Malignant Behaviors in Glioma.* DNA Cell Biol, 2018. **37**(9): p. 791-797.
108. Li, G., et al., *A novel circular RNA, hsa_circ_0046701, promotes carcinogenesis by increasing the expression of miR-142-3p target ITGB8 in glioma.* Biochem Biophys Res Commun, 2018. **498**(1): p. 254-261.
109. Li, G.F., et al., *Hsa_circ_0007534/miR-761/ZIC5 regulatory loop modulates the proliferation and migration of glioma cells.* Biochem Biophys Res Commun, 2018. **499**(4): p. 765-771.
110. Xie, G., *Circular RNA hsa-circ-0012129 Promotes Cell Proliferation and Invasion in 30 Cases of Human Glioma and Human Glioma Cell Lines U373, A172, and SHG44, by Targeting MicroRNA-661 (miR-661).* Med Sci Monit, 2018. **24**: p. 2497-2507.
111. Bian, A., et al., *Circular RNA Complement Factor H (CFH) Promotes Glioma Progression by Sponging miR-149 and Regulating AKT1.* Med Sci Monit, 2018. **24**: p. 5704-5712.
112. Xu, H., et al., *NFIX Circular RNA Promotes Glioma Progression by Regulating miR-34a-5p via Notch Signaling Pathway.* Front Mol Neurosci, 2018. **11**: p. 225.
113. Jin, P., et al., *CircRNA circHIPK3 serves as a prognostic marker to promote glioma progression by regulating miR-654/IGF2BP3 signaling.* Biochem Biophys Res Commun, 2018. **503**(3): p. 1570-1574.
114. Wang, R., et al., *CircNT5E Acts as a Sponge of miR-422a to Promote Glioblastoma Tumorigenesis.* Cancer Res, 2018. **78**(17): p. 4812-4825.
115. He, Q., et al., *circ-SHKBP1 Regulates the Angiogenesis of U87 Glioma-Exposed Endothelial Cells through miR-544a/FOXP1 and miR-379/FOXP2 Pathways.* Mol Ther Nucleic Acids, 2018. **10**: p. 331-348.
116. Zhou, J., et al., *Circular RNA hsa_circ_0008344 regulates glioblastoma cell proliferation, migration, invasion, and apoptosis.* J Clin Lab Anal, 2018. **32**(7): p. e22454.
117. Li, F., et al., *Identification of the tumor-suppressive function of circular RNA ITCH in glioma cells through sponging miR-214 and promoting linear ITCH expression.* Am J Transl Res, 2018. **10**(5): p. 1373-1386.
118. Zheng, J., et al., *TTBK2 circular RNA promotes glioma malignancy by regulating miR-217/HNF1beta/Derlin-1 pathway.* J Hematol Oncol, 2017. **10**(1): p. 52.
119. Barbagallo, D., et al., *Dysregulated miR-671-5p / CDR1-AS / CDR1 / VSNL1 axis is involved in glioblastoma multiforme.* Oncotarget, 2016. **7**(4): p. 4746-59.
120. Yang, Y., et al., *Novel Role of FBXW7 Circular RNA in Repressing Glioma Tumorigenesis.* J Natl Cancer Inst, 2018. **110**(3).
121. Begum, S., et al., *Novel tumour suppressive protein encoded by circular RNA, circ-SHPRH, in glioblastomas.* Oncogene, 2018. **37**(30): p. 4055-4057.
122. Zhang, M., et al., *A novel protein encoded by the circular form of the SHPRH gene suppresses glioma tumorigenesis.* Oncogene, 2018. **37**(13): p. 1805-1814.

123. Wang, Y., et al., *Decreased circular RNA hsa_circ_0001649 predicts unfavorable prognosis in glioma and exerts oncogenic properties in vitro and in vivo.* Gene, 2018. **676**: p. 117-122.
124. Montes, M., et al., *RNA Splicing and Disease: Animal Models to Therapies.* Trends Genet, 2019. **35**(1): p. 68-87.
125. Pajares, M.J., et al., *Alternative splicing: an emerging topic in molecular and clinical oncology.* Lancet Oncol, 2007. **8**(4): p. 349-57.
126. Collesi, C., et al., *A splicing variant of the RON transcript induces constitutive tyrosine kinase activity and an invasive phenotype.* Mol Cell Biol, 1996. **16**(10): p. 5518-26.
127. Ghigna, C., et al., *Cell motility is controlled by SF2/ASF through alternative splicing of the Ron protooncogene.* Mol Cell, 2005. **20**(6): p. 881-90.
128. Bartel, F., H. Taubert, and L.C. Harris, *Alternative and aberrant splicing of MDM2 mRNA in human cancer.* Cancer Cell, 2002. **2**(1): p. 9-15.
129. Lukas, J., et al., *Alternative and aberrant messenger RNA splicing of the mdm2 oncogene in invasive breast cancer.* Cancer Res, 2001. **61**(7): p. 3212-9.
130. Yu, F. and W.M. Fu, *Identification of differential splicing genes in gliomas using exon expression profiling.* Mol Med Rep, 2015. **11**(2): p. 843-50.
131. Sadeque, A., et al., *Identification and characterization of alternative exon usage linked glioblastoma multiforme survival.* BMC Med Genomics, 2012. **5**: p. 59.
132. Loilome, W., et al., *Glioblastoma cell growth is suppressed by disruption of Fibroblast Growth Factor pathway signaling.* J Neurooncol, 2009. **94**(3): p. 359-66.
133. Pedersen, M.W., et al., *The type III epidermal growth factor receptor mutation. Biological significance and potential target for anti-cancer therapy.* Ann Oncol, 2001. **12**(6): p. 745-60.
134. Feng, H., et al., *EGFRvIII stimulates glioma growth and invasion through PKA-dependent serine phosphorylation of Dock180.* Oncogene, 2014. **33**(19): p. 2504-12.
135. Kinzler, K.W., et al., *Identification of an amplified, highly expressed gene in a human glioma.* Science, 1987. **236**(4797): p. 70-3.
136. Wang, X.Q. and J.A. Rothnagel, *Post-transcriptional regulation of the gli1 oncogene by the expression of alternative 5' untranslated regions.* J Biol Chem, 2001. **276**(2): p. 1311-6.
137. Zhu, H., et al., *The GLI1 splice variant TGLI1 promotes glioblastoma angiogenesis and growth.* Cancer Lett, 2014. **343**(1): p. 51-61.
138. Lo, H.W., et al., *A novel splice variant of GLI1 that promotes glioblastoma cell migration and invasion.* Cancer Res, 2009. **69**(17): p. 6790-8.
139. Dvinge, H., et al., *RNA splicing factors as oncoproteins and tumour suppressors.* Nat Rev Cancer, 2016. **16**(7): p. 413-30.
140. Brinkman, B.M., *Splice variants as cancer biomarkers.* Clin Biochem, 2004. **37**(7): p. 584-94.
141. Dreyfuss, G., V.N. Kim, and N. Kataoka, *Messenger-RNA-binding proteins and the messages they carry.* Nat Rev Mol Cell Biol, 2002. **3**(3): p. 195-205.
142. Tu, H.C., et al., *LIN28 cooperates with WNT signaling to drive invasive intestinal and colorectal adenocarcinoma in mice and humans.* Genes Dev, 2015. **29**(10): p. 1074-86.
143. Galante, P.A., et al., *A comprehensive in silico expression analysis of RNA binding proteins in normal and tumor tissue: Identification of potential players in tumor formation.* RNA Biol, 2009. **6**(4): p. 426-33.
144. Kechavarzi, B. and S.C. Janga, *Dissecting the expression landscape of RNA-binding proteins in human cancers.* Genome Biol, 2014. **15**(1): p. R14.
145. Kafasla, P., et al., *Defining the roles and interactions of PTB.* Biochem Soc Trans, 2012. **40**(4): p. 815-20.
146. Fontana, L., et al., *Suggestive evidence on the involvement of polypyrimidine-tract binding protein in regulating alternative splicing of MAP/microtubule affinity-regulating kinase 4 in glioma.* Cancer Lett, 2015. **359**(1): p. 87-96.
147. Zong, F.Y., et al., *The RNA-binding protein QKI suppresses cancer-associated aberrant splicing.* PLoS Genet, 2014. **10**(4): p. e1004289.
148. Bechara, E.G., et al., *RBM5, 6, and 10 differentially regulate NUMB alternative splicing to control cancer cell proliferation.* Mol Cell, 2013. **52**(5): p. 720-33.
149. Radisky, D.C. and M.J. Bissell, *Matrix metalloproteinase-induced genomic instability.* Curr Opin Genet Dev, 2006. **16**(1): p. 45-50.
150. Singh, R. and J. Valcarcel, *Building specificity with nonspecific RNA-binding proteins.* Nat Struct Mol Biol, 2005. **12**(8): p. 645-53.
151. Lefave, C.V., et al., *Splicing factor hnRNPH drives an oncogenic splicing switch in gliomas.* EMBO J, 2011. **30**(19): p. 4084-97.
152. Golan-Gerstl, R., et al., *Splicing factor hnRNP A2/B1 regulates tumor suppressor gene splicing and is an oncogenic driver in glioblastoma.* Cancer Res, 2011. **71**(13): p. 4464-72.

153. Pereira, B., M. Billaud, and R. Almeida, *RNA-Binding Proteins in Cancer: Old Players and New Actors.* Trends Cancer, 2017. **3**(7): p. 506-528.
154. Boggs, R.T., et al., *Regulation of sexual differentiation in D. melanogaster via alternative splicing of RNA from the transformer gene.* Cell, 1987. **50**(5): p. 739-47.
155. Krainer, A.R., G.C. Conway, and D. Kozak, *Purification and characterization of pre-mRNA splicing factor SF2 from HeLa cells.* Genes Dev, 1990. **4**(7): p. 1158-71.
156. Roth, M.B., A.M. Zahler, and J.A. Stolk, *A conserved family of nuclear phosphoproteins localized to sites of polymerase II transcription.* J Cell Biol, 1991. **115**(3): p. 587-96.
157. Zahler, A.M., et al., *SR proteins: a conserved family of pre-mRNA splicing factors.* Genes Dev, 1992. **6**(5): p. 837-47.
158. Graveley, B.R., *Sorting out the complexity of SR protein functions.* RNA, 2000. **6**(9): p. 1197-211.
159. Kataoka, N., J.L. Bachorik, and G. Dreyfuss, *Transportin-SR, a nuclear import receptor for SR proteins.* J Cell Biol, 1999. **145**(6): p. 1145-52.
160. Blencowe, B.J., *Exonic splicing enhancers: mechanism of action, diversity and role in human genetic diseases.* Trends Biochem Sci, 2000. **25**(3): p. 106-10.
161. Shepard, P.J. and K.J. Hertel, *The SR protein family.* Genome Biol, 2009. **10**(10): p. 242.
162. Mermoud, J.E., P.T. Cohen, and A.I. Lamond, *Regulation of mammalian spliceosome assembly by a protein phosphorylation mechanism.* EMBO J, 1994. **13**(23): p. 5679-88.
163. Kanopka, A., O. Muhlemann, and G. Akusjarvi, *Inhibition by SR proteins of splicing of a regulated adenovirus pre-mRNA.* Nature, 1996. **381**(6582): p. 535-8.
164. Caceres, J.F., G.R. Screaton, and A.R. Krainer, *A specific subset of SR proteins shuttles continuously between the nucleus and the cytoplasm.* Genes Dev, 1998. **12**(1): p. 55-66.
165. Michlewski, G., J.R. Sanford, and J.F. Caceres, *The splicing factor SF2/ASF regulates translation initiation by enhancing phosphorylation of 4E-BP1.* Mol Cell, 2008. **30**(2): p. 179-89.
166. Zhang, J. and J.L. Manley, *Misregulation of pre-mRNA alternative splicing in cancer.* Cancer Discov, 2013. **3**(11): p. 1228-37.
167. David, C.J. and J.L. Manley, *Alternative pre-mRNA splicing regulation in cancer: pathways and programs unhinged.* Genes Dev, 2010. **24**(21): p. 2343-64.
168. Karni, R., et al., *The gene encoding the splicing factor SF2/ASF is a proto-oncogene.* Nat Struct Mol Biol, 2007. **14**(3): p. 185-93.
169. Anczukow, O., et al., *The splicing factor SRSF1 regulates apoptosis and proliferation to promote mammary epithelial cell transformation.* Nat Struct Mol Biol, 2012. **19**(2): p. 220-8.
170. Vivanco, I. and C.L. Sawyers, *The phosphatidylinositol 3-Kinase AKT pathway in human cancer.* Nat Rev Cancer, 2002. **2**(7): p. 489-501.
171. Shaw, R.J. and L.C. Cantley, *Ras, PI(3)K and mTOR signalling controls tumour cell growth.* Nature, 2006. **441**(7092): p. 424-30.
172. Jia, R., et al., *SRp20 is a proto-oncogene critical for cell proliferation and tumor induction and maintenance.* Int J Biol Sci, 2010. **6**(7): p. 806-26.
173. Jensen, M.A., J.E. Wilkinson, and A.R. Krainer, *Splicing factor SRSF6 promotes hyperplasia of sensitized skin.* Nat Struct Mol Biol, 2014. **21**(2): p. 189-97.
174. Cohen-Eliav, M., et al., *The splicing factor SRSF6 is amplified and is an oncoprotein in lung and colon cancers.* J Pathol, 2013. **229**(4): p. 630-9.
175. Zhou, X., et al., *BCLAF1 and its splicing regulator SRSF10 regulate the tumorigenic potential of colon cancer cells.* Nat Commun, 2014. **5**: p. 4581.
176. Lai, M.C. and W.Y. Tarn, *Hypophosphorylated ASF/SF2 binds TAP and is present in messenger ribonucleoproteins.* J Biol Chem, 2004. **279**(30): p. 31745-9.
177. Sanford, J.R., et al., *A novel role for shuttling SR proteins in mRNA translation.* Genes Dev, 2004. **18**(7): p. 755-68.
178. Wu, H., et al., *A splicing-independent function of SF2/ASF in microRNA processing.* Mol Cell, 2010. **38**(1): p. 67-77.
179. Loomis, R.J., et al., *Chromatin binding of SRp20 and ASF/SF2 and dissociation from mitotic chromosomes is modulated by histone H3 serine 10 phosphorylation.* Mol Cell, 2009. **33**(4): p. 450-61.
180. Pelisch, F., et al., *The serine/arginine-rich protein SF2/ASF regulates protein sumoylation.* Proc Natl Acad Sci U S A, 2010. **107**(37): p. 16119-24.
181. Fregoso, O.I., et al., *Splicing-factor oncoprotein SRSF1 stabilizes p53 via RPL5 and induces cellular senescence.* Mol Cell, 2013. **50**(1): p. 56-66.
182. Das, S., et al., *Oncogenic splicing factor SRSF1 is a critical transcriptional target of MYC.* Cell Rep, 2012. **1**(2): p. 110-7.

183. Valacca, C., et al., *Sam68 regulates EMT through alternative splicing-activated nonsense-mediated mRNA decay of the SF2/ASF proto-oncogene.* J Cell Biol, 2010. **191**(1): p. 87-99.
184. Gautrey, H.L. and A.J. Tyson-Capper, *Regulation of Mcl-1 by SRSF1 and SRSF5 in cancer cells.* PLoS One, 2012. **7**(12): p. e51497.
185. Ge, H. and J.L. Manley, *A protein factor, ASF, controls cell-specific alternative splicing of SV40 early pre-mRNA in vitro.* Cell, 1990. **62**(1): p. 25-34.
186. Nowak, D.G., et al., *Expression of pro- and anti-angiogenic isoforms of VEGF is differentially regulated by splicing and growth factors.* J Cell Sci, 2008. **121**(Pt 20): p. 3487-95.
187. Rennel, E.S., et al., *VEGF(121)b, a new member of the VEGF(xxx)b family of VEGF-A splice isoforms, inhibits neovascularisation and tumour growth in vivo.* Br J Cancer, 2009. **101**(7): p. 1183-93.
188. Thobe, M.N., et al., *The Ron receptor promotes prostate tumor growth in the TRAMP mouse model.* Oncogene, 2011. **30**(50): p. 4990-8.
189. Ajiro, M., et al., *A genome landscape of SRSF3-regulated splicing events and gene expression in human osteosarcoma U2OS cells.* Nucleic Acids Res, 2016. **44**(4): p. 1854-70.
190. Bedard, K.M., S. Daijogo, and B.L. Semler, *A nucleo-cytoplasmic SR protein functions in viral IRES-mediated translation initiation.* EMBO J, 2007. **26**(2): p. 459-67.
191. Lou, H., et al., *Regulation of alternative polyadenylation by U1 snRNPs and SRp20.* Mol Cell Biol, 1998. **18**(9): p. 4977-85.
192. Auyeung, V.C., et al., *Beyond secondary structure: primary-sequence determinants license pri-miRNA hairpins for processing.* Cell, 2013. **152**(4): p. 844-58.
193. Ohta, S., et al., *Global splicing pattern reversion during somatic cell reprogramming.* Cell Rep, 2013. **5**(2): p. 357-66.
194. Anko, M.L., et al., *The RNA-binding landscapes of two SR proteins reveal unique functions and binding to diverse RNA classes.* Genome Biol, 2012. **13**(3): p. R17.
195. Jumaa, H. and P.J. Nielsen, *The splicing factor SRp20 modifies splicing of its own mRNA and ASF/SF2 antagonizes this regulation.* EMBO J, 1997. **16**(16): p. 5077-85.
196. Nishida, N., et al., *Angiogenesis in cancer.* Vasc Health Risk Manag, 2006. **2**(3): p. 213-9.
197. Semenza, G., *Signal transduction to hypoxia-inducible factor 1.* Biochem Pharmacol, 2002. **64**(5-6): p. 993-8.
198. Carmeliet, P., *VEGF as a key mediator of angiogenesis in cancer.* Oncology, 2005. **69 Suppl 3**: p. 4-10.
199. Ferrara, N. and T. Davis-Smyth, *The biology of vascular endothelial growth factor.* Endocr Rev, 1997. **18**(1): p. 4-25.
200. Ferrara, N., H.P. Gerber, and J. LeCouter, *The biology of VEGF and its receptors.* Nat Med, 2003. **9**(6): p. 669-76.
201. Park, J.E., G.A. Keller, and N. Ferrara, *The vascular endothelial growth factor (VEGF) isoforms: differential deposition into the subepithelial extracellular matrix and bioactivity of extracellular matrix-bound VEGF.* Mol Biol Cell, 1993. **4**(12): p. 1317-26.
202. Ferrara, N., *Vascular endothelial growth factor as a target for anticancer therapy.* Oncologist, 2004. **9 Suppl 1**: p. 2-10.
203. Thomas, K.A., *Vascular endothelial growth factor, a potent and selective angiogenic agent.* J Biol Chem, 1996. **271**(2): p. 603-6.
204. Alon, T., et al., *Vascular endothelial growth factor acts as a survival factor for newly formed retinal vessels and has implications for retinopathy of prematurity.* Nat Med, 1995. **1**(10): p. 1024-8.
205. Sato, K., et al., *Expression of vascular endothelial growth factor gene and its receptor (flt-1) gene in urinary bladder cancer.* Tohoku J Exp Med, 1998. **185**(3): p. 173-84.
206. Xia, G., et al., *Expression and significance of vascular endothelial growth factor receptor 2 in bladder cancer.* J Urol, 2006. **175**(4): p. 1245-52.
207. Mylona, E., et al., *The prognostic value of vascular endothelial growth factors (VEGFs)-A and -B and their receptor, VEGFR-1, in invasive breast carcinoma.* Gynecol Oncol, 2007. **104**(3): p. 557-63.
208. Ghosh, S., et al., *High levels of vascular endothelial growth factor and its receptors (VEGFR-1, VEGFR-2, neuropilin-1) are associated with worse outcome in breast cancer.* Hum Pathol, 2008. **39**(12): p. 1835-43.
209. Takahashi, Y., et al., *Expression of vascular endothelial growth factor and its receptor, KDR, correlates with vascularity, metastasis, and proliferation of human colon cancer.* Cancer Res, 1995. **55**(18): p. 3964-8.
210. Ozdemir, F., et al., *The effects of VEGF and VEGFR-2 on survival in patients with gastric cancer.* J Exp Clin Cancer Res, 2006. **25**(1): p. 83-8.
211. Kyzas, P.A., I.W. Cunha, and J.P. Ioannidis, *Prognostic significance of vascular endothelial growth factor immunohistochemical expression in head and neck squamous cell carcinoma: a meta-analysis.* Clin Cancer Res, 2005. **11**(4): p. 1434-40.

212. Seto, T., et al., *Prognostic value of expression of vascular endothelial growth factor and its flt-1 and KDR receptors in stage I non-small-cell lung cancer.* Lung Cancer, 2006. **53**(1): p. 91-6.
213. Carrillo de Santa Pau, E., et al., *Prognostic significance of the expression of vascular endothelial growth factors A, B, C, and D and their receptors R1, R2, and R3 in patients with nonsmall cell lung cancer.* Cancer, 2009. **115**(8): p. 1701-12.
214. Strizzi, L., et al., *Vascular endothelial growth factor is an autocrine growth factor in human malignant mesothelioma.* J Pathol, 2001. **193**(4): p. 468-75.
215. Latil, A., et al., *VEGF overexpression in clinically localized prostate tumors and neuropilin-1 overexpression in metastatic forms.* Int J Cancer, 2000. **89**(2): p. 167-71.
216. Kollermann, J. and B. Helpap, *Expression of vascular endothelial growth factor (VEGF) and VEGF receptor Flk-1 in benign, premalignant, and malignant prostate tissue.* Am J Clin Pathol, 2001. **116**(1): p. 115-21.
217. Knizetova, P., et al., *Autocrine regulation of glioblastoma cell cycle progression, viability and radioresistance through the VEGF-VEGFR2 (KDR) interplay.* Cell Cycle, 2008. **7**(16): p. 2553-61.
218. Hamerlik, P., et al., *Autocrine VEGF-VEGFR2-Neuropilin-1 signaling promotes glioma stem-like cell viability and tumor growth.* J Exp Med, 2012. **209**(3): p. 507-20.
219. Plate, K.H., et al., *Up-regulation of vascular endothelial growth factor and its cognate receptors in a rat glioma model of tumor angiogenesis.* Cancer Res, 1993. **53**(23): p. 5822-7.
220. Plate, K.H., et al., *Vascular endothelial growth factor and glioma angiogenesis: coordinate induction of VEGF receptors, distribution of VEGF protein and possible in vivo regulatory mechanisms.* Int J Cancer, 1994. **59**(4): p. 520-9.
221. Hadjipanayis, C.G. and E.G. Van Meir, *Brain cancer propagating cells: biology, genetics and targeted therapies.* Trends Mol Med, 2009. **15**(11): p. 519-30.
222. Xu, C., X. Wu, and J. Zhu, *VEGF promotes proliferation of human glioblastoma multiforme stem-like cells through VEGF receptor 2.* ScientificWorldJournal, 2013. **2013**: p. 417413.
223. Bao, S., et al., *Stem cell-like glioma cells promote tumor angiogenesis through vascular endothelial growth factor.* Cancer Res, 2006. **66**(16): p. 7843-8.
224. Chi, A.S., et al., *Angiogenesis as a therapeutic target in malignant gliomas.* Oncologist, 2009. **14**(6): p. 621-36.
225. Keunen, O., et al., *Anti-VEGF treatment reduces blood supply and increases tumor cell invasion in glioblastoma.* Proc Natl Acad Sci U S A, 2011. **108**(9): p. 3749-54.
226. Hu, Y.L., et al., *Hypoxia-induced autophagy promotes tumor cell survival and adaptation to antiangiogenic treatment in glioblastoma.* Cancer Res, 2012. **72**(7): p. 1773-83.
227. Kurebayashi, J., et al., *Expression of vascular endothelial growth factor (VEGF) family members in breast cancer.* Jpn J Cancer Res, 1999. **90**(9): p. 977-81.
228. Shaheen, R.M., et al., *Antiangiogenic therapy targeting the tyrosine kinase receptor for vascular endothelial growth factor receptor inhibits the growth of colon cancer liver metastasis and induces tumor and endothelial cell apoptosis.* Cancer Res, 1999. **59**(21): p. 5412-6.
229. Yoshiji, H., et al., *KDR/Flk-1 is a major regulator of vascular endothelial growth factor-induced tumor development and angiogenesis in murine hepatocellular carcinoma cells.* Hepatology, 1999. **30**(5): p. 1179-86.
230. Droller, M.J., *Vascular endothelial growth factor is a predictor of relapse and stage progression in superficial bladder cancer.* J Urol, 1998. **160**(5): p. 1932.
231. Karayiannakis, A.J., et al., *Circulating VEGF levels in the serum of gastric cancer patients: correlation with pathological variables, patient survival, and tumor surgery.* Ann Surg, 2002. **236**(1): p. 37-42.
232. Balbay, M.D., et al., *Highly metastatic human prostate cancer growing within the prostate of athymic mice overexpresses vascular endothelial growth factor.* Clin Cancer Res, 1999. **5**(4): p. 783-9.
233. Higa, G.M. and J. Abraham, *Biological mechanisms of bevacizumab-associated adverse events.* Expert Rev Anticancer Ther, 2009. **9**(7): p. 999-1007.
234. Willett, C.G., et al., *Direct evidence that the VEGF-specific antibody bevacizumab has antivascular effects in human rectal cancer.* Nat Med, 2004. **10**(2): p. 145-7.
235. Niyazi, M., et al., *Bevacizumab and radiotherapy for the treatment of glioblastoma: brothers in arms or unholy alliance?* Oncotarget, 2016. **7**(3): p. 2313-28.
236. McCarty, J.H., *Glioblastoma resistance to anti-VEGF therapy: has the challenge been MET?* Clin Cancer Res, 2013. **19**(7): p. 1631-3.
237. Hamdollah Zadeh, M.A., et al., *Alternative splicing of TIA-1 in human colon cancer regulates VEGF isoform expression, angiogenesis, tumour growth and bevacizumab resistance.* Mol Oncol, 2015. **9**(1): p. 167-78.
238. Caltabiano, R., et al., *ADAM 10 expression in primary uveal melanoma as prognostic factor for risk of metastasis.* Pathol Res Pract, 2016. **212**(11): p. 980-987.
239. Paz, I., et al., *RBPmap: a web server for mapping binding sites of RNA-binding proteins.* Nucleic Acids Res, 2014. **42**(Web Server issue): p. W361-7.

240. Amin, E.M., et al., *WT1 mutants reveal SRPK1 to be a downstream angiogenesis target by altering VEGF splicing.* Cancer Cell, 2011. **20**(6): p. 768-80.
241. Mavrou, A., et al., *Serine-arginine protein kinase 1 (SRPK1) inhibition as a potential novel targeted therapeutic strategy in prostate cancer.* Oncogene, 2015. **34**(33): p. 4311-9.
242. Ye, X., et al., *Altered ratios of pro- and anti-angiogenic VEGF-A variants and pericyte expression of DLL4 disrupt vascular maturation in infantile haemangioma.* J Pathol, 2016. **239**(2): p. 139-51.
243. Madhavan, S., et al., *Rembrandt: helping personalized medicine become a reality through integrative translational research.* Mol Cancer Res, 2009. **7**(2): p. 157-67.
244. Tomczak, K., P. Czerwinska, and M. Wiznerowicz, *The Cancer Genome Atlas (TCGA): an immeasurable source of knowledge.* Contemp Oncol (Pozn), 2015. **19**(1A): p. A68-77.
245. Siede, D., et al., *Identification of circular RNAs with host gene-independent expression in human model systems for cardiac differentiation and disease.* J Mol Cell Cardiol, 2017. **109**: p. 48-56.
246. Das, S. and A.R. Krainer, *Emerging functions of SRSF1, splicing factor and oncoprotein, in RNA metabolism and cancer.* Mol Cancer Res, 2014. **12**(9): p. 1195-204.
247. Anczukow, O., et al., *SRSF1-Regulated Alternative Splicing in Breast Cancer.* Mol Cell, 2015. **60**(1): p. 105-17.
248. Martinez-Terroba, E., et al., *The oncogenic RNA-binding protein SRSF1 regulates LIG1 in non-small cell lung cancer.* Lab Invest, 2018. **98**(12): p. 1562-1574.
249. Van Nostrand, E.L., et al., *Robust transcriptome-wide discovery of RNA-binding protein binding sites with enhanced CLIP (eCLIP).* Nat Methods, 2016. **13**(6): p. 508-14.
250. Guo, J., J. Jia, and R. Jia, *PTBP1 and PTBP2 impaired autoregulation of SRSF3 in cancer cells.* Sci Rep, 2015. **5**: p. 14548.
251. Lareau, L.F., et al., *Unproductive splicing of SR genes associated with highly conserved and ultraconserved DNA elements.* Nature, 2007. **446**(7138): p. 926-9.
252. Ni, J.Z., et al., *Ultraconserved elements are associated with homeostatic control of splicing regulators by alternative splicing and nonsense-mediated decay.* Genes Dev, 2007. **21**(6): p. 708-18.
253. Cheung, H.C., et al., *Splicing factors PTBP1 and PTBP2 promote proliferation and migration of glioma cell lines.* Brain, 2009. **132**(Pt 8): p. 2277-88.
254. Gilbert, M.R., et al., *A randomized trial of bevacizumab for newly diagnosed glioblastoma.* N Engl J Med, 2014. **370**(8): p. 699-708.
255. Holdt, L.M., A. Kohlmaier, and D. Teupser, *Circular RNAs as Therapeutic Agents and Targets.* Front Physiol, 2018. **9**: p. 1262.
256. Fukuhara, T., et al., *Utilization of host SR protein kinases and RNA-splicing machinery during viral replication.* Proc Natl Acad Sci U S A, 2006. **103**(30): p. 11329-33.